Summer 8-19-2016

Study of the Structure-Related Functions of Eukaryotic Primase-POL ALPHA Complex During Replication

Yinbo Zhang
University of Nebraska Medical Center

STUDY OF THE STRUCTURE-RELATED FUNCTIONS OF EUKARYOTIC PRIMASE-POL ALPHA COMPLEX DURING REPLICATION

By

Yinbo Zhang

A DISSERTATION

Presented to the Faculty of

The University of Nebraska Graduate College

In Partial Fulfillment of the Requirements

For the Degree of Doctor of Philosophy

Department of Biochemistry and Molecular Biology

Under the Supervision of Professor Youri I. Pavlov

University of Nebraska Medical Center

Omaha, Nebraska

May, 2016

Supervisory Committee:

Prof. Youri I. Pavlov (chair)

Prof. Gloria E. Borgstahl

Prof. Steve Caplan

Associate Prof. Polina V. Shcherbakova

Prof. Tahir H. Tahirov

ACKNOWLEDGEMENT

I feel very fortunate to be a Ph.D. student at the University of Nebraska Medical Center in the Biochemistry and Molecular Biology (BMB) program. Over the years, both BMB program and Eppley Institute for Research in Cancer provided essential support to my study. Through the curriculum and seminars I have been exposed to many aspects of science and become a determined scientist. Additionally, staffs from both departments have been patient to address my numerous and various questions and problems. In particular I would like to thank Jennifer Pace and Karen Hankins from the BMB department and Darcy Jackson and Ashley Ryan from Eppley Institute for always being available to help and point me in the right direction. I thank Dan Teet for all his help with visa, immigration-related issues, and other matter related to student affairs. I would also like to thank Drs. Surinder K. Batra and Richard G. MacDonald for their important and valuable advice in my first year on how to choose a laboratory and set the goals for my Ph.D. study.

I was fortunate to work with great lab-mates from Dr. Pavlov's laboratory. Artem, Hollie, Corinn, Miriam, and Irina created a friendly and enjoyable environment to work in. I would like to also thank people from Dr. Polina Shcherbakova's lab: Tony, Olga, Matt, Dan, Stephanie, Chelsea, and Xuan. I am grateful to Krista Brown and Liz Moore for their expert help with maintenance of the laboratory. Together, everybody around has provided essential comments to my work, thoughtful scientific discussions, and joyful conversation during the years in the lab, at lab meetings, or in the bar. A special thanks to

UNMC radiation safety office, especially Pamela Cox, who helped me through the radiation training and maintained the radiation lab.

I would like to thank my supervisory committee members for providing constructive critique and suggestions to my project. Dr. Gloria Borgstahl also served on my comprehensive exam committee (together with Drs. Laurey Steinke and Duygu Dee Harrison-Findik). The work during preparation of the exam helped me to stay on the correct path of my graduate study. Dr. Steve Caplan is a valuable expert in biochemistry but whose study is outside of my research field. His critiques and suggestions to my work ensure its quality meets the standards of a broader audience. I would like to extend a special thank you to Dr. Tahir Tahirov and his laboratory, especially Dr. Andrey Baranovskiy, who provided amazing collaboration opportunity for my project. The major part of my work would not be possible without this collaboration. I would also like to thank Drs. Sergei Mirkin (Tufts University) and Peter Burgers (Washington University in St. Louis) laboratories for sending materials for some of my work.

My mentor, Dr. Youri Pavlov, and my supervisory committee member, Dr. Polina Shcherbakova, have created a unique work environment by joining two independent laboratories together to share resources from materials to knowledge. This environment allowed efficient collaborations and information-exchange on a day-to-day basis. Youri has had a great impact on me that beyond just the scientific aspect. I have learned not only how to conduct scientific projects, present the data, and developed my critical thinking and writing skills, but also how to be a better person. I would like to express my

deep gratitude for his generous support and guidance over the years. I only hope that I have contributed a fraction as much to him and his lab.

Finally I would like to thank my parents who gave me life and have raised me and educated me during my childhood. All my friends who have helped me to reveal myself are extremely valuable. UNMC is a magical place where I met the love of my life, Xiaolin Zhou, whom became my wife in my third year here. This achievement has really made my journey of my Ph.D. study very special. I am fortunate enough to marry someone with whom I share the same life goals and turns out to be my best friend. No words can describe my gratitude but simply a “thank you”.

ABSTRACT

During eukaryotic replication primase•polymerase α (prim•polα) complex synthesizes *de novo* chimeric primers composed of about 10 nt RNA and 20 nt DNA, which are subsequently extended by main replicative DNA polymerases (pol), polε and polδ, on leading and lagging strands, respectively. It is estimated that prim•polα initiates more than 10 millions of lagging strand Okazaki fragments in human genome in each replication cycle. A concerted action of the two active sites, RNA pol and DNA pol, is required to ensure the efficient priming. A remarkable feature of the prim•polα complex is the "programmed" synthesis of the chimeric primer, where the lengths of the RNA and DNA parts are tightly regulated. It is likely achieved by emerging intrinsic structural features of the complex and components of replication fork. To get a better understanding of the mechanism and biological importance of priming by the primase•polα, we utilized biochemical and genetic approaches to examine the protein-protein interactions, *de novo* synthesis and primer extension by prim•polα and the genome stability in primase mutants.

A direct interaction between the N-terminal domain of the human primase accessory subunit (p58N) and the C-terminal domain of the polα (p180C) catalytic subunit was found. The function of the C-terminal domain

of primase containing Fe-S cluster and linker connecting it with p58N in the regulation of primase and polα synthesis was revealed. A novel interaction between the C-terminal domain with the 5' triphosphate group of the RNA primer as well as the phosphodiester backbone of the template at the primer/template junction defines the length of the RNA primer, and the position where polα synthesis starts. We describe two mechanisms of decrease of apparent processivity of polα induced by divalent metal ions. The increased genomic instability in yeast mutants defective in primer initiation during Okazaki fragment synthesis led to a hypothesis on mutation-prone Okazaki fragment maturation when priming is delayed.

LIST OF ABBREVIATIONS

7DdATP	7-Deaza-dATP
AEP	archaeo-eukaryotic primase
CMG	Cdc45-MCM-GINS complex, active eukaryotic helicase
CTD	C-terminal domain
DTT	Dithiothreitol
fission yeast	*Schizosaccharomyces pombe*
MCM	Minichromosome maintenance factor, historic name for hexameric part of eukaryotic helicase
MMR	mismatch repair
p180	human DNA polymerase α catalytic subunit (in yeast encoded by*POL1* gene)
p180ΔN-core	human DNA polymerase α catalytic subunit without the N-terminal unstructured region
p180ΔN•p78	human DNA polymerase α dimer
p180C	human DNA polymerase α catalytic subunit C-terminal domain
p49	human primase catalytic subunit
p49•p58	human primase dimer

p49•p58•p180ΔN•p78	purified human primase DNA polymerase α tetramer
p58	human primase accessory subunit
p70	human DNA polymerase α accessory subunit
PCNA	proliferating cell nuclear antigen
PMSF	phenylmethylsulfonyl fluoride
pol	polymerase
polα	DNA polymerase α (catalytic sunbunit is encoded by the *POL1* gene in yeast)
polδ	DNA polymerase δ (catalytic sunbunit is encoded by the *POL3* gene in yeast)
polε	DNA polymerase ε (catalytic sunbunit is encoded by the *POL2* gene in yeast)
polζ	DNA polymerase ζ (catalytic sunbunit is encoded by the *REV3* gene in yeast)
prim	primase
prim•polα	Eukaryotic primase DNA polymerase alpha complex
RF-C	replication factor C
RPA	replication protein A
SsoPriSL	*Sulfolobus solfataricus* primase

TNR	Tri-nucleotide repeats
tri-P	triphosphate
yeast (or budding yeast, bakers yeast, *S.cerevisiae*)	*Saccharomyces cerevisiae*
Y2H	yeast-two-hybrid system for analysis of protein-protein interactions
YPDAU	yeast medium contain yeast extract peptone dextrose with adenine and uracil

Table of Contents

CHAPTER 1: INTRODUCTION - DNA polymerase alpha and eukaryotic DNA replication 6

1.1 The requirement of RNA primers during replication initiation. 7

1.2 DNA polymerase alpha is specialized enzyme for initiation of DNA synthesis de novo in eukaryotic cells. 12

1.3 Dissertation Overview 25

CHAPTER 2: Materials and methods 27

2.1 Protein-protein interactions between subunits of human primase-polα 28

2.1.1 Construction of plasmids that express human DNA prim•polα genes for Y2H assay. 28

2.1.2 Y2H assay to detect protein-protein interaction 29

2.1.3 Construction of plasmids that express human DNA prim•polα genes for over-expression in E.coli and pull-down assay 30

2.1.4 Induction of gene expression in bacterial cultures 31

2.1.5 Nickel-iminodiacetic acid (Ni-IDA) Pulldown Assay 31

2.2 De novo primase activity assay. 33

2.2.1 Primers and template used in de novo primase activity and primase- polα primer extension assays were purchased from IDT Inc., Coralville, Iowa 33

2.2.2 Primer and template preparation and purification 37

2.2.2.1. 5’ end labeling reaction using 32P-γ-ATP 37

2.2.2.2. Purification of labeled primers using C-18 column 37

2.2.2.3. Purification of non-labeled templates or fluorescent-labeled primers using denaturing PAGE and C-18 column..... 37

2.2.3 Primase Assay (de novo synthesis of RNA primers on single-stranded templates)..... 38

2.2.4. Primer Extension Assay by DNA pols using fluorescent- or 5'^{32}P- labeled primers..... 39

2.2.5 Primer Extension Assay (incorporation of α-^{33}P-labeled nucleotide triphosphates)..... 40

2.3. Yeast as a model organism to study primase-polα function during replication..... 41

2.3.1. Saccharomyces cerevisiae strains and plasmids..... 41

2.3.2. CAN1 forward mutation assay and fluctuation analysis for determination of mutation rates..... 42

2.3.3 Measurement of the $(GAA)_{100}$ tri-nucleotide expansion in pri2-2 strain..... 43

CHAPTER 3: Primase structure and function: primase counting and switching during primer synthesis..... 46

3.1 Introduction..... 47

3.2. Results..... 48

3.2.1. The C-terminal domain (CTD) of the catalytic subunit of human polα interacts with the N-terminal part of the large subunit of primase..... 48

3.2.2. The role of polα in regulating primase activity..... 54

3.2.3. The role of dATP in regulating primase activity..... 58

3.2.4 The C-terminal domain of polα regulates its DNA polymerase activity..... 61

3.2.5. Primase and polα activities in a quaternary prim•polα complex on poly-dT template 64

3.2.6. Recapitulation of the key observations from 3.2.3 and 3.2.4 using ^{32}P-labeled primers 67

3.2.7 The importance of the C-terminal domain of primase large subunit and the linker that attach it to the N-terminal domain in primase synthesis de novo. 69

3.2.8. The C-terminal domain of p58 subunit interacts with the 5' triphosphate (tri-P) group of the RNA primer during primer extension and thus determines what number of nucleotides primase synthesizes. 79

3.2.9. Primase to polα switch in the presence of polα and dNTP 88

3.3 Discussion 90

CHAPTER 4: Interplay between divalent metal ions and substrates during DNA synthesis by polymerase α and other DNA polymerases. 95

4.1. Introduction 96

4.2. Results 102

4.2.1. Polα preferentially uses RNA primers and synthesizes only around 20 nt on poly-dT_{70} template 102

4.2.2. $Mg^{2+}$and Mn^{2+} -induced barrier to polα progression simulates the effect of "counting" of the number of nucleotides in the product on the poly-dT_{70}. 107

4.2.3 Mg^{2+}-induced restraining of pol activity is relieved when synthesis occurs in the presence of 7-Deaza-dATP. 113

4.2.4. Mg^{2+}-induced poly-dT template-specific stalling is characteristic of different DNA pols. 115

4.2.5. Zn^{2+} -catalyzed polymerase reactions. 119

4.3. Discussion 130

4.3.1. Structure of DNA polymerase substrates, metal ions and pol reactions... 130

4.3.2. Dynamics of metals in the polymerase active site and the effect of Zn^{2+}. 132

CHAPTER 5: Polα integration into replication fork: preliminary results and future directions..... 136

5.1. How does polα stop synthesis?..... 137

5.1.1. Background..... 137

5.1.2 Exploration of the self-counting by polα. 138

5.1.3. Approaches to delineate the size of primers synthesized by polα and examine the switch to main replicative pols. 149

5.2 Genome instability induced by defect of prim•polα and proposed function of prim•polα in double-strand break repair 152

5.2.1. Background..... 152

5.2.2. Preliminary results: Malfunction of primase induces genome instability in yeast 154

5.2.2.1 CAN1 forward mutagenesis assay..... 154

5.2.2.2 Tri-nucleotide expansion in pri2-2 cells 162

5.2.3. Proposed mechanism for pri2-2 induced genome instability..... 165

5.2.4 Polα fidelity depends on the presence of free hydroxyl group at the 2' carbon (deoxyribose vs ribose) of the nucleoside monophosphate 168

Reference List..... 171

CHAPTER 1: INTRODUCTION - DNA polymerase alpha and eukaryotic DNA replication

1.1 The requirement of RNA primers during replication initiation.

DNA replication is a fundamental biological process to store and transmit genetic information. DNA molecules adopt double helical structure (1) and are replicated semi-conservatively (2) by a specialized class of enzymes called DNA polymerases (pols), capable copying template DNA using preformed primers. DNA synthesis in living organisms is almost universally initiated by *de novo* synthesis of RNA primers. There are only a few exceptions. Mammalian primpol and the heterodimeric archaeal *Sulfolobus solfataricus* (Sso) primase are two known primases that can use both ribonucleotide triphosphate (rNTP) and deoxyribonucleotide triphosphate (dNTP) to initiate primer synthesis (3,4). However, these two enzymes are not the main primases in their respective organisms. In mammalian cells, a complex of primase with DNA polymerase α (prim•polα) is used exclusively for initiation of DNA synthesis during chromosomal replication (following section), whereas primpol is not essential (5). The archaeal heterodimeric eukaryotic-like primases coexist with orthologs of bacterial DnaG-like primase that uses exclusively rNTPs (6,7). This type of primases can synthesize DNA up to 3 kb, and hypothetically function during DNA repair (7). It is not known which primase is normally used in archaeal DNA replication. Another exception is the reverse transcription by retroviruses (e.g. HIV) and retrotransposons (long terminal repeats (LTR) and non-LTR type (e.g. telomerase)), where either tRNA or the 3' chromosomal DNA ends are utilized to serve as the primer for DNA synthesis (8).

There are two possible reasons why genome replication requires specially dedicated primase and starts with RNA. The first reason is purely structural and becomes evident from the mode of interaction of DNA pols with DNA. All known DNA pols adopt a

conformation resembling right-hand with functional domains called palm, fingers, and thumb. In addition, most replicative DNA polymerases also have additional 3'-5' exonuclease domain for proofreading activity ((9,10) Figure 1.1). The polymerase active site locates at the highly conserved palm domain, where both template DNA and 3' -OH of the growing DNA strand make contacts with protein residues, thus providing the information on the identity of next nucleotide that could be incorporated. The fingers domain is adjacent to the palm domain making contacts with the incoming dNTP and undergoes a large conformational change when the incoming nucleotide is positioned near the metals, template, and the 3' end of the growing strand in the active site. Both template and growing strand upstream of the 3'-hydroxyl group interact with the thumb domain, and this arrangement determines either the editing or polymerization modes of the enzyme ((11); Figure 1.2). For example, thumb, palm and exonuclease subdomains in yeast polε make close contacts with at least 11 bases behind the 3'OH group ((12); Figure 1.3). **Therefore, a single deoxynucleotide with a free 3'OH group (*de novo* DNA synthesis) is not enough to provide a stable ternary complex with pol and template to activate the synthesis**. DNA polymerases evolved to bind to template with a primer of certain length, On the other hand, RNA polymerases can form stable structures with single or di-nucleotides, which provide a more stable foundation for further extension (13). Still, in the primase reaction products *in vitro* many di-nucleotides remain unextended, which is a sign of aborted synthesis due to some unstable complexes (14).

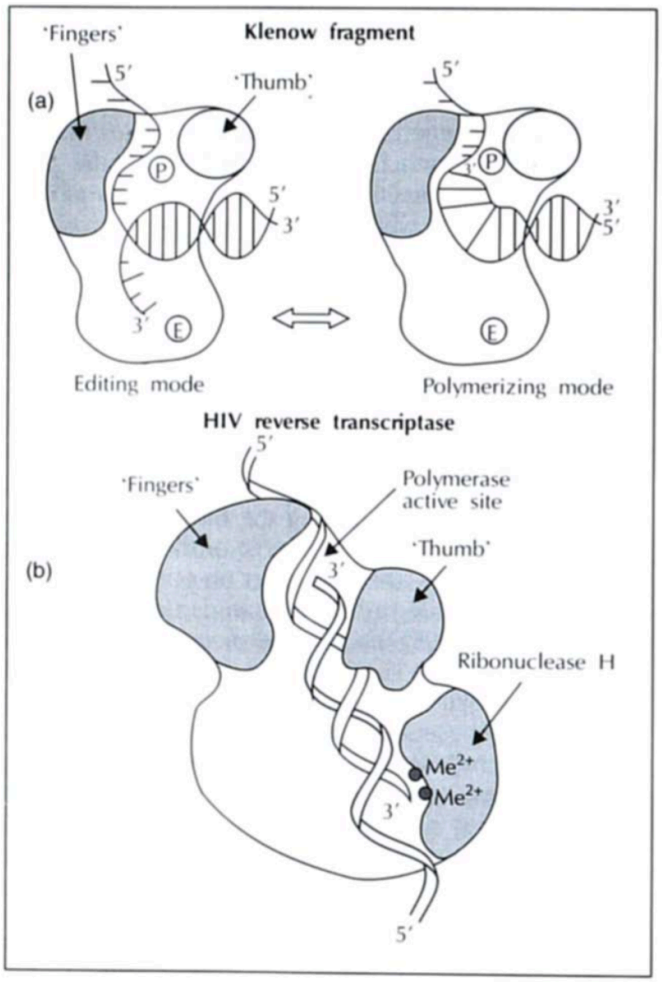

Figure 1.1, **DNA synthesis and position of primer template in polymerase and exonuclease active sites in Klenow fragment (a) and in polymerase site of Reverse Transcriptase (b) (9).** It is noticeable that the direction of DNA synthesis relative to the conserved polymerase catalytic subdomain is the same in both polymerases. P and E mark the locations of the Klenow fragment's polymerase (palm) and 3',5'-exonuclease active sites, respectively. The 3',5'-exonuclease (E) removes wrong misincorporated nucleotides as sensed by the thumb domain binding to the upstream growing strand. Any factor that destabilizes duplex DNA (which contacts thumb), such as a mismatched base pair, will favor the switch to editing complex and excision of the nucleotide.

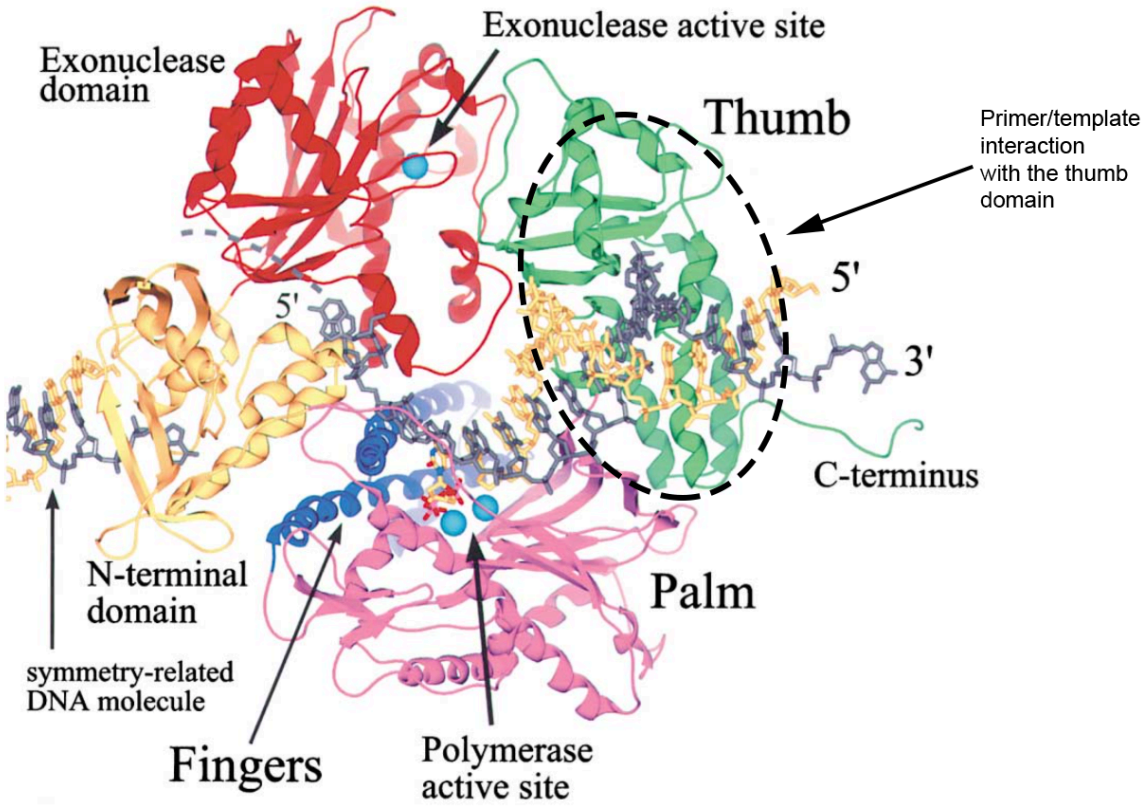

Figure 1.2. **X-ray crystal structure of the B-family DNA polymerase RB69, including N-terminal domain (yellow), exonuclease domain (red), palm (magenta), fingers (blue), and thumb (green), shown as a ribbon representation (11)**. The primer and template strands of the DNA are shown in a stick representation, with the primer (gold) and the template (gray). The two calcium ions bound at the polymerase active site are shown as light blue spheres, along with a calcium ion at the exonuclease active site. The incoming dTTP is shown colored according to atom type, with carbons in gold.

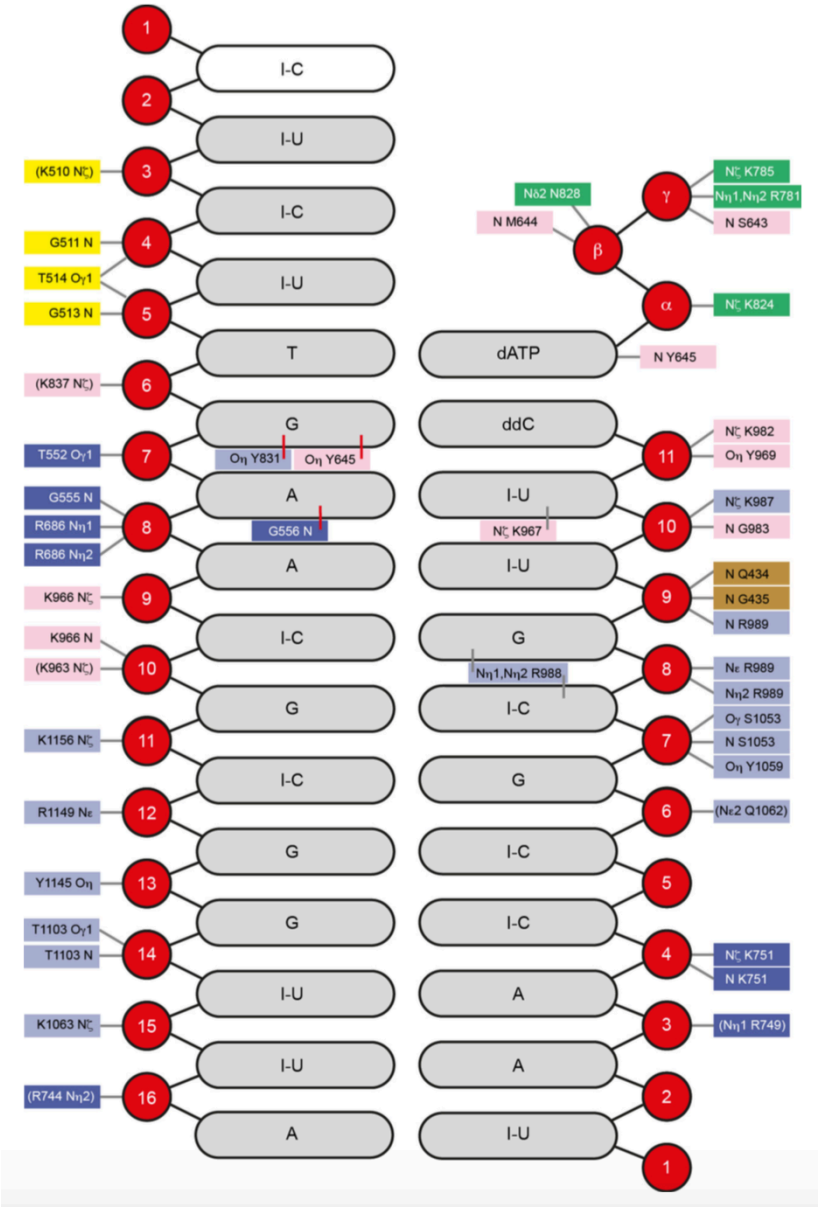

Figure 1.3. **Schematic diagram showing the interactions between yeast pol ε and the DNA primer template (12)**. Residues interacting with DNA are color coded according to the domains they belong to (fingers (green), palm (pink), thumb (light blue), exonuclease (gold) and N-terminal domains (light yellow)) Residues in brackets indicate that these residues have side chains positioned in the vicinity of the DNA with the potential to form direct salt-bridges to the phosphodiester backbone.

The second reason to use of ribonucleotides for priming lies in the kinetics of the reaction. The cellular rNTPs concentrations, necessary for transcription, are usually at least ten-fold higher than the concentrations of dNTPs, and purine (A and G) rNTPs levels are generally higher than pyrimidine (T and C) (15). The formation of the first two nucleotides (di-NT) is the rate-limiting step of primer synthesis. The 5' nucleotide in RNA primer synthesized by primase is a purine (A or G). The second nucleotide is generally a purine too but this is not exclusive and pyrimidine can also be added (16). Therefore making two-base purine RNA is catalytically easier in cells then synthesis of DNA.

1.2 DNA polymerase alpha is specialized enzyme for initiation of DNA synthesis de novo in eukaryotic cells.

In eukaryotes, primase is a two-subunit enzyme that in complex with a two-subunit DNA polymerase constitutes four-subunit primase-polα complex (prim•polα). Along with catalytic subunits of DNA polymerases δ, ε, and ζ, the catalytic subunit of polα belongs to the B-family DNA polymerases, which carry out the major task of accurate nuclear genome replication in eukaryotes (17-21). Polε plays an important role in the assembly of the replisomes at origins (22), whereas prim•polα generates primers *de novo* (23), polδ (24) and polε (25) elongate primers synthesized by polα and participate in bulk DNA synthesis (10,26,27), and polζ is a key player in the synthesis on templates that are difficult to replicate (28,29). The critical essential step of the replication in eukaryotes is extension of the RNA primers, made by primase, by polα.

All B-family polymerases are four-subunit complexes (the latest addition to the group was polζ that shares two accessory subunits with polδ)(30-34), where the largest catalytic subunit has a unique regulatory C-terminal domain binding zinc or iron-sulfur clusters (30,35-37). These C-terminal domains share sequence similarities and are evolutionarily conserved from yeast to humans (30,38). Human polα is composed of a 180-kDa catalytic subunit (p180) and a 70-kDa B subunit (p70) (23)(Figure 1.4). The primase part is composed of a 49-kDa catalytic subunit (p49) and a 58-kDa accessory subunit (p58) (23,39). Two metal binding sites that are located on the C-terminal domain of p180 (p180C) are occupied by Zn atoms in crystal structure in both yeast and human analogs (36,40). When p180C fragment was partially purified from bacteria under anaerobic conditions, it contained a detectable level of iron-sulfur clusters (37), which may be an artificial peculiarity of the heterologous expression in bacteria (30). The p58 primase subunit possesses an evolutionarily conserved, C-terminal four-cysteine motif that coordinates a [4Fe-4S] cluster necessary for the formation and stabilization of the initial di-ribonucleotide of the RNA primer (41-44).

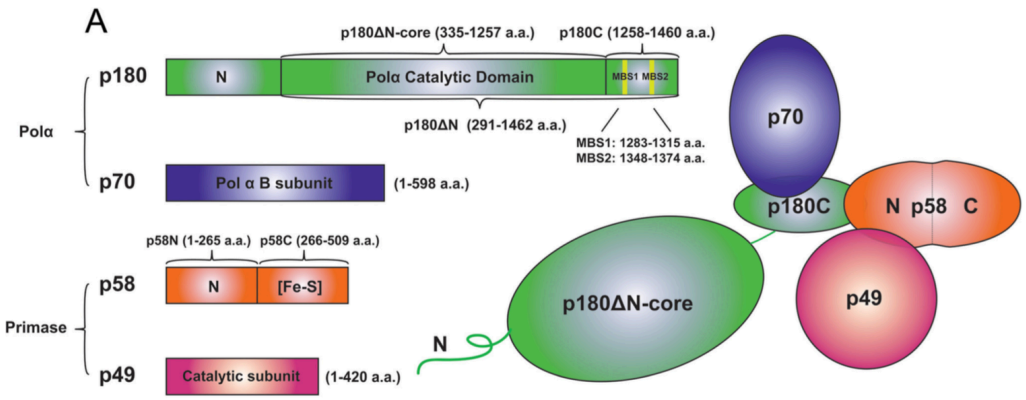

Figure 1.4. **Overall structure of human prim•polα.** *A*, schematic representation of the four-subunit complex, p180 (*green*), p70 (*blue*), p58 (*orange*), and p49 (*red*). The primary amino acids sequence and the domains of each subunit and various recombinant constructs studied in the current work are shown as *stick diagrams on the left*. Metal binding motifs in p180 are marked by *yellow vertical lines* and named metal binding sites MBS1 and MBS2.

Mouse and yeast homologs of the polα p180C domain interact with the B subunit and primase, working as a scaffold to tether the catalytic part of p180, B subunit and primase (45,46). The large interaction interface (4,500 $Å^2$) between the C-terminus of yeast Pol1 and the B-subunit suggests tight contact between two polypeptides (36). The B subunit has an N-terminal helical subdomain, an oligonucleotide-oligosaccharide binding (OB) subdomain and a C-terminal phosphoesterase (PE) subdomain. The N-terminal helical domain can interact with SV40 viral helicase, thus explaining how polα is recruited for viral genome replication (47). The structural information is consistent with the idea that p180C•p70 might tether the prim•polα to the other components of replication machinery (45,48). The B-subunit and C-terminal domain of the catalytic subunits are highly conserved. Alignment of the B-subunits of human polα, δ, and ε as well as archaeal DNA pol II (also the B-family DNA pol) shows the conservation of all three subdomains, except the B-subunit of polδ does not possess the N-terminal helical domain. However, a similar winged helix-turn-helix domain exists in the third subunit of polδ (Figure 1.5), which may fulfill the function of the missing domain in the second subunit (49). Structure and sequence alignment of the polα B-subunit of human and yeast (*S. cerevisiae*) indicates that, despite the sequence identity is only 27%, the subdomains are conserved and structures are highly similar (50). Addition of the polα B-subunit from fruit fly and zebrafish to yeast and human sequence alignment shows an overall 26.3% sequence similarity (Figure 1.6)

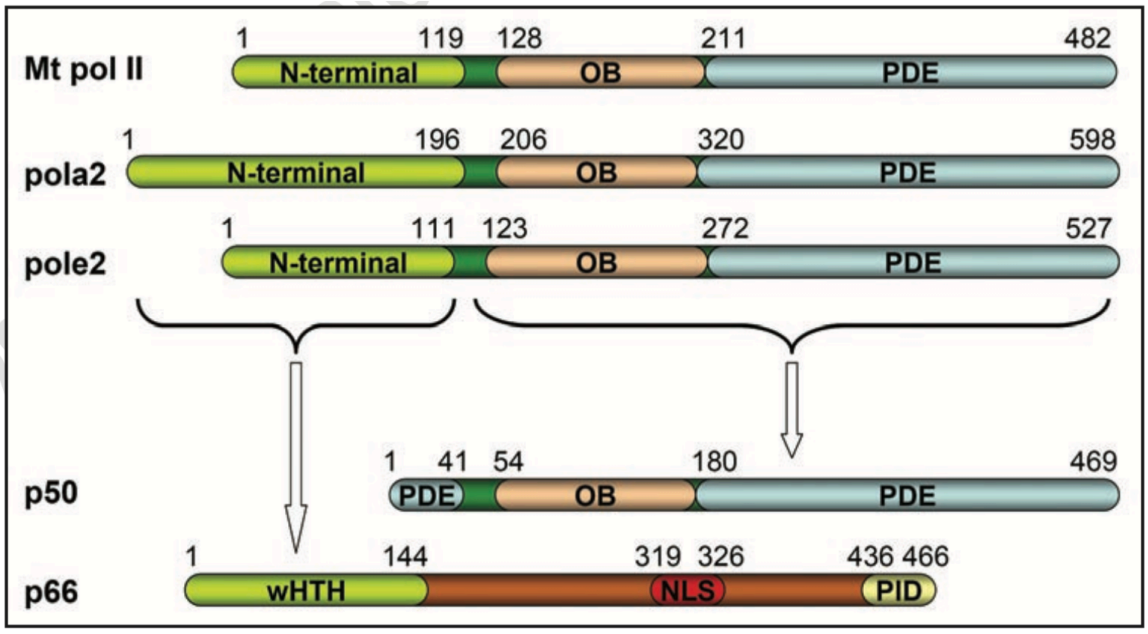

Figure 1.5. **Highly conserved domains of the B family DNA polymerase second subunits (49)**. The subdomains of second subunits of B-family DNA pols are including the archaeal *Methanothermobacter thermautotrophicus* DNA polymerase II (Mt pol II), human polα (pola2), human pol ε (pole2) and pol δ (p50). The third subunit of human Pol δ (p66) contains the winged helix-turn-helix domain similar to the other second subunits of B-family pols.

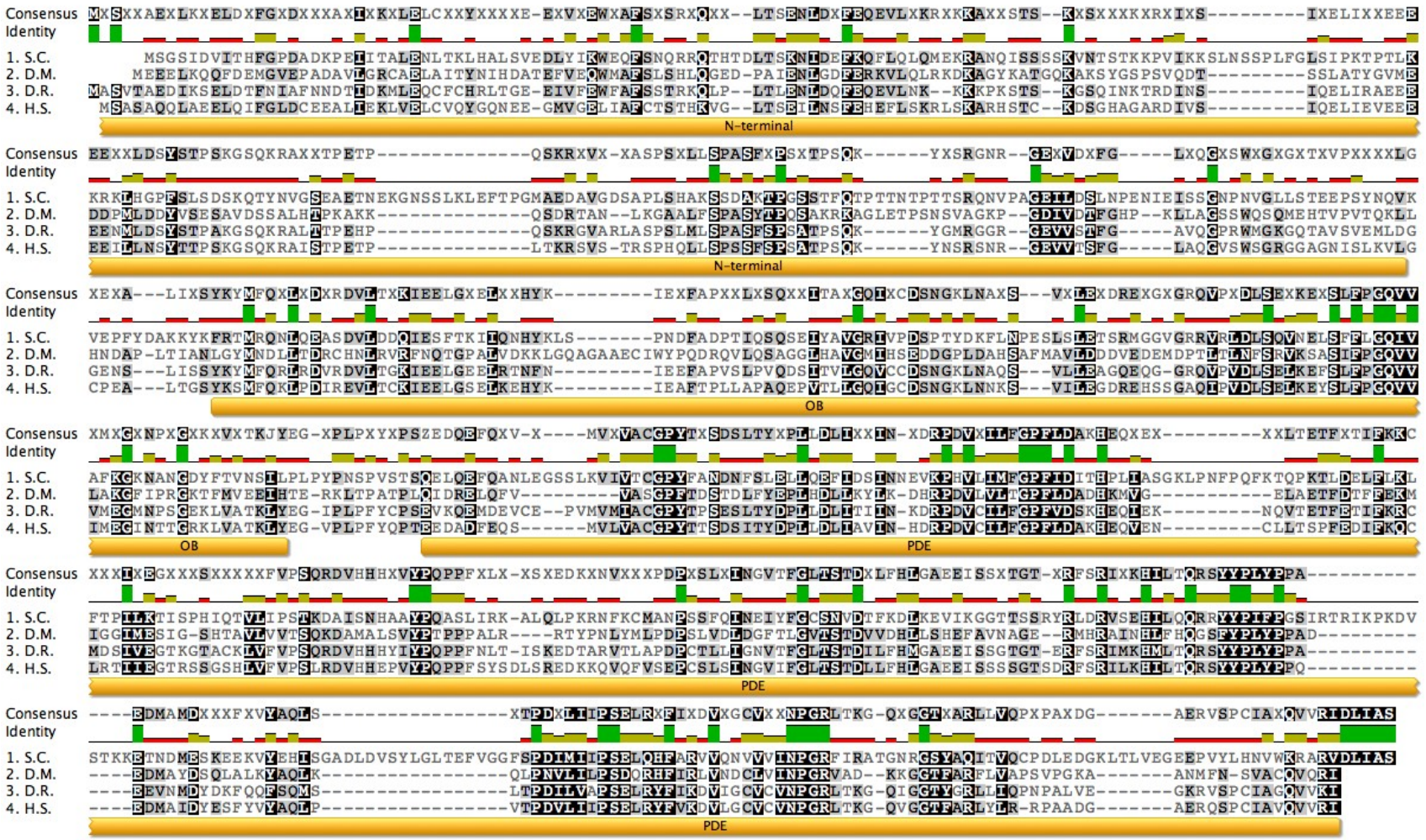
Consensus
Identity
1. S.C.
2. D.M.
3. D.R.
4. H.S.
N-terminal
OB
PDE

Figure 1.6. **Sequence alignments of the yeast, *Drosophila melanogaster*, *Danio rerio*, and human polα B subunits**. The conserved residues are highlighted with black background; similar but not identical residues are highlighted in grey background. Sequences were aligned using clustalx-2.1 software and visualized by Geneious R6 software.

Prim•polα is the only B-family polymerase complex that possesses an RNA polymerase and a DNA polymerase. The knowledge on this enzyme before recent break-through structural discoveries (40) is summarized below. Polα lacks proofreading exonuclease activity, a feature that can facilitate DNA synthesis during transition from RNA to DNA. The synthetic activity of the complex is limited to the synthesis of RNA/DNA hybrids that serve as primers for the synthesis of genomic DNA. During the initiation of DNA synthesis, primase first synthesizes a short RNA primer in a two-phase reaction, the rate-limiting synthesis of dinucleotide, and the subsequent faster, further elongation to reach the length of around ten ribonucleotides (51). Then, polα takes over and extends the primer by approximately 20 nucleotides of DNA. The ability to determine the size of RNA and DNA parts (called "counting") is thought to be an intrinsic property of primase and polα (52,53). This primer is elongated by polδ/polε for synthesis of the bulk of chromosomal DNA. The nature of the replication on the lagging strand requires multiple initiations by the polα-prim, which leads to the formation of 165 bp Okazaki fragments (Figure 1.7A) that correspond to unit size of nucleosomal repeats (54).

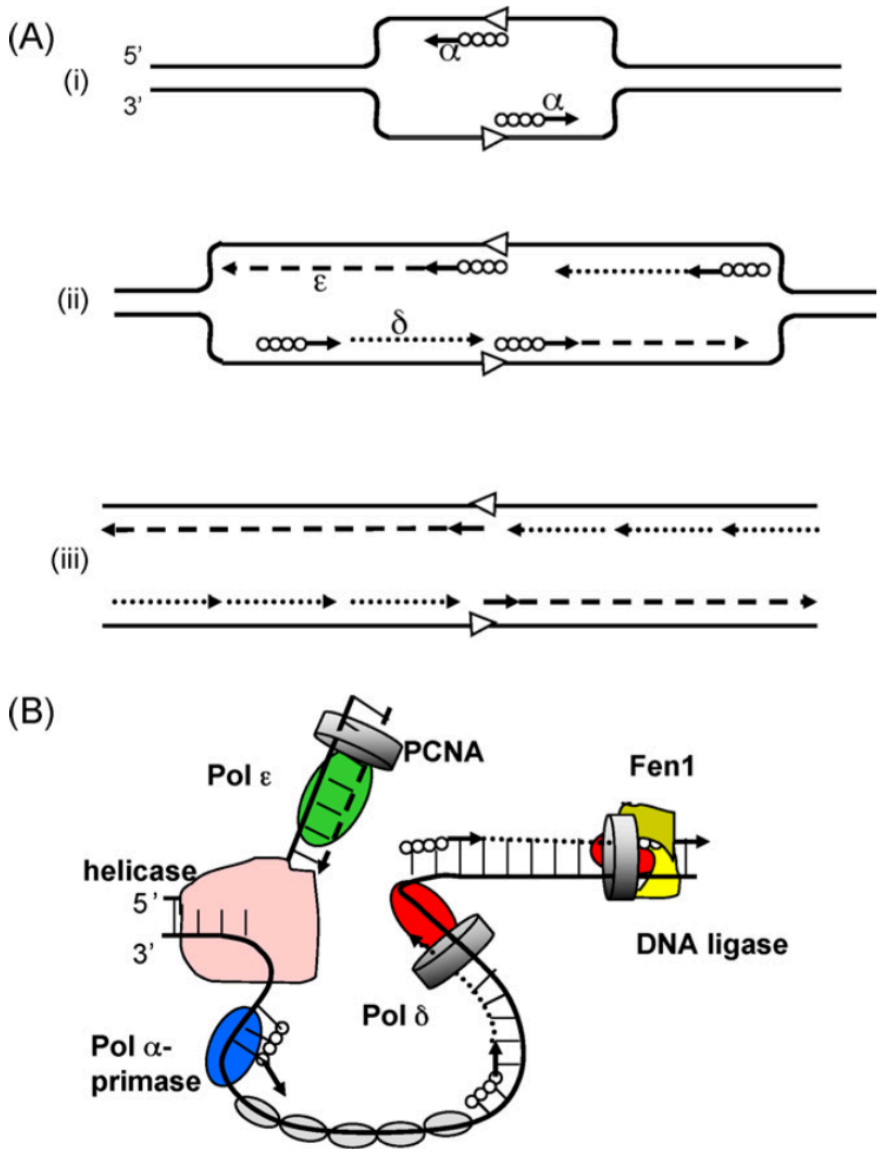
(A)
(i)
5'
3'
α
α
(ii)
ε
δ
(iii)
(B)
Pol ε
PCNA
Fen1
helicase
5'
3'
DNA ligase
Pol δ
Pol α-
primase

Figure 1.7. **Three-polymerase model of replication fork in eukaryotes (27).** (A) Original model of replication fork, proposed by Sugino group (55). Polα start synthesis of short RNA-DNA primers on the leading strand upon origin firing. Then on leading strand the primers are extended by polε. On the lagging strand, polα synthesizes short fragments on the opposite direction of the fork multiple times (forms Okazaki fragments), which are extended by polδ. (B) The currently most widely accepted model of the replicases at eukaryotic replication fork. The model illustrates that the MCM helicase (pink) unwinds the DNA and determines the direction of the fork; Polε (green oval) replicates the leading DNA strand; and Polδ (red oval) replicates the lagging strand; Polα-primase (blue oval) synthesizes RNA–DNA primers (open circles and straight lines); the eukaryotic replication protein A (RPA; gray ovals) covers and stabilizes the single-stranded DNA; the sliding clamp proliferating cell nuclear antigen (PCNA; gray ring) forms complex with Polε and δ to increase polymerase processivity; and the Fen1–DNA ligase complex (yellow) processes and maturates the Okazaki fragments.

Due to the 5' to 3' DNA synthesis replication polarity, the leading strand is co-directional to the active helicase, CMG complex, positioned on this strand and presumably is primed by polα and synthesized by polε, tightly bound to helicase. The lagging strand is replicated in the opposite direction, primed by polα and extended by polδ (Figure 1.7B). Since the lagging strands are constantly primed in the opposite direction in respect of the replication fork movement, the downstream Okazaki fragment extended by polδ encounters the upstream RNA/DNA primer synthesized by primase-polα. Polδ can displace the primers into 5' flaps of various lengths. Depending on the length of the flaps, they will be either removed by Fen1 (short flaps) or Dna2 (long flaps), and subsequently ligated to form a continuous strand of DNA (Figure 1.8). Stodola and Burgers (56) showed that the activities of polδ and Fen1 are sufficient to process the RNA primer of the earlier Okazaki fragment, in the absence of RNase H. During a single round of nuclear DNA replication in *S. cerevisiae* ~100,000 Okazaki fragments are made and maturated (17). Despite of the processing and maturation of Okazaki fragments, approximately 1.5% of the *S. cerevisiae* genome contains the traces of the DNA synthesized by polα (57). Human genome contains approximately 3 billion base pairs (3 billion bases of each leading and lagging strand during replication). If the size of Okazaki fragments in humans is the same as in yeast, approximately 90 million bases in human genome are traces of DNA synthesized by polα.

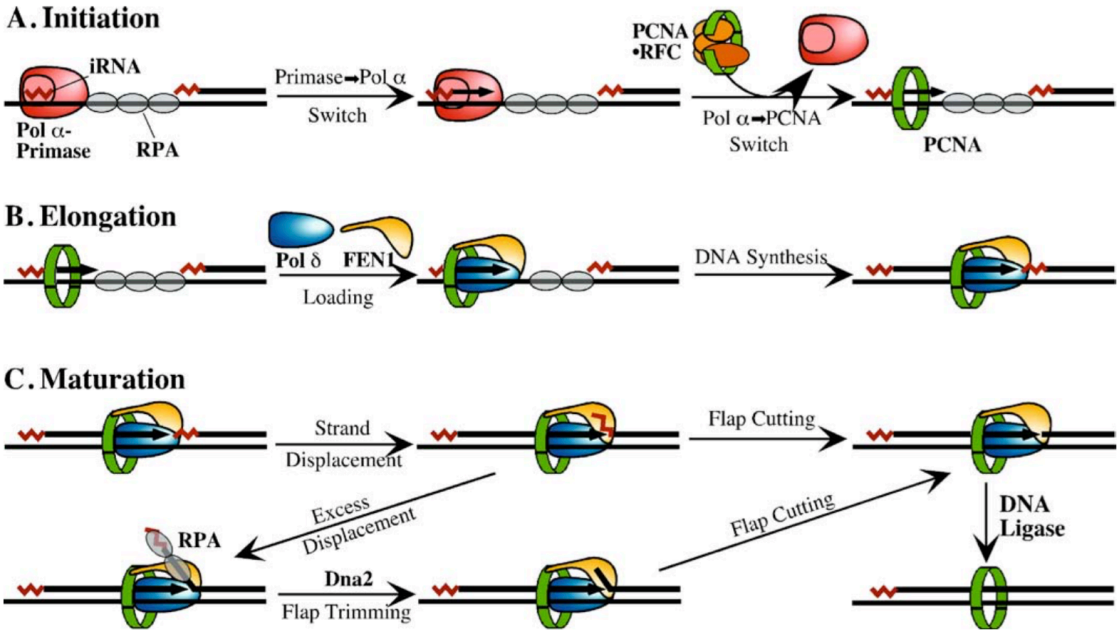
A. Initiation
iRNA
Pol α-
Primase
RPA
Primase➡Pol α
Switch
PCNA
•RFC
Pol α➡PCNA
Switch
PCNA
B. Elongation
Pol δ
FEN1
Loading
DNA Synthesis
C. Maturation
Strand
Displacement
Flap Cutting
Excess
Displacement
RPA
Dna2
Flap Trimming
Flap Cutting
DNA
Ligase

Figure 1.8. **Replication stages of the lagging strand.** Since the lagging strand goes to the opposite direction of the replisome, the downstream Okazaki fragment encounters the upstream fragment from the 5' direction. (A) Before the synthesis of the downstream, the region that unwound by the helicase is temporarily covered by RPA. Polα-primase competes with the RPA for template binding and initiates the RNA-DNA primer synthesis. The primer synthesized by polα is extended by polδ that is loaded to PCNA by RFC. (B) During elongation, FEN1 is loaded together with Polδ on PCNA. (C) Polδ displaces the encountered upstream Okazaki fragment, which leaves the flap to be processed by RNase H and FEN1. Longer flaps are stabilized by RPA that inhibits FEN1 but promotes the Dna2 exonuclease activity. The trimmed flaps are processed by FEN1. Then DNA ligase seals the nick (17).

1.3 Dissertation Overview

Although eukaryotic prim•polα (including human) has been studied for more than 20 years, many details of the operations of this enzymatic complex at the replication fork were still not understood. For example, it was still enigmatic how primase and polα work together during the RNA-DNA primer synthesis. **In chapter three**, we describe genetic and biochemical studies to identify the interacting parts of primase and polα domains. The study provided insights on how primase and polymerase activities could be regulated. Several primase and polymerase activity assays were designed to address different questions. In the *de novo* primer synthesis assays with prim•polα variants possessing combinations of catalytic and regulatory domains we examined how polα might regulate primase processivity and activity. The interaction between primase regulatory domain and the triphosphate of the first ribonucleotide in nascent RNA primer appears to serve as an important mechanism of primase synthesis and counting the number of nucleotides in the RNA primer. **Chapter four** is dedicated to description of two distinct roles that divalent metal cations play in DNA synthesis by polα in comparison to other DNA pols. On DNA templates with repetitive sequence, Mg divalent ions, normally catalyzing the reaction, promote the formation of triplex structure and cause DNA pols stalling. Experiments with polymerase reaction catalyzed by another divalent ion, Zn^{2+}, revealed a critical step of ion removal within pol reaction cycle. In **Chapter five** we present some new preliminary data, discuss possible outcomes of the whole work and future directions. We outline the design of new experiments to study switches between polα and pol δ or ε. Based on preliminary yeast genetics data, we

present hypothetical mechanisms of induction of genome instability by defective primase function.

CHAPTER 2: Materials and methods

This chapter describes methodology used in biochemical analysis and yeast genetics studies. The main goal of this work is to analyze the structure-related function of primase and polα in the *de novo* synthesis of RNA primer and its further extension. First, protein-protein interactions between four subunits of primase-polα were analyzed using yeast-two-hybrid (Y2H) and bacterial over-expression pull-down assay. Then *de novo* synthesis by human primase was analyzed using purified human primase with several polα variants and ^{32}P or ^{33}P radiolabeled ribonucleotides. Primase activities during extension were analyzed using either fluorescent-labeled primers or unlabeled primers in reactions containing radiolabeled ribonucleotides. Polα activities were analyzed by either coupled with primase *de novo* synthesis, or by extension of pre-existing RNA or DNA primers. Yeast primase-polα mutants were made to study the phenotypic changes *in vivo* to get insights into biological roles of primase using mutation accumulation and tri-nucleotide repeat expansions as the endpoints.

2.1 Protein-protein interactions between subunits of human primase-polα

2.1.1 Construction of plasmids that express human DNA prim•polα genes for Y2H assay.

Material: The cDNAs for the p49 (encoding for 420 amino acids, (aa)) and p58 (509 aa) subunits of human primase cloned into pETDUET1 vector (pETDUET1-p49-p58His6 plasmid) and human polα B subunit (598 aa) and C-terminal of *POLA1* encoding for (p180C, aa 1265-1462 aa) and human polδ subunit p66 cloned into pColaDuet1 (pColaDuet1-p70His6-SUMOp180C-p66N) were provided by Dr. Baranovskiy from from Dr. Tahirov laboratory.

For Y2H assay, I amplified the coding sequences (cs) of all four genes of human

primase-polα subunits by PCR using pETDUET1-p49-p58His6 and pColaDuet1-p70His6-SUMOp180C as templates with attached sequences of restriction sites at both ends. Then the four amplified PCR products were ligated into the pGADT7 and pGBKT7 vectors (eight constructs total; Clontech, Mountain View, CA) containing *TRP1* and *LEU2* selection markers, respectively.

2.1.2 Y2H assay to detect protein-protein interaction

The yeast strain AH109 with three reporter genes, *HIS3*, *ADE2*, and *lacZ*, was a generous gift from Dr. Paul Sorgen laboratory at UNMC. AH109 cells were transformed by combinations of the plasmids constructed in 2.1.1. The co-transformations by plasmids with cs-p49/cs-p58 and cs-p180C/cs-p70 combinations as well as the murine cs-p53/cs-SV40 large T-antigen served as positive controls. The co-transformations by each construct with an empty vector served as negative controls. The cells were allowed to grow three days on Synthetic Complete drop-out plates lacking leucine and tryptophan ($SC\text{-}Leu^{-}Trp^{-}$). Grown colonies of transformants were replica-plated on SC plates additionally lacking histidine ($SC\text{-}Leu^{-}Trp^{-}$ His), adenine ($SC\text{-}Leu^{-}Trp^{-}Ade^{-}$), or both ($SC\text{-}Leu^{-}Trp^{-}$ $His^{-}Ade^{-}$). Growth of colonies on each plate was evaluated after 3 days of incubation at 30 °C. Activation of both *HIS3* and *ADE2* reporters was recorded as an interaction if 80% of the colonies with prey and bait genes were His^{+} and Ade^{+} (the single activation of the *HIS3* reporter produces many "false positives"; therefore, only the concomitant Ade^{+} phenotype suggests that proteins under study really interact).

2.1.3 Construction of plasmids that express human DNA prim•polα genes for over-expression in E.coli and pull-down assay.

Several expression constructs were made for bacterial over-expression (Table 2.1).

Table 2.1. **Bacterial expression plasmid constructs used for studies of protein-protein interactions of human prim•polα parts.**

Name	Coding sequence (cDNA)	Backbone
pE1	*cs-p58-HIS$_6$*, *cs-SUMOp180C*	pETDuet-1
pE2	*cs-p58-HIS$_6$*	pETDuet-1
pE3	*cs-p49, cs-p58*	pETDuet-1
pE4	*cs-p49, cs-p58N (encoding amino acids 1-265)*	pETDuet-1
pE5	*cs-p49, cs-p58C (encoding amino acids 266-509)*	pETDuet-1
pC1	*cs-p70-HIS$_6$*, *cs-SUMOp180C*, *cs-p66N*	pColaDuet-1
pC2	*cs-p70-HIS$_6$*	pColaDuet-1
pC3	*cs-SUMOp180C*	pColaDuet-1

The *cs-p58-HIS$_6$* and *cs-SUMO-p180C* were cloned together into the MCS1 and MCS2 of pETDuet-1 (vector named as pE1, Table 2.1), respectively, using a two-step insertion method (58). A single insertion of *cs-p58-HIS$_6$* (pE2) into pETDuet-1 served as a control. Non-tagged *cs-p49* and *cs-p58* were cloned into the MCS1 and MCS2 of pETDuet-1(pE3), respectively. The *cs-p58N* (encoding amino acids 1-265) or *cs-p58C* (amino acids (aas) 266-509) was cloned into the MCS2 of the pETDuet-1 that contains *cs-p49* at MCS1. To obtain a pColaDuet-1 vector producing only SUMO-p180C (for negative controls) a premature stop-codon was introduced into the *cs-p70-HIS$_6$*.

2.1.4 Induction of gene expression in bacterial cultures

The pETDuet-1 and pColaDuet-1 constructs were introduced into the Rosetta-2 (DE3) cells by transformation and selected on the LB with antibiotics (ampicillin /kanamycin /chloramphenicol) medium. Individual colonies of transformants were inoculated in 5 ml LB broth with antibiotic for 16 hour growth at 37 °C (overnight). Then 300 µl of overnight culture were inoculated into 100 ml of LB broth and the cultures were allowed to grow to OD600 of 0.8. Then cultures were cooled on ice, transferred to 25 °C shaker. 1 mM of IPTG was added to each culture and they grew for another 16 hours.

2.1.5 Nickel-iminodiacetic acid (Ni-IDA) Pulldown Assay

After induction of gene expression in bacterial cultures (2.1.4), cells were harvested and kept in aliquots at -80 °C. Cells were disrupted in tubes immersed in ice-chilled water by sonication in lysis buffer containing 20 mM Tris (pH 7.8), 0.15 M NaCl, 10 mM KH_2PO_4, 3% glycerol, 3 mM β-mercaptoethanol, 0.5 mM phenylmethylsulfonyl fluoride

(PMSF), and 1 μg/ml leupeptin. After centrifugation, 0.2 ml of cleared lysate (corresponding to a 2.5-ml culture volume) was incubated for 1 h with rocking at 4 °C with 10 μl of Ni-IDA resin. The resin was washed once with 0.2 ml of lysis buffer and 2 times with 0.2 ml of the lysis buffer containing 0.5 M NaCl. The bound proteins were eluted by 30 μl of 0.3 M imidazole in the lysis buffer (pH 7.7). Proteins of bacterial lysates and samples eluted from Ni-IDA resin were separated by 12% SDS-PAGE and detected by Coomassie Blue (R250) staining or Western blotting using the Mini-PROTEAN Tetra cell system (Bio-Rad). Anti-His monoclonal antibody and anti-SUMO monoclonal antibodies (6G2A9 and 4G11E9, respectively; GenScript, Piscataway, NJ) were used to detect His_6-tagged human p58 and p70 and SUMO-tagged p180C, respectively.

2.2 De novo primase activity assay.

2.2.1 Primers and template used in de novo primase activity and primase- polα primer extension assays were purchased from IDT Inc., Coralville, Iowa.

Table 2.2 DNA **Templates used in *de novo* primase activity assay**

Name	Sequence
Poly-dT70	$(dT)_{70}$
35a2	5’ GCG AAG GAG AAG CAG AGG AGA GGA GGATAAAAAAA
60a5	5’ GGA GAG AAG GAG CAA GGA GAG GAA GAC GAA GGA GAA GCA GAG GAG AGG AGG ATAAAAAAA
TA15	5’ AAAAAAAAAAAAAAATAAAAAAA
GA6	5’ AAAGAGAGAGAGAGATAAAAAAA

Table 2.3 **DNA Templates used in primer extension assay**

Name	Sequence
Poly-dT70	$(dT)_{70}$
73a	5’$(T)_{35}$AGCGTCTTAATCTAAGCACTCGCTATGTTTTCAAGTTT
73b	5’GTCTGGAATGATGAAGATTACTAGTGAAGATTCTGAGCGTCTTAATCTAAGC ACTCGCTATGTTTTCAAGTTT
73 C-rich	5’ CCTAA$(CCCTAA)_8$CTCGCTATGTTTTCAAGTTT
73 G-rich	5’ $(TTAGGG)_9$TCGCTATGTTTTCAAGTTT
46A1	5’ GATTCACACGACTAGCACACTAAGCACTCGCTATGTTTTCAAGTTT
60a7	5’GTGAGAGAAGGAGAAGGAGAGGAAGAGAAGGAGAAGAGGAGAGAAACGC CGCCAAAAAAA
60a10	5’GCGAGAGAAGGAGAAGGAGAGGAAGAGAAGGAGAAGAGGAGACCCGACC AGCCAAAAAAA
53a1	5’GTGAGAGAAGGAGAAGGAGAGGAAGAGAAGGAGAAGAGGAGAGAAACGC CGCC
33a5	5’GGAGTACGAATCAGTTAGACGCCGCCAAGAATA
22a6	5’ ATACAACCCGCACGCCAACATA
25a3	5’ ATACTATCCCGACCAGCCAATACAA
59a	5’GTGAGAGAAGGAGAAGGAGAGGAAGAGAAGGAGAAGAGGAGAG**AA**CGCC GCCAAAAAAA
58a	5’GTGAGAGAAGGAGAAGGAGAGGAAGAGAAGGAGAAGAGGAGAG**A**CGCCG CCAAAAAAA

18a1	5 -AAACACCGAGCCAACATA
12a1	5 -AAACACCGAGCC
60a9	5’GCGAGAGAAGGAGAAGGAGAGGAAGAGAAGGAGAAGAGGAGATCCGACCAGCCAAAAAAA
53a2	5’GCGAGAGAAGGAGAAGGAGAGGAAGAGAAGGAGAAGAGGAGATCCGACCAGCC
59a2	5’GCGAGAGAAGGAGAAGGAGAGGAAGAGAAGGAGAAGAGGAGATCCGCACGCCAAAAAAA
52a2	5’GCGAGAGAAGGAGAAGGAGAGGAAGAGAAGGAGAAGAGGAGATCCGCACGCC

Table 2.4 **Primers used in extension assay**

-TYE_{665}: is the fluorescent label (Cy5 equivalent); PPP is the triphosphate group

Name	Sequence
Poly-dA15	5'TYE_{665} -$(dA)_{15}$
Poly-rA15	5' TYE_{665}-$(rA)_{15}$
Hetero-DNA	5' TYE_{665}-CTTGAAAACATAGCGA
Hetero-RNA	5' TYE_{665}-rCrTrTrGrArArArArCrArTrArGrCrGrA
5' tri-P6	5'PPP-rGrGrCrGrGrC
P6	5'GGCGGC
5' tri-P7	5' PPP-GGCUCGG
P7	5' GGCUCGG
5'Tri-P9	5'PPP-rGrGrCrGrUrGrCrGrG
5'Tri-P10	5'PPP-rGrGrCrUrGrGrUrCrGrG
P10	5'-rGrGrCrUrGrGrUrCrGrG

2.2.2 Primer and template preparation and purification

The labeled primers and templates (non-labeled) were carefully purified before future use.

2.2.2.1. 5' end labeling reaction using 32P-γ-ATP

To label the primers, 50 µl of reaction containing 50 pmol of each primers were added to reaction containing 50 pmoles of ^{32}P-γ-ATP, 20 units of T4 Polynucleotide Kinase (T4-PNK) in 1X T4-PNK reaction buffer on ice. Then reactions were started by incubation at 37 ºC for 1 hour. Then reactions were stopped by adding EDTA to a final concentration of 20 mM on ice.

2.2.2.2. Purification of labeled primers using C-18 column

The labeled oligonucleotides were dissolved in 2 ml TE buffer (10 mM Tris-HCl, 1 mM EDTA, pH 8.0] with 150 mM NaCl and purified using Waters C18 Sep-Pak cartridges. The cartridges were prepared by flushing them with 10 ml of methanol and subsequently rinsing the cartridge two times with 10 ml of water, before passing the oligonucleotide solutions slowly through the cartridge. The flow-through was collected and passed through the cartridge two more times. The column was then washed with 10 ml of water, and a small amount of air was pushed through the cartridge to remove any excess water. The labeled single-stranded primers were then eluted with 1.2 ml of 60% methanol and dried in a Savant Speed Vac.

2.2.2.3. Purification of non-labeled templates or fluorescent-labeled primers using denaturing PAGE and C-18 column.

The oligos were suspended in solutions contain 50% formamide, 2.5 mM EDTA, and 0.01% Orange-G of concentration of 400 µM. 2 pmol of each oligo were loaded to 14-18% Urea-PAGE gel (depending on the oligo size) and ran 3 hours at 2000 V. After the

run, gel cassette was disassembled to uncover the gel for slicing out the oligo band. The fluorescent-labeled primers were visible by naked eye since the oligos had attached blue dye. The template unlabeled oligos were stained first by GelStar^{TM} Nucleic Acid Gel Stain (Lonza Rockland, Inc., Rockland, ME, USA), visualizing using blue-filtered lamp with orange glass and corresponding parts of the gels were cut out. The gels parts with bands were sliced and chopped into small pieces, placed in 1 to 3 ml of 1x TE buffer, subjected to 3 freeze/thaw cycles and eluted overnight at 30 °C. The eluted oligos were further cleaned and concentrated by C-18 column as described in section 2.2.2.2.

2.2.3 Primase Assay (de novo synthesis of RNA primers on single-stranded templates).

The activity of full-length human primase variants was tested on several different single-stranded DNA templates as indicated in corresponding figures. Reactions (20 µl) were assembled on ice in the following order: 100 nM template was added to reaction buffer (30 mM HEPES-KOH (pH 7.9), 1 mM DTT, 7 mM $MgCl_2$ or $MnCl_2$) followed by the addition of 100 M rATP or 1 mM dATP with 0.15 µM [α-^{32}P]-rATP (3000 Ci/mmol) or 0.15 µM [α-^{32}P]dATP (3000 Ci/mmol; MP Biomedicals, Santa Ana, CA). Then 0.1 µM primase with or without 0.025, 0.05, or 0.1 µM p70 p180C or 0.2 µM p70 p180 N was added, and reaction tubes were incubated at 37 °C for 20 min in a thermo cycler (Thermolyne Amplitron I). A molecular weight marker was created by 5' phosphorylation of the single-stranded 70-mer poly(dT) by T4 polynucleotide kinase (New England Biolabs, Ipswich, MA) following the manufacturer's instructions with [γ-^{32}P]rATP (4500 Ci/mmol, MP Biomedicals). Reaction products were mixed with formamide loading buffer (95% formamide, 5 mM EDTA, 0.02% bromphenol blue, and 0.02% xylene cyanol), heated at 65 °C for 10 min, and resolved by 20% urea-PAGE

(UreaGel System (19:1 acrylamide/ bisacrylamide); National Diagnostics, Atlanta, GA) for 5 h at 2000 V. The gel was dried at 65 °C for 45 min using a Bio-Rad 583 gel dryer. The reaction products were visualized by phosphorimaging (Typhoon 9410, GE Healthcare). The intensities of bands were quantified using the ImageQuant software (version 5.2, Molecular Dynamics).

2.2.4. Primer Extension Assay by DNA pols using fluorescent- or 5'^{32}P- labeled primers

Activities of the p180ΔN-core, p70•p180 N, or p70•p180•N•p49•p58 were compared in reactions (20 µl) that contained 0.75 µM poly-dT_{70} template with 0.50 µM 5 -TYE665 fluorophore-labeled poly-dA_{15} DNA or poly-rA_{15} RNA oligos or 73a (73b) templates pre-annealed with hetero-DNA or RNA primers. The annealing of the 73a or the 73b template with RNA or DNA primers was done by a decrease of temperature from 80 to 25 °C in 0.5 °C/min gradient in the thermo cycler (50 µl volume, 50 mM NaCl). The activity of primase p49·p58 heterodimer was analyzed using close to an equal 1:1.5 ratio of enzyme to template. The activities of primase p49·p58·p70p·180 N heterotetramer were analyzed using a low 1:15 ratio of enzyme to primer/template. The low ratio of primase to template allowed us to approach single-hit conditions, whereas at the equal ratio the primase was able to synthesize longer products due to multiple binding events with substrate. This allowed us better access the inhibitory effect of dATP. Reactions were assembled on ice in the following order. The primer/template was added to the buffer containing 20 mM Tris-HCl, pH 8.0, 50 mM NaCl, 10 mM $MgCl_2$, 0.2 mg/ml BSA, and 2 mM DTT followed by the addition of dATP (200 µM or otherwise indicated) or 200 µM dNTPs for the poly-dT70 and 73a (or 73b) template, respectively. Then, the p180ΔN-core, p70·p180 N, or p70·p180 N p49·p58 was added into the reaction to

concentrations indicated in the figure legends. Reactions were held for the indicated time points at 37 °C in the thermo cycler. T4 DNA polymerase (Promega Corporation; stock concentration 25 nM) was used as a control for the primer extensions on hetero-DNA and RNA. Reaction products were mixed with formamide loading buffer (95% formamide, 0.025% Orange G, 5 mM EDTA, and 0.025% SDS) and heated at 70 °C for 5 min. The reaction products were separated as described previously. Visualization of the products used the Typhoon 9410 imager (emission of fluorescence at 645 nm or phosphorimaging described in 2.2.3).

2.2.5 Primer Extension Assay (incorporation of α-^{33}P-labeled nucleotide triphosphates)

Activity of primase or polα in extension of ribo-primers with or without terminal 5'-triphosphate annealed to different DNA templates was tested in a 20 µl reaction containing 30 mM Hepes-KOH (pH 7.9), 50 mM KCl, 1mM DTT, 2 mM $MgCl_2$, 100µM UTP, 100 µM CTP , 0.25 µM [α-^{33}P]-GTP (3000 Ci/mmol; PerkinElmer, Inc.), 1 µM template- primer, and various concentrations of primase variants or polα (polα-core, dimer, tetramer). Reactions were incubated at 35°C in a thermal cycler (Thermolyne Amplitron I) and stopped by mixing with an equal volume of formamide loading buffer (95% v/v formamide, 5 mM EDTA 0.02% Bromophenol blue, 0.02% Xylene cyanol, and 0.025% SDS), heated at 65°C for 10 min, and resolved by 20% Urea-PAGE for 5 hours at 2000 V. The gel was processed as described in 2.2.3.

2.3. Yeast as a model organism to study primase-polα function during replication

2.3.1. Saccharomyces cerevisiae strains and plasmids

Diploid yeast strain YPOM258 resulted from a cross of two haploid yeast strains, BY4742 (*MATα his3*Δ*-1 leu2*Δ*-0 lys2*Δ*-0 ura3*Δ*-0*) and Δ1 (*MAT***a** *CAN1 his7-2 leu2-*Δ*::kanMX ura3-*Δ *trp1-289 ade2-1 lys2-*Δ*GG2899-2900ψ*), Dr. Pavlov, unpublished. The haploid strain LAN201 (*MAT*α *ade5-1 lys2*-Tn*5-13 trp1-289 his7-2 leu2-3,112 ura3-4*) (59) was provided by Dr. Artem Lada.

The coding sequence corresponding to the C-terminal domain of yeast primase large subunit within the *PRI2* gene (named *PRI2-CT*) was amplified by PCR and cloned into yeast integrative vector pRS306 with the *URA3* selectable marker giving pRS306-*PRI2-CT*. The *pri2-2* (C434Y) allele was generated by site-directed mutagenesis PCR on the plasmid. Briefly, two semi-complementary primers (described in Liu and Naismith (60)) were used to PCR-amplify the plasmid and change "TGC (Cys)" to "TAC (Tyr)" at position corresponding to C434. The PCR product was then digested by DpnI and used for transformation of XL-10 *E. coli* cells. Plasmids were isolated and sequenced.

Then pRS306-*PRI2-CT* (C434Y) was digested by AgeI restriction enzyme and this preparation was used to transform the diploid YPOM258 or haploid LAN201 yeast strains. Transformants were selected on synthetic complete (SC) medium lacking uracil. The haploid transformants were plated on 5-fluoroorotate (5-FOA) medium forced the loss of the *URA3* marker by intrachromatid ''pop-out'' recombination. The single colonies of FOA-resistant cells were isolated and streaked on complete (yeast extract peptone dextrose with adenine and uracil (YPDAU)) plate. Clones containing the mutation in *PRI2* region were found after PCR amplification and sequencing of the

corresponding region of genomic DNA isolated from the colonies.

The diploid YPOM258 yeast cells containing one copy of wild type *PRI2* and one copy of *pri2-2* mutation were plated onto sporulation medium (contain 1% potassium acetate and minimum nutrient required) for induction of meiosis. The cell walls of asci were digested in 2 mg/ml zymolyase solution and individual spores from tetrads were isolated using micromanipulator. After tetrad dissection the haploid clones carry the pri2-2 were isolated by "pop-out" recombination method (see above). The *pri2-2/rev3*Δ(rev3::LEU2) strain was made by transforming XbaI digested pAM56 plasmid (described in (61)) into *pri2-2* strain and selected on SC- Leu^- media.

2.3.2. CAN1 forward mutation assay and fluctuation analysis for determination of mutation rates.

Mutations at *CAN1* locus were selected for on synthetic complete media lacking arginine and containing canavanine (SC-Arg^- CAN^+). Cells with wild-type *CAN1* gene (encodes for arginine permease) take up canavanine, a toxic arginine analog, and die. Forward mutations that inactivate *CAN1* (e.g. base substitution, insertion, deletion) allow for growth on such medium.

A patch test was performed at first for preliminary qualitative characterization of strains mutability. The quantitative analysis was then done using fluctuation test. Briefly, nine individual colonies from each of the yeast variants wild type, *pri2-2*, and *pri2-2 rev3Δ* were randomly picked and re-suspended into 5 ml of liquid YPDAU medium. The wild-type culture was grown at 30 °C in rotating incubator for 48 hours, while the *pri2-2* and *pri2-2 rev3Δ* cultures were grow at 30 °C for 96 hours. Then each culture was proper diluted and plated on synthetic complete (SC) and SC-Arg^-+Can agar plates and

incubated for another 3 to 5 days. Mutant frequency in each culture was calculated by the number of colonies on selective plates (mutant frequency) divided by number of colonies on complete medium and then multiplied by dilution factor (survival). The mutation rates (μ) were calculated using formula originated from Drake (62) as described in (29) as $\mu=f/\ln(N\mu)$ (where "f" is median frequency of mutants, "N" is final number of cells) that was solved by iteration.

To study mutations induced in the presence of Cd^{2+}, we modified the method as follows. After resuspension of individual colonies in 5 ml of medium, each culture was split equally into 2.5 ml cultures with or without 10 μM $CdCl_2$ and then shaken at 30 °C for another 48 and 96 hours, for wild type or the *pri2-2*, respectively as processed as before.

2.3.3 Measurement of the $(GAA)_{100}$ tri-nucleotide expansion in pri2-2 strain.

The $(GAA)_{100}$ cassette plasmid (described in (63), Figure 2.1) was digested with SwaI restriction enzyme. Then LAN201 wild-type and *pri2-2* strains were transformed by this digested plasmid, and transformants selected on SC-Ura^- plates. The single colonies isolated from Ura^- plates were inoculated in 5 ml of YPDAU broth and streaked on YPDAU plates at the same time. The 5 ml cultures were grown in the shaker at 28°C for 3 days (4 days for *pri2-2* strain). After growth, the cultures were harvested and plated on 5-FOA (100 μl of 10^{-1} dilution), SC-URA^- (100 μl of 10^{-4} dilution), and YPDAU (100 μl of 10^{-6} dilution). The streaked colonies on YPDAU were used for genomic DNA isolation, to evaluate the status of repeat before expansion. The colonies from 5-FOA plates were streaked on YPDAU for genomic DNA isolation, to evaluate the status of repeat after

expansion. The $(GAA)_{100}$ cassettes were PCR-amplified and run on 1.2% agarose gel to visualize the extent of expansion.

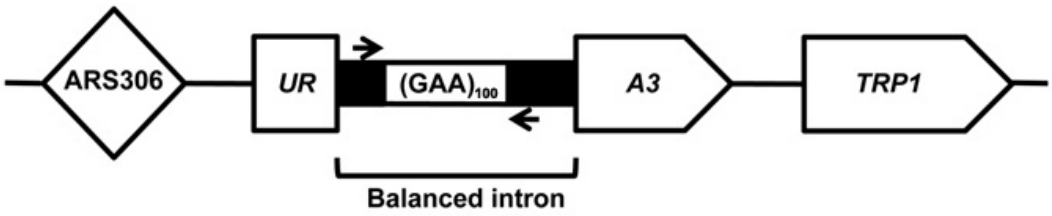

Figure 2.1 Cassette for the detection of expansions of the $(GAA)_{100}$ repeats within the *URA3* marker. The expansion of the repeats leads to the non-functional gene. Arrows show positions of primers used for the PCR analysis of repeat lengths.

CHAPTER 3: Primase structure and function: primase counting and switching during primer synthesis

Most of the material presented in this chapter was published in the following articles:

Zhang, Y., Baranovskiy, A. G., Tahirov, T. H., Pavlov, Y. I. (2014) "The C-terminal Domain of the DNA Polymerase Catalytic Subunit Regulates the Primase and Polymerase Activities of the Human DNA Polymerase α-Primase Complex" J. Biol. Chem. 289: 22021-34

Baranovskiy, A. G., ***Zhang, Y***., Suwa, Y., Babayeva, N. D., Gu, J., Pavlov, Y. I., Tahirov, T. H. (2014) "Crystal Structure of the Human Primase" J. Biol. Chem. 290: 5635-46

Baranovskiy, A. G., ***Zhang, Y.***, Suwa, Y., Gu, J., Babayeva, N. D., Pavlov, Y. I., Tahirov, T. H. (2016) "Insight into the Human DNA Primase Interaction with Template-primer" J. Biol. Chem. 291(9):4793-802.

Baranovskiy, A.G., Babayeva, N.D., ***Zhang, Y***., Gu, J., Suwa, Y., Pavlov, Y.I., Tahirov, T.H. (2016) "Mechanism of concerted RNA-DNA primer synthesis by human primosome". J. Biol. Chem. Accepted.

3.1 Introduction

We already described the eukaryotic prim•polα heterotetrameric complex that constitutes two polymerases, an RNA polymerase and a DNA polymerase in Chapter 1 (Figure 1.4). It is a unique complex of polymerases different from pols that can incorporate both ribo- and deoxy-NTPs by the same polymerase active site (e.g. primpol). The polα p180 catalytic subunit is divided into the N-terminal catalytic domain and a highly conserved C-terminal domain with two Zn motifs, which are connected by a flexible linker (Chapter 1, Fig. 1.4). The p58 regulatory subunit of primase contains a flexible linker that separates the N- and C-terminal domain (40). The C-terminal domain of p58 contains a Fe-S cluster, which is critical in the initiation of primer synthesis. The structure similarity between yeast analog priL-CTD with a DNA photolyase from cryptochrome family of flavoproteins was the first hint that the C-terminal domain of the large primase subunit may be involved in di-NT synthesis ((64)). The current sequential synthesis model indicates that after primase synthesizes the 7- to 10-mer RNA primer, there is a switch to polα synthesis (40). While primase synthesizes, polα remains inactive. After the switch to polα, the primase activity is not required. It is likely that the activity of these parts is a subject of tight regulation. In this part of my work the goal was to determine how primase subunit(s) interacts with polα part(s), and how each part of the complex regulates the activity of prim•polα.

3.2. Results

3.2.1. The C-terminal domain (CTD) of the catalytic subunit of human polα interacts with the N-terminal part of the large subunit of primase

Mammalian polα interacts with the large subunit of primase (39). The structure of artificially-made, chimeric primase-CTD of polα (amino acids 1445-1462) protein suggested that the CTD of polα interacts with the N-terminus of the large subunit of primase (65). To examine the inter-subunit interactions between primase and polα *in vivo* we have used a yeast two-hybrid assay. As expected, a strong interaction was detected between the two primase-subunits as well as the C-terminal domain of polα (p180C) with the second subunit of polα (p70) (Table 3.1), while no interaction was seen between p180C and p49. The presence of two plasmids containing cs-p58 fused to activation domains (AD) and cs-p180C (encoding for aas 1258-1462) fused to BD led to a positive signal for both *HIS3* and *ADE2* reporters. However, there was no activation of reporters when p58 was fused to BD and p180C was fused to AD. We concluded that the large subunit of human primase interacts with the CTD domain of polα.

Table 3.1. Activation of the reporter genes (*HIS3* and *ADE2*) by the co-transformation of the yeast two-hybrid (Y2H) plasmids in yeast strain AH109.

	vector combination		activation of reporter genes	
	pGADT7	pGBKT7	*HIS3*	*ADE2*
negative controls	vector	vector		
	vector	p49		
	vector	p58		
	vector	p70		
	vector	p180CTD		
	p49	vector		
	p58	vector	+	
	p70	vector		
	p180CTD	vector		
positive control	*SV40 large T-antigen	murine p53	+	+
	p49	p58	+	+
	p58	p49	+	+
	p70	p180CTD	+	+
	p180CTD	p70	+	+
experiments	p49	p49		
	p58	p58	+	
	p70	p70	+	
	p180CTD	p180CTD		
	p49	p180CTD		
	p180CTD	p49		
	p58	p70	+	
	p70	p58	+	
	p49	p70	+	
	p70	p49		
	p58	p180CTD	+	+
	p180CTD	p58	+	

Footnotes: * SV40 large T-antigen is in the pTD1 vector and the murine p53 is cloned in pVA3 vector. Each combination was tested in more than 30 yeast colonies. "+" ≥ 80% of the colonies have the positive phenotype of the activated reporter gene.

To get more precise information about the interaction, we explored the binding of the same proteins produced in bacteria, in Rosetta-2 (DE3) cells (Figure 3.1). Co-expression of the genes encoding the SUMO-tagged p180C and HIS6-tagged p58 allowed us to obtain a stable binary complex by affinity purification on the Ni-IDA resin (Figure 3.1A, lane 5). The stoichiometry of the binding between p58- HIS6 and SUMO-p180C was similar to the positive control (Figure 3.1A, lane 4). The identities of p58- HIS6 and p70-HIS6 purified by Ni-IDA resin, as well as the SUMO-p180C were verified by the Western-blot analysis (Figure 3.1B).

In the crystal structure, p58N is tightly bound to the p49 subunit of primase (65), although it lacks the C-terminal domain with the [Fe-S] cluster (amino acids 287-509). Weiner et al. (42,43) noted that the purification of the p58N alone is problematic, because it is largely insoluble in the absence of p49. In our experiments, only a 24 kDa proteolytic product was seen (Figure 3.1A and B, lane 1) in the pull-down of p58-HIS6 alone, which likely represents the C-terminal part of the p58 subunit. To investigate the role of the primase domain containing [Fe-S] cluster in interaction with polα, plasmids encoding for two subunits of primase (p49•p58) and two subunits of polα (SUMO-p180C•p70-HIS6) were constructed and the four-subunit complex was produced. An N-terminal SUMO tag was added to the p180C to address the problem of poor solubility of the protein in *E. coli*. The levels of primase are typically higher than polα when produced in *E. coli* cells. The HISx6 tag, therefore, was placed in the N-terminal of the p70 subunit to obtain a quaternary complex with more even stoichiometry after pull-down. Similar to the p49•p58•SUMO-p180C•p70-HISx6 (positive control; Figure 3.1C, lane 4), the p49•p58N and SUMO-p180C•p70-HISx6 are represented by stable quaternary complexes

after affinity purification on the Ni-IDA resin (Figure 3.1C, lane 5). After the production of p49•p58C and SUMO-p180C•p70-HISx6, only a binary complex SUMO-p180C•p70-HISx6 was present on the gel after pull-down (Figure 3.1C, lane 6). We concluded that the polα interaction with primase is through the p180C-p58N. Neither p49, nor the part containing the [Fe-S] domain of p58, play a role in the interaction. Our data are consistent with the recent finding that the last 18 residues of the C-terminal region of the yeast Polα catalytic subunit are important for binding to the N-terminus of the primase large subunit (45,65).

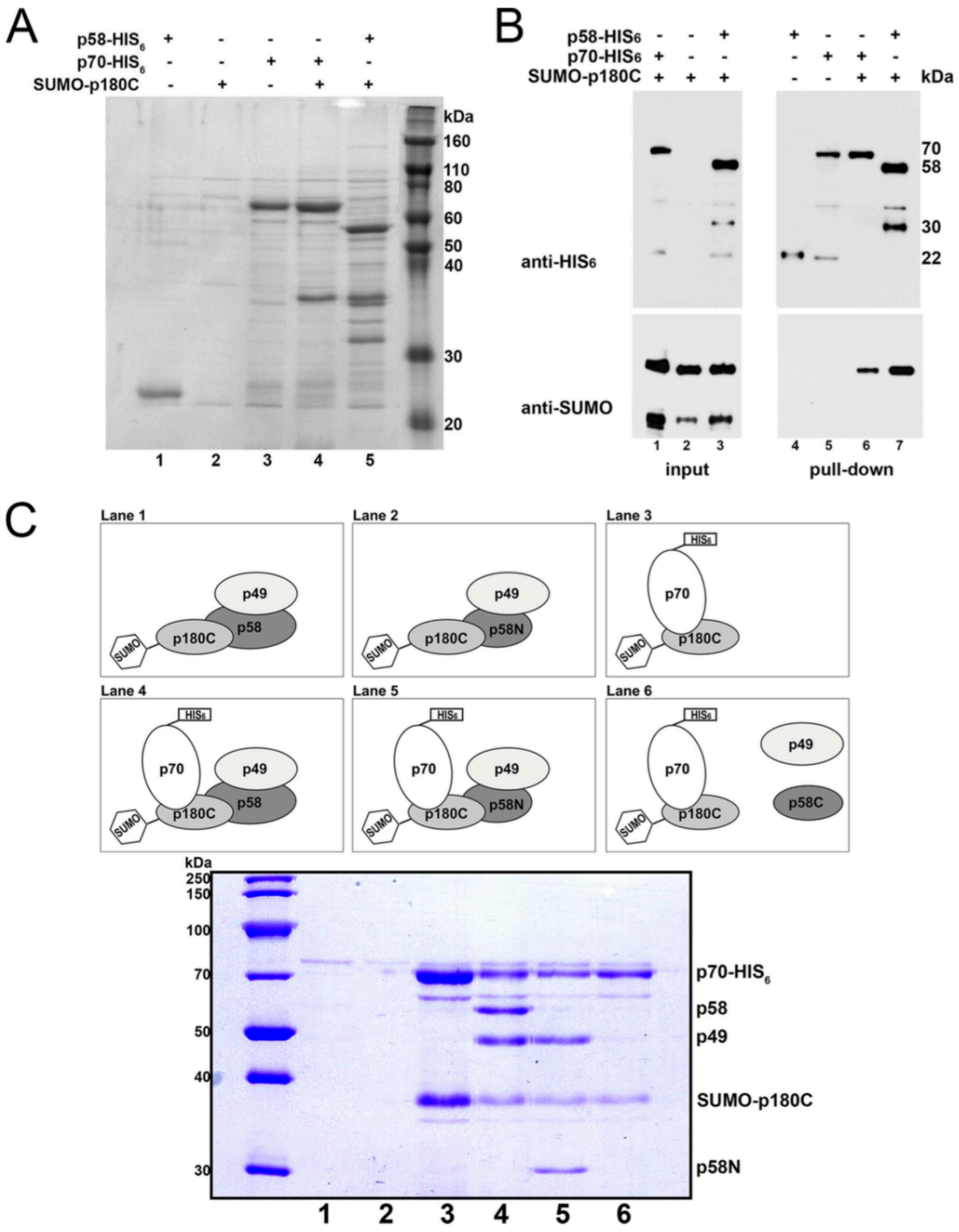
A
p58-HIS6
p70-HIS6
SUMO-p180C
kDa
160
110
80
60
50
40
30
20
1 2 3 4 5
B
p58-HIS6
p70-HIS6
SUMO-p180C
kDa
anti-HIS6
anti-SUMO
70
58
30
22
1 2 3 4 5 6 7
input
pull-down
C
Lane 1
Lane 2
Lane 3
Lane 4
Lane 5
Lane 6
p49
p58
p180C
SUMO
p58N
HIS6
p70
p58C
kDa
250
150
100
70
50
40
30
p70-HIS6
p58
p49
SUMO-p180C
p58N
1 2 3 4 5 6

Figure 3.1. **N-terminus of the large subunit of primase tethers it to polα.** Analysis of the pulldown of proteins separated on SDS-PAGE and stained by Coomassie Blue (R250). *A*, direct interaction between p58 and p180C. *Lane 1*, p58-Hisx6 is self-cleaved to a 24-kDa product in the absence of its binding partner; *lane 2*, SUMO-p180C does not bind to Ni-IDA resins; *lane 3*, p70-Hisx6 pulldown by Ni-IDA resin; *lane 4*, SUMO-p180C binds to p70-Hisx6; *lane 5*, p180C sumo binds to p58-Hisx6. *B*, Western blot detection of the interacting proteins seen in *A*. *C*, finding a region of p58 that is responsible for its interaction with pol. *Lanes 1* and *2*, p49, p58, p58N, or SUMO-p180C do not bind to Ni-IDA resin in the absence of p70-Hisx6 (negative controls); *lane 3*, SUMO-p180C binds to p70-Hisx6 (positive control). *Lane 4*, p58 p49 interacts with pol (SUMO-p180C p70-Hisx6; positive control); *lane 5*, p49 p58N interacts with SUMO-p180C p70-Hisx6; *lane 6* shows the absence of interaction of p58C or p49 with SUMO-p180C p70-Hisx6.

3.2.2. The role of polα in regulating primase activity

To study the functional relevance of the subunit contacts in polα-prim, several variants of recombinant human primase and polα were purified in laboratory of our collaborator, Dr. Tahirov. Similar to yeast polα (52), where N-terminus interacts with Ctf4 for the integration of polα into the replication fork (66), the N-terminus of human p180 is poorly folded and has no conserved motifs necessary for DNA polymerizing activity, so it has been deleted to increase protein solubility and simplify its purification. B-subunit (p70) with catalytically proficient catalytic DNA pol subunit, p180ΔN is called two-subunit polα (or p70•p180ΔN). The C-terminal domain of p180 (p180C) in complex with p70 is called polα-CTD (or p70•p180C). The catalytic domain of p180 without the N-terminal unstructured region and C-terminal part is called p180ΔN-core, or simply p180-core. Two-subunit primase is p49•p58.

We analyzed *de novo* RNA synthesis and the extension of these primers on the poly-dT template with radioactive [α-^{32}P]-ATP by p49•p58 heterodimer of primase alone, or in the complex with heterodimer of p70•p180C, or p70•p180ΔN. The heterodimeric primase synthesized RNA primers of an average of 8-10 nucleotides unit-length and multiples of this unit. They were extended to around 20 nucleotides and, more frequently, to around 30 nucleotides, and, less efficiently, they were extended further to 50 and 60 nucleotides (Figure 3.2A, lane 2). The addition of dATP dramatically inhibited the activity of primase (Figure 3.2B, lane 3-5). In the presence of p70•p180C the majority of products became longer, around 70 nucleotides in length (Figure 3.2A, lane 3 and titration of p70•p180C concentration in Figure 3.2B, lane 7-9). The explanation for the predominance of the long products could be the elevated activity/processivity of the primase and non-random

initiation/extension by primase in the presence of p70•p180C biased toward the 3'-end of the template. The presence of catalytically active heterodimeric polα, conversely, inhibited the extension of unit-length primers when there was no dATP in the reaction (Figure 3.2A, lane 4 and titration of p70•p180ΔN in Figure 3.2B lanes 10-12). This observation is consistent with earlier studies (67). The addition of dATP with p70•p180ΔN, as expected, led to a rapid synthesis of the full-length products (Figure 3.2A, lane 5). The quantification of the product distribution and band intensity in the case of primase alone, plus p70•p180C or p70•p180ΔN with or without dATP, (Figure 3.2C) provides support to the visual analysis of the gel shown in Figure 3.2A.

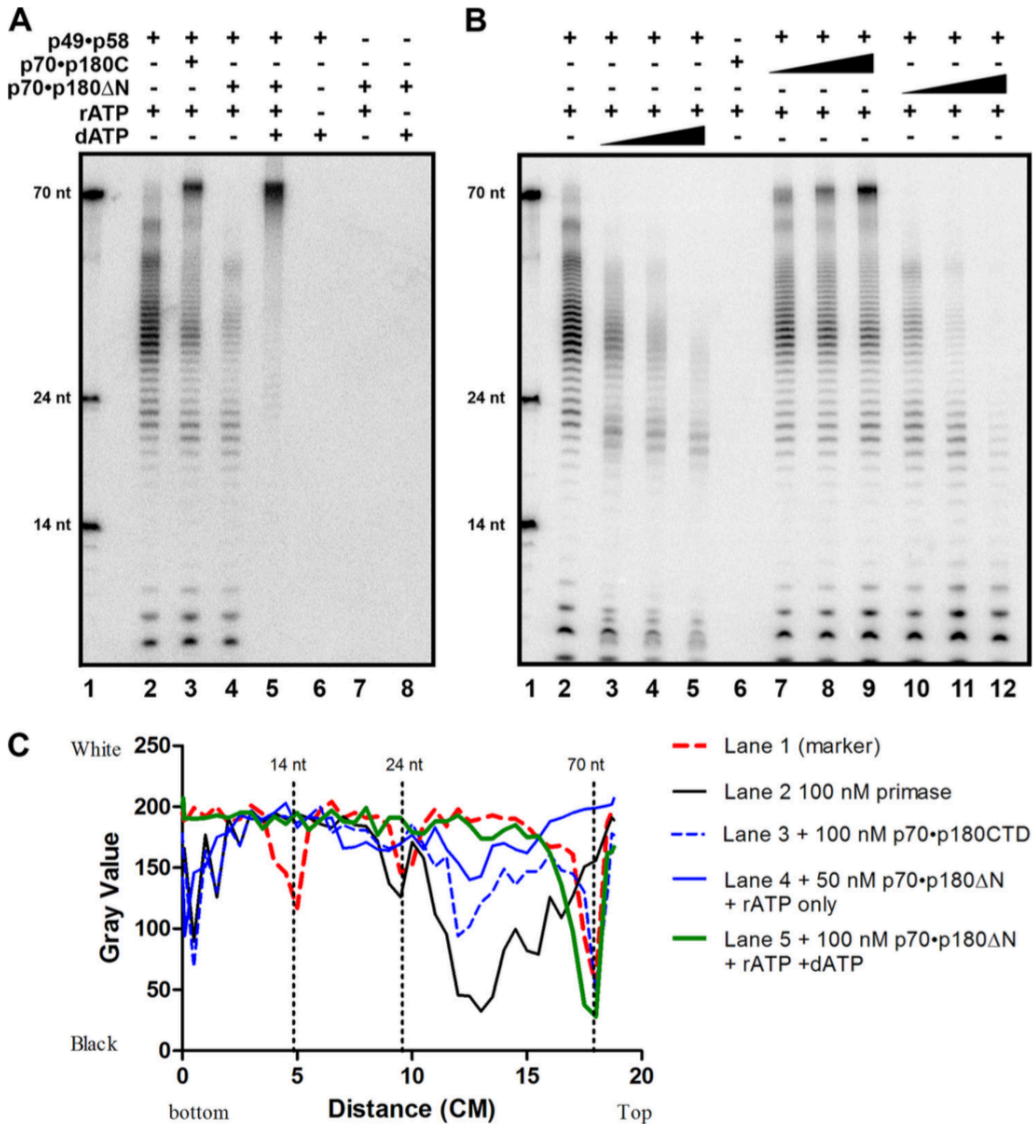
A
p49•p58
p70•p180C
p70•p180ΔN
rATP
dATP
70 nt
24 nt
14 nt
1 2 3 4 5 6 7 8
B
70 nt
24 nt
14 nt
1 2 3 4 5 6 7 8 9 10 11 12
C
White
Black
Gray Value
250
200
150
100
50
0
14 nt
24 nt
70 nt
0 5 10 15 20
bottom
Distance (CM)
Top
Lane 1 (marker)
Lane 2 100 nM primase
Lane 3 + 100 nM p70•p180CTD
Lane 4 + 50 nM p70•p180ΔN + rATP only
Lane 5 + 100 nM p70•p180ΔN + rATP +dATP

Figure 3.2. Regulation of *de novo* primase activity by polα.

Polα-primase activity assay was done on the poly-dT_{70} template (0.1 μM).

(A) Effect of polα on primase activity. Lane 1, nucleotide size marker; Lane 2, RNA primers synthesized by 0.1 μM p49•p58 alone; Lane 3, RNA primers synthesized by 0.1 μM p49•p58 with the addition of 0.1 μM p70•p180C; Lane 4, RNA primers synthesized by 0.1 μM p49•p58 with the addition of 0.05 μM of p70•p180ΔN; Lane 5, hybrid RNA-DNA fragments synthesized by 0.1 μM p49•p58•p70•p180ΔN complex with both the rATP and the dATP in reaction; and Lanes 6-8, negative controls.

(B) Primase activity assays with the titration of the polα variants. Lane 1, nucleotide size marker; Lane 2, RNA primers synthesized by p49•p58 alone; Lanes 3-5, RNA synthesized by p49•p58 in the presence of increasing concentrations of dATP (25, 50, 100 μM); Lane 6, no activity by p70•p180C with rATP (negative control); Lanes 7-9, the effect of increasing concentrations of p70•p180C (0.025-0.1 μM) on RNA synthesized by p49•p58; and Lane 10-12, RNA synthesized by p49•p58 with 0.05-0.2 μM p70•p180ΔN.

(C) Quantification of gel shown in panel (A). The Mean Gray Value of each lane was selected from the bottom to the top of the gel image and analyzed by Image J. The distribution of the band (X-axis: distance from bottom to the top of the gel) versus the intensity of the band (Y-axis: gray value closer to 0 means black, 250 means white).

3.2.3. The role of dATP in regulating primase activity

To further study how the primase activity is inhibited by dATP (Figure 3.2B, lanes 3-5), we analyzed the ability of the heterodimeric primase to extend ribonucleotide primers in the presence of ribo- versus deoxynucleotides or a mixture of both. We have used the high ratio of enzyme to template to push the primase to its limits in order to see the extent of dNTP effects. Primase robustly extended the poly-rA15 primers on the poly-dT70 template with rATP. The extent of primer utilization and the length of products increased with longer reaction time, indicating the multiple cycles of binding and synthesis (Figure 3.3, lanes 2-4). Deoxy-ATP was a poor substrate for the primase reaction: it was incorporated in the +1 position quite efficiently but further incorporations were not favored, with no products longer than +4 (Figure 3.3, lanes 5-7). The primase extended about half of the RNA primers with dAMP in 30 sec, while the addition of second dAMP was almost ten times slower. The primer extension was also limited when both rATP and dATP were present (Figure 3.3, lanes 8-10). The primase incorporated both dATP and rATP with comparable efficiency (Fig. 3, lanes 8-10, note that oligonucleotides containing only RNA s migrate slower than RNA primers extended with dNTPs). These results indicate that primase does not greatly discriminate against dATP, but the products with incorporated dAMP are poor substrates for the following extension.

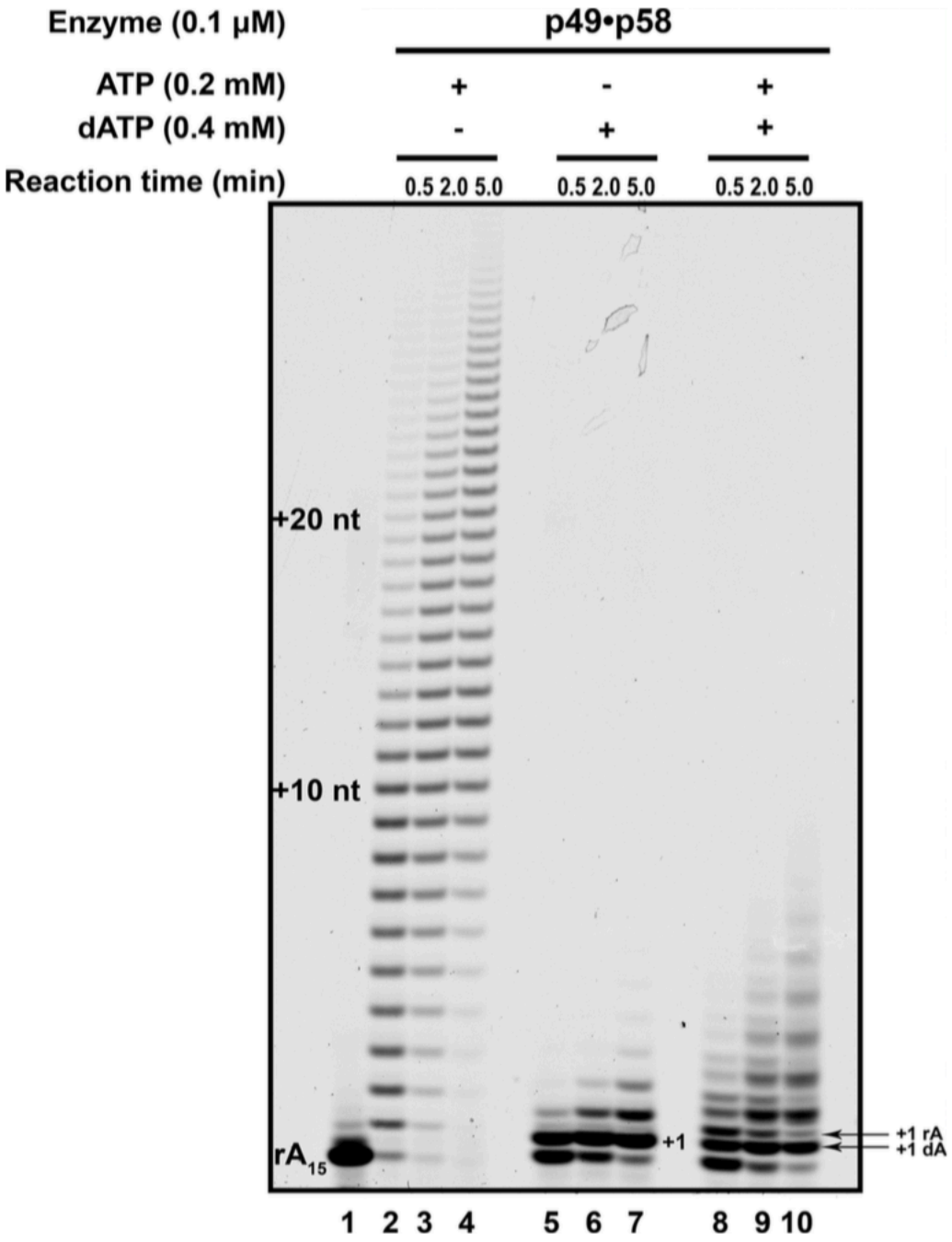
Enzyme (0.1 μM)
p49•p58
ATP (0.2 mM)
+
-
+
dATP (0.4 mM)
-
+
+
Reaction time (min)
0.5 2.0 5.0
0.5 2.0 5.0
0.5 2.0 5.0
+20 nt
+10 nt
rA15
+1
+1 rA
+1 dA
1 2 3 4 5 6 7 8 9 10

Figure 3.3. **Primase can incorporate a few deoxyribonucleotides and this attenuates further RNA synthesis.**

The poly-rA15 primer (enzyme to primer/template ratio = 1:1.5) was extended by heterodimeric primase (p49·p58) in the presence of rATP, dATP or both. Lane 1, reaction without nucleotides; lanes 2-4, reaction with 0.2 mM ATP for 0.5, 2.0, and 5.0 minutes, respectively; lanes 5-7, reaction with 0.4 mM dATP for 0.5, 2.0, and 5.0 minutes, respectively; lanes 8-10, reaction with 0.2 mM ATP plus 0.4 mM dATP for 0.5, 2.0, and 5.0 minutes, respectively.

3.2.4 The C-terminal domain of polα regulates its DNA polymerase activity

In comparison to the p180ΔN-core, the primer extension activity of the dimeric polα complex (p180ΔN•p70) on the poly-dT70 template with RNA primer is much lower (note a two-fold higher enzyme concentration of p180ΔN•p70, Figure 3.4A). It is interesting that the average length of the synthesized fragments is also decreased to around 10 nucleotides. The increase of concentrations of dATP in reaction with the RNA primer on the poly-dT70 template did not result in stimulation of the primer usage (Figure 3.4B). The presence of CTD with metal binding sites rendered the dimeric enzyme sensitive to DTT (Figure 3.4C), while DTT did not modulate the activity of the p180ΔN-core (Figure 3.4D). With an increased reaction time and more than a five-fold excess of the enzyme, we obtained a comparable activity of the p70•p180ΔN and p180ΔN-core on RNA15/poly-dT70. The synthesis by the dimeric polα was still terminated a few nucleotides earlier than the synthesis by the p180ΔN-core (Figure 3.4E). The lower activity of the p70•p180ΔN dimer compared to the p180ΔN-core was also observed on the hybrid homo-heteropolymeric 73a template with the RNA primer (Figure 3.4F).

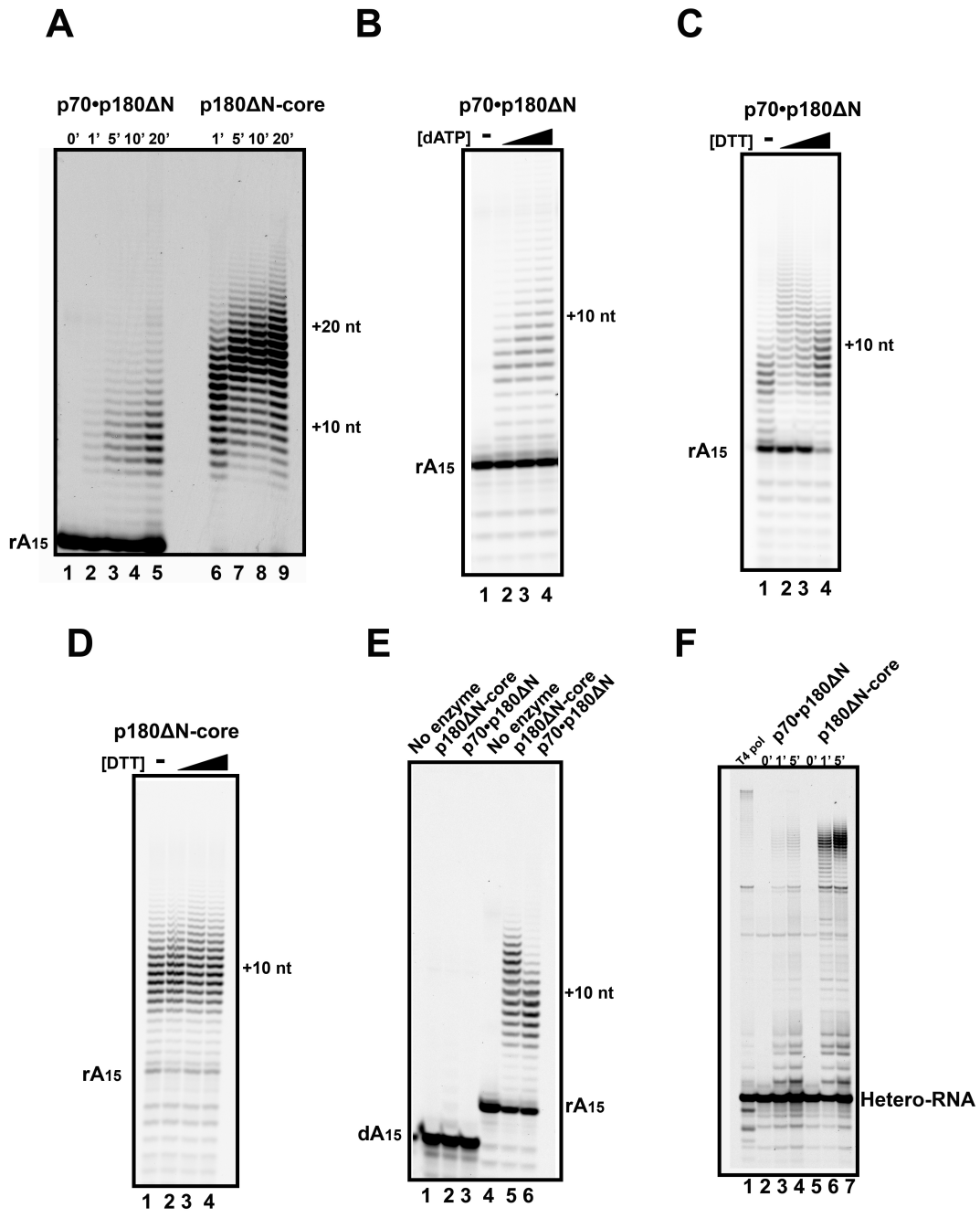
A
p70•p180ΔN
p180ΔN-core
0' 1' 5' 10' 20'
1' 5' 10' 20'
+20 nt
+10 nt
rA15
1 2 3 4 5 6 7 8 9
B
p70•p180ΔN
[dATP] -
+10 nt
rA15
1 2 3 4
C
p70•p180ΔN
[DTT] -
+10 nt
rA15
1 2 3 4
D
p180ΔN-core
[DTT] -
+10 nt
rA15
1 2 3 4
E
No enzyme
p180ΔN-core
p70•p180ΔN
No enzyme
p180ΔN-core
p70•p180ΔN
+10 nt
rA15
dA15
1 2 3 4 5 6
F
T4 pol
p70•p180ΔN
p180ΔN-core
0' 1' 5'
0' 1' 5'
Hetero-RNA
1 2 3 4 5 6 7

Figure 3.4 **Inhibitory effect of p70•p180C on the primer extension by polα.**

(A) The time course of the extension of the poly-rA15 primers on the poly-dT70 template by p70•p180ΔN (enzyme to primer/template ratio = 1: 50; lane 2-5) or by the polα-core (enzyme to primer/template ratio = 1: 100; lanes 6-9). (B) Extension of the poly-rA15 primers by p70•p180ΔN on the poly-dT70 template (enzyme to primer/template ratio = 1: 50, reaction time was 5 minutes). The black triangle indicates that the reactions were carried out with the increase of dATP concentrations of 0.01, 0.1, and 1 mM, respectively. (C, D) Effect of DTT on the ability of polα to extend the poly-rA15 primer. (C) polα p70•p180ΔN (enzyme to primer/template ratio = 1: 50, reaction time 10 in); (D) p180ΔN-core (enzyme to primer/template ratio = 1: 100, reaction time 5 min). The black triangle indicates that the reactions were carried out with the increase of DTT concentrations of 0, 0.5, 1.0, 2.0 mM DTT, respectively.(E) Smaller fragments in primer extension by excess of dimeric polα (p70•p180ΔN) in comparison to the polα core. Extension of the poly-dA15 and poly-rA15 primers in long reactions by the excess of p70•p180ΔN (enzyme to primer/template ratio = 1: 50, reaction time 15 min) or by the p180ΔN-core (enzyme to primer/template ratio = 1: 250, reaction time 2 min) with 0.2 mM dATP.(F) Lower activity of dimeric polα in comparison to the polα core on hybrid DNA template. Extension of the RNA primers on the DNA template 73a by p70•p180ΔN (0.025 μM) or by p180ΔN-core (enzyme to primer/template ratio = 1:50) for the indicated time points. As a control, T4 DNA polymerase (~1:2500, reaction time 2 min) was used to obtain a completely extended, full-length product.

3.2.5. Primase and polα activities in a quaternary prim•polα complex on poly-dT template

During the initiation of DNA replication, the utilization of ribo-nucleotides and deoxy-nucleotides by prim•polα should happen in a sequential order. Primase first synthesizes RNA, then, polα synthesizes the DNA part of the primer. To study the primase activity in the polα-prim complex, we analyzed the activities of primase and polα within the four-subunit complex in the primer extension assay with ribo- versus deoxynucleotides or a mixture of both. In these experiments we have used a low 1:15 ratio of enzyme to template to bring reactions closer to single-hit conditions. Primase p49·p58 and polα p70·p180ΔN were used as internal controls (Figure 3.5). The primase is a non-processive enzyme and was able to incorporate only a few nucleotides (up to 10) (lanes 2-4). Oligonucleotides with a higher number of incorporations seen after four minutes of reaction most likely represent rebinding of the enzyme (lane4). The dimer of polα processively added many more nucleotides with the median around position +15. In complex with polα, primase activity was less than the primase alone (Figure 3.5, compare lanes 8-10 and 2-4). This was likely due to the hand-over of primers from primase to polα. Polα robustly extended the primer in complex with primase with only dATP (Figure 3.5, lanes 11-13). In comparison to p70·p180ΔN alone (Figure 3.5, lanes 5-7), there is a slight increase of primer usage and product length. In the reactions with both rATP and dATP, only a few rAMPs were attached by primase to the rA15, (position +1) and polα rapidly outcompeted primase for the primer 3' end and robustly extended it (Figure 3.5, lanes 14-16).

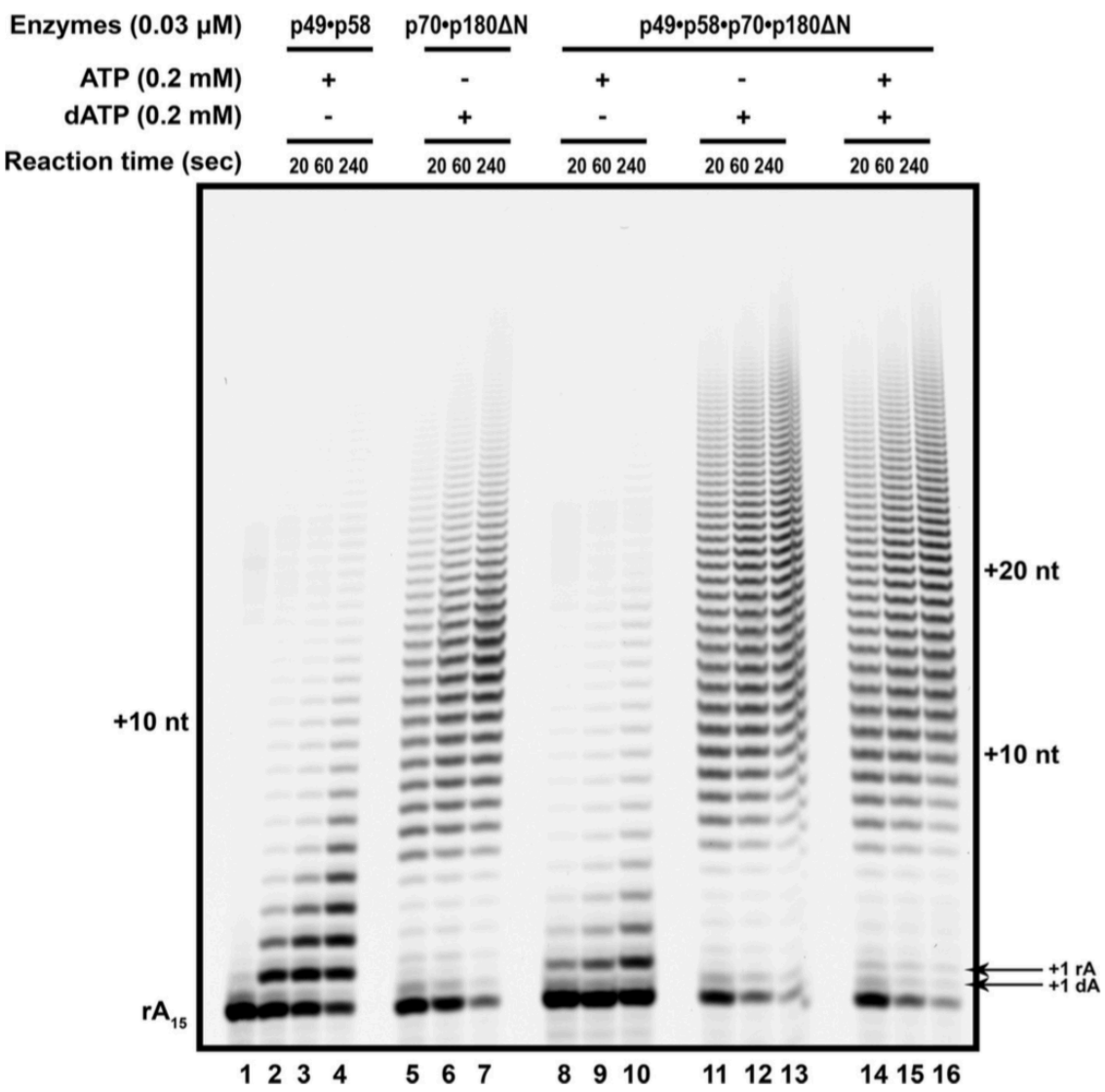
Enzymes (0.03 μM)
p49•p58
p70•p180ΔN
p49•p58•p70•p180ΔN
ATP (0.2 mM)
+ - + - +
dATP (0.2 mM)
- + - + +
Reaction time (sec)
20 60 240 20 60 240 20 60 240 20 60 240 20 60 240
+20 nt
+10 nt
+10 nt
+1 rA
+1 dA
rA15
1 2 3 4 5 6 7 8 9 10 11 12 13 14 15 16

Figure 3.5. **Primase and DNA polymerase activities of the tetrameric polα-primase complex during the extension of the RNA primer on the poly-dT template**.

The poly-rA15 primer annealed to poly-dT and extended by primase (lanes 2-4: 0.2 mM rATP), polα (lanes 5-7: 0.2 mM dATP), or the polα-prim complex (lanes 8-16). Lane 1, reaction without nucleotides; Lanes 8-10, reactions containing 0.2 mM rATP; Lanes 11-13, reactions containing 0.2 mM dATP; Lanes 14-16, reactions containing 0.2 mM of mixture of rATP and dATP. All reactions have an enzyme to primer/template ratio of 1:15 for balanced RNA and DNA pols activities. In each case, the time course of the reaction included points of 20, 60, and 240 seconds.

3.2.6. Recapitulation of the key observations from 3.2.3 and 3.2.4 using ^{32}P-labeled primers

To ensure some of the results observed in primer extension assay using fluorescent-labeled primers (TYE665, a Cy5 equivalent) were not artifacts related to the presence of the fluorescent group at the 5' end of our primers (Figure 3.6A) at the 5' of the primer, we repeated the key observations documented in Figure 3.3 and 3.4 using ^{32}P-γ-ATP-labeled primers. The result shows that the dimer p70·p180ΔN possess less activity than the p180ΔN-core (Figure 3.6B) and dATP is poisonous to primase (Figure 3.6C). The results are in line with results obtained with fluorescent primers.

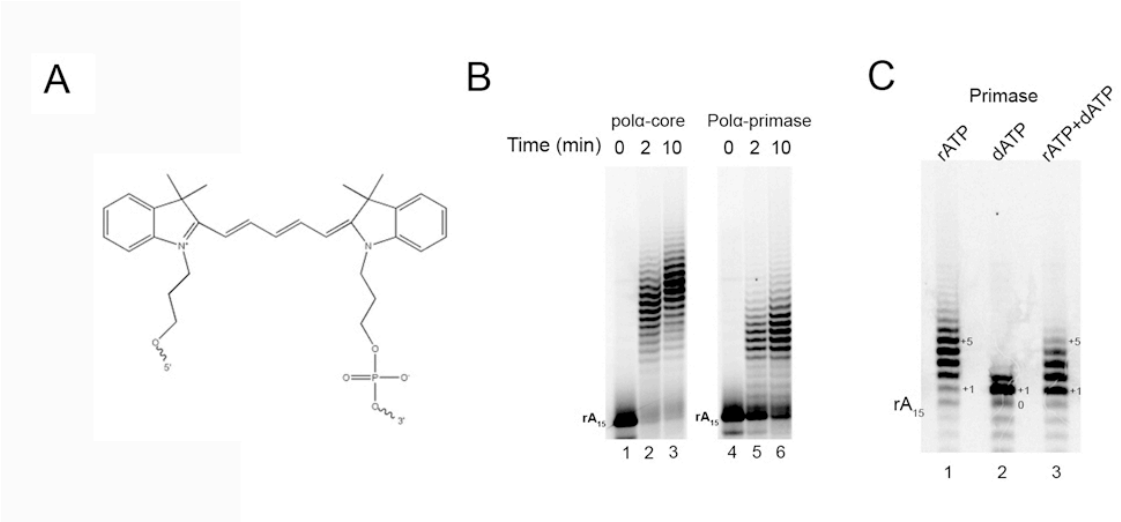

Figure 3.6. **Extension from radioactively labeled primers radioactive give results similar to extension of fluorescent primers**.

(A) Structure of the TYE-665 fluorescent dye (Integrated DNA Technologies, Inc.). (B) The extension of the 5' ^{32}P-labeled poly-rA15 primers (approximately 100 nM, labeled primers lost in purification) on the poly-dT_{70} template (100 nM) by human p180ΔN-core (10 nM; lanes 2 and 3) or polα-primase (10 nM; lanes 5 and 6) in 2 and 10 minutes. (C) Human primase extends the same concentration of substrate as part (B) using 100 μM rATP (lane 1), dATP (lane 2), and rATP + dATP (lane 3).

3.2.7 The importance of the C-terminal domain of primase large subunit and the linker that attach it to the N-terminal domain in primase synthesis de novo.

Zerbe and Kuchta (53) presented initial evidence for a potential importance of the p58C in human primase counting. They found a p58 deletion variant with abnormal counting, which accumulated during *de novo* synthesis RNA products over 40 nucleotides long. However, there was a technical problem in their analysis. The authors used for *de novo* synthesis a human p49•p58 variant with a deletion of the region M288 to L313 that could potentially disrupt the Fe-S cluster (first Cys residue that coordinates the cluster is C287) (68). Moreover, the only critical residue in p58 that participates in *de novo* synthesis (R306) (65)63) is also in this deleted region. Therefore the results presented in the paper (53) are difficult to interpret. Nevertheless, these experiments led to one the first mechanistic models of counting by primase by Kuchta and Stengel (51). The two subunits of eukaryotic primase work together like a hinge. The "hinge-opening" model describe the mechanism of the de novo synthesis as the two subunits binds to the template as a closed hinge, p58 stays at the 5' of the primer and the hinge opens up when p49 subunit starts the synthesis. The p49 stops the synthesis as the "hinge" opens to its maximum distance. The reciprocal "hinge-closing" model describes the initial binding of the primase as an open "hinge", where the direction of the p49 synthesis is towards the p58 subunit. The p49 stops primer synthesis when it bumps into the p58 (Figure 3.7).

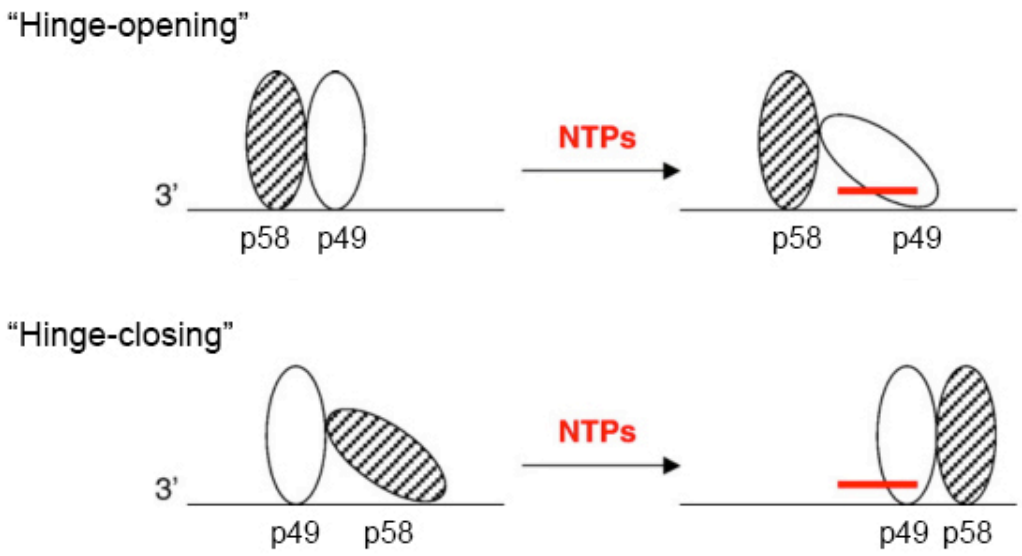

Figure 3.7. **The hinge-opening and hinge-closing model for primase counting**. The catalytic p49 subunit is in white oval shape, and the large p58 subunit is in oval shape filled with dashed-lines. Adapted from Kuchta and Stengel (51).

Primase large subunit connects primase catalytic subunit with polα via its N-terminal domain (section 3.2.1). The C-terminal domain of p58 does not appear to interact with other primase or polα parts, based on protein-protein interaction study or crystal structures (Figure 3.8 (crystalized and solved by Dr. Tahirov's group at UNMC) and structure not shown (40)). The N- and C-terminal parts of p58 are connected by an 18-residue flexible linker (a.a. 253–270) (68). The C-terminal domain of p58 may take advantage of the flexibility of the linker during *de novo* synthesis.

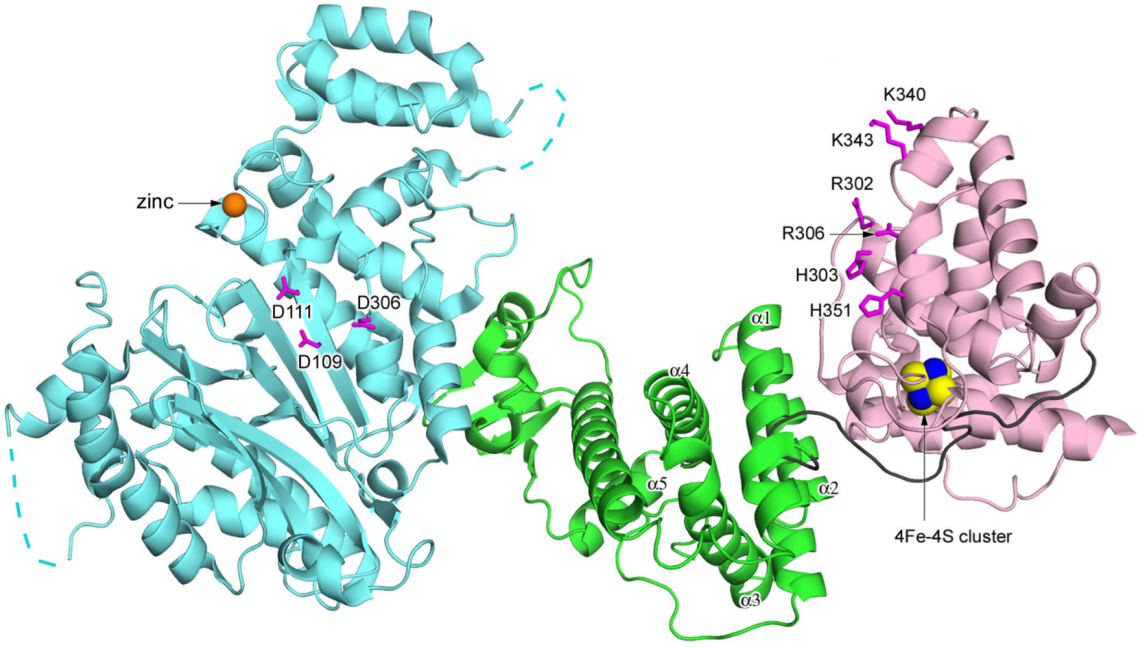

Figure 3.8. **X-ray crystal structure of human primase p49•p58 (68)**. The p49, p58N, p58C, and the linker between p58N and p58C are colored cyan, green, light pink, and gray, respectively. Zinc is shown as an orange sphere, and the 4Fe-4S cluster is shown as a space-filled representation, with iron and sulfur atoms colored blue and yellow, respectively. The disordered regions in p49 are shown by dashed lines. Side chains of catalytic aspartates on p49 and residues forming the proposed NTP/DNA binding site on p58C are shown as sticks and colored magenta.

Several human primase linker mutants were generated to investigate its role in primase activity. Two of these mutants (Prim-Δ5 and Prim-Δ15) have a deletion of 5 (a.a. 256-260) or 15 (a.a. 256-270) residues in p58. The third mutant (Prim-Ins5) has an insertion of 5 residues (GSASG) after Ser-263. The activity of the full-length human primase and its linker mutants was initially tested on the template TA15 (Table 2.2). This template was designed to provide a single start position that simplifies the analysis of product distribution and processivity. One drawback of the template used in de novo synthesis (e.g. poly-dT_{70}) is that the longer products contain theoretically more radiolabeling than the shorter products, which could affect the interpretation of the results. The TA15 and GA6 templates possess only one pyrimidine (dT) that allows a single unique primer start position with only one radiolabeled ATP, thus eliminates the drawback.

In the *de novo* assay with TA15 template, primase synthesized primer up to 9-nt (Figure 3.9A). The activity of Prim-Δ15 was decreased about five fold (Figure 3.9*A*, compare lane 4 with lane 2), the activity of Prim-Δ5 was decreased about two fold (lane 3), while increasing of the linker size by 5 residues had no effect on activity (lane 5). Deletion of $p58_C$ results in complete loss of *de novo* synthesis (Figure 3.9*A*, lane 6), which confirms that $p58_C$ plays a critical role in dinucleotide formation (41,43,69). Addition of purified $p58_C$ at two fold molar excess does not recover primase activity (Figure 3.9*A*, lane 7) indicating that $p58_C$ must be connected to the rest of primase molecule for proper orientation in regard to p49 active site. The residual activity of Prim-Δ15 means the p58C is probably still mobile and can reach the active site in p49.

The template GA6 was designed as a control template for TA15 to test different template sequence variations. Surprisingly, we observed more processive synthesis by primase (Figure 3.9B) than on TA15 template (Figure 3.9A). The majority syntheses were all the way up to 16 nt, where the 9 nt stop present with TA15 disappeared. To elucidate the influence of GA vs poly-A template on primase processivity in de novo synthesis, two longer templates (35a2, and 60a5; Table 2.2) were used. The addition of cytidine increases the heterogeneity to the template. Similar to the GA6 template (Figure 3.9B), primase synthesis de novo does not stop at the unit length (Figure 3.10, lane 1 compare to Figure 3.9A) on 35a2 template and the synthesis primarily reaches to the end of the template (28 nt). There is a stop at 16^{th} position, which is a result of primase inaccurate synthesis across template C using either UTP or CTP. The addition of polα decreases the primase activity, but has no effect on product size (Figure 3.10, lane 2). The known inhibitor of polα, aphidicolin, surprisingly decreased the amount of the full-length products by primase, without changing the di-nt synthesis and intermediate product (Figure 3.10, lane 3). The addition of deoxyribonucleoside triphosphates G, C, and T to the reaction condition as lane 3 showed an accumulation of full-length extended product, probably synthesized moderately by polα (Figure 3.10, lane 4). This suggest that the long stretch of RNA primer synthesis is due to the rebinding of primase for extension, which is probably a different mechanism from a single-hit *de novo* synthesis. On the other hand, the linker deletion mutant Δ15 exhibited a decreased activity but was also more processive (Figure 3.10, lane 5). The similar effect is observed on a longer template (60a5; Figure 3.10, lane 6-9). It is interesting that primase-polα bypasses only two

template Cs, but not the third one. More studies on primase-polα infidelity are described in chapter 5.

We also analyzed primer extension by primase variants. The shortening or increasing size of the linker by 5 residues minimally affects primase ability in extending hetero-RNA primer while the deletion of $p58_C$ domain or 15 linker residues reduced the activity about five fold (Figure 3.9*C*). These results confirm the observation from previous study (69) on the importance of p58C in primer extension and suggest that this domain interacts with a substrate during all steps of primer synthesis. The deletion of the linker between p58N and $p58_C$ leads to a much stronger impact on initiation step (di-nt synthesis) when compared to extension.

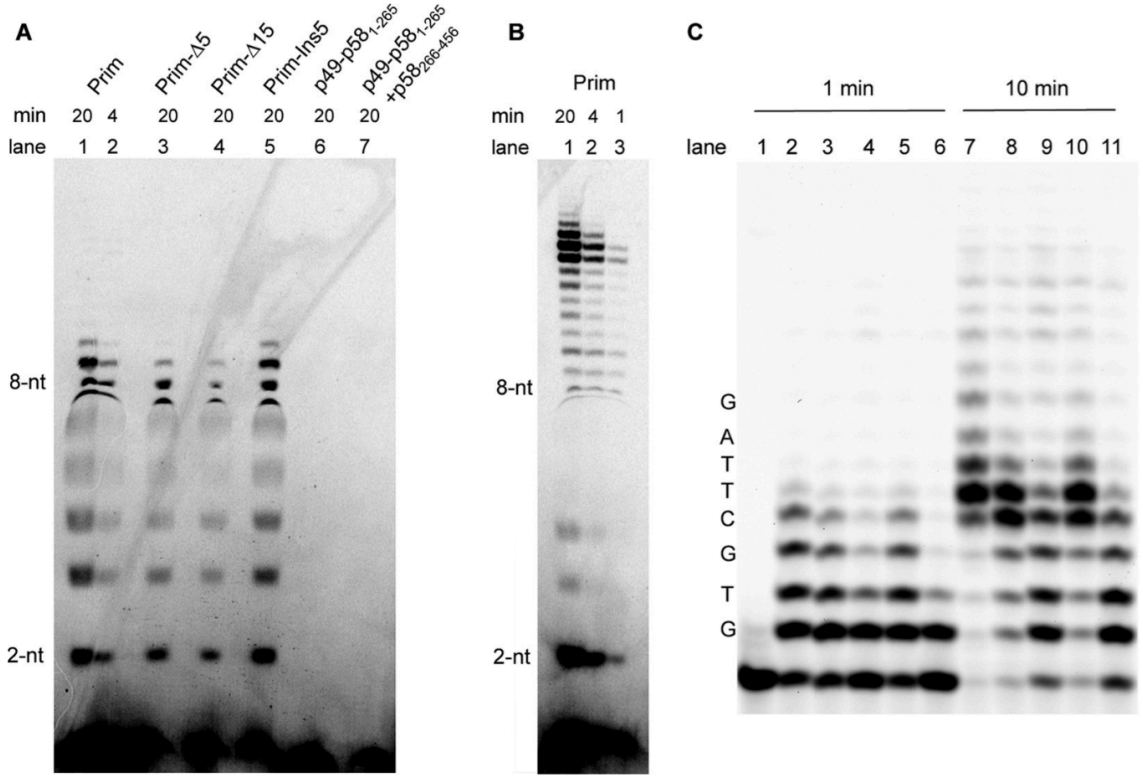

Figure 3.9. **Activity analysis of the human primase and mutants with shortened linker of p58.** (***A***) *De novo* activity on template TA15. $p58_C$ was added at two-fold molar excess over p49-$p58_N$. (***B***) *De novo* activity of the wild-type primase on template GA6. (***C***) Extension assay using fluorophore-labeled RNA primer annealed to template 46A1 (Table 2.3). Lane 1 – control incubation (no enzyme); lanes 2 and 7 – wild-type primase; lanes 3 and 8 – PrimΔ5; lanes 4 and 9 – Prim-Δ15; lanes 5 and 10 – Prim-Ins5; lanes 6 and 11 – p49-$p58_N$. Reactions were incubated 1 min (lanes 2–6) and 10 min (lanes 1 and 7–11) at 35 °C. Activity of primase samples was analyzed in presence of p70-$p180_C$. We assume all RNA products shown in panels A and B were labeled at 5' end because of using [γ-^{33}P]-ATP without adding cold ATP.

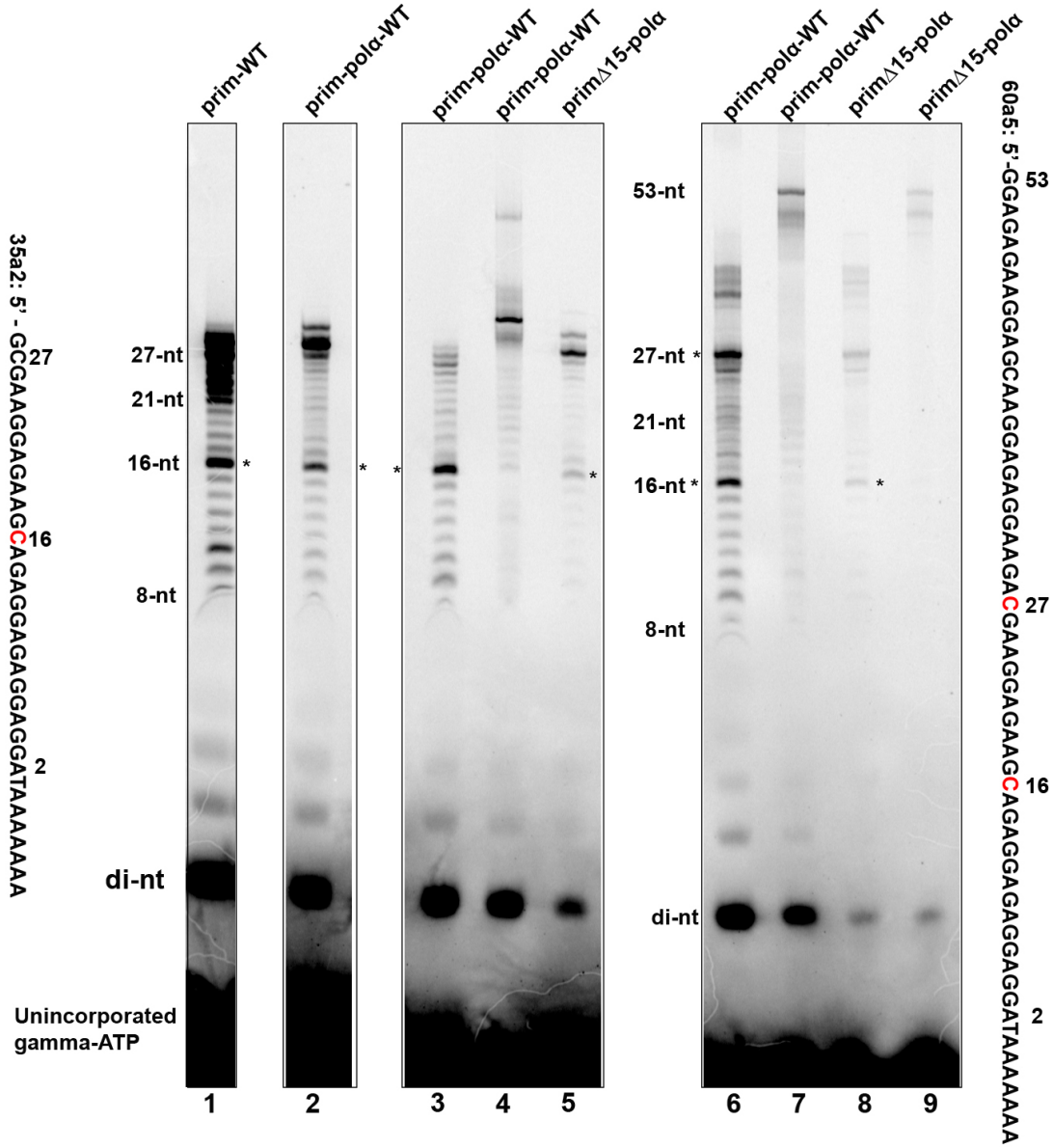
prim-WT
prim-polα-WT
prim-polα-WT
prim-polα-WT
primΔ15-polα
prim-polα-WT
prim-polα-WT
primΔ15-polα
primΔ15-polα
35a2: 5' - GCGAAGGAGAAGCAGAGGAGAGGAGGATAAAAAA
60a5: 5'-GGAGAGAAGGAGCAAGGAGAGGAAGACGAAGGAGAAGCAGAGGAGAGGAGGATAAAAAA
27
16
2
53
27-nt
21-nt
16-nt
8-nt
di-nt
Unincorporated
gamma-ATP
1
2
3
4
5
6
7
8
9

Figure 3.10. ***De novo*** **activity of the human primase and mutants with shortened linker of p58 on longer 35a2 and 60a5 templates.** Lanes 1-5, *de novo* activity on 35a2 template; lanes 6-9, *de novo* activities on 60a5 template. Sequences of two templates are labeled on each borders of the figure. The mis-incorporation by primase across template in lanes 1, 2, 3, 5, 6, and 8 are labeled as "*". Lane 1, wild-type primase dimer with 100 μM ribo-CTP and UTP; Lane 2 and 6, wild-type primase-polα tetramer with 100 μM ribo-CTP and UTP; Lane 3, addition of 400 μM aphidicolin compare to lane 2; Lane 4, addition of 10 μM dTTP, dCTP, dGTP compare to lane 3; Lane 5 and 8, primase(Δ15)-polα tetramer with 100 μM ribo-CTP and UTP; lanes 7 and 9, wild-type primase-polα tetramer or Δ15 variant with 100 μM ribo-CTP and UTP and 10 μM dTTP, dCTP, dGTP.

3.2.8. The C-terminal domain of p58 subunit interacts with the 5' triphosphate (tri-P) group of the RNA primer during primer extension and thus determines what number of nucleotides primase synthesizes.

RNA primers synthesized by primases or RNA polymerases are from the *de novo* syntheses and contain the triphosphate moiety at the 5'-terminus (70). Gel shift analysis of the DNA template annealed with RNA primers that contain 5' tri-P and template that has 3' overhangs enhanced binding with primase and p58C (71). The K_d values for different template/primer substrates containing 5' tri-P in primer or possessing 3' overhang in the template were determined using competitive inhibition assay. The inhibitors used in this assay were unlabeled templates/primer duplex that templates contain either 3' overhang (18a1; Table 2.3) or not (12a1; Table 2.3) when anneal with primers that contain either with (5'tri-P7; Table 2.3) or without (P7; Table 2.3) the 5' tri-P. The fluorescent-labeled rA_{15} annealed with poly-dT_{70} resembles an analog of T1-P2 because it is missing tri-P. The optimal substrate 18a1/5'tri-P7 showed fairly high affinity to primase (Kd = 36.0 nM), while the absence of the 3'-overhang or tri-P or both reduced the enzyme-DNA/RNA complex strength approximately 90-, 360-, and 4,000-fold, respectively. (Figure 3.11). Moreover, primase exhibited similar affinities to ssDNA (18a1) and the DNA/RNA duplex without tri-P and the 3'-overhang (12a1-P7). Together with the gel shift data these results indicate that the 5'tri-P in the primer and the 3'-overhang on the template play a key role in template-primer binding.

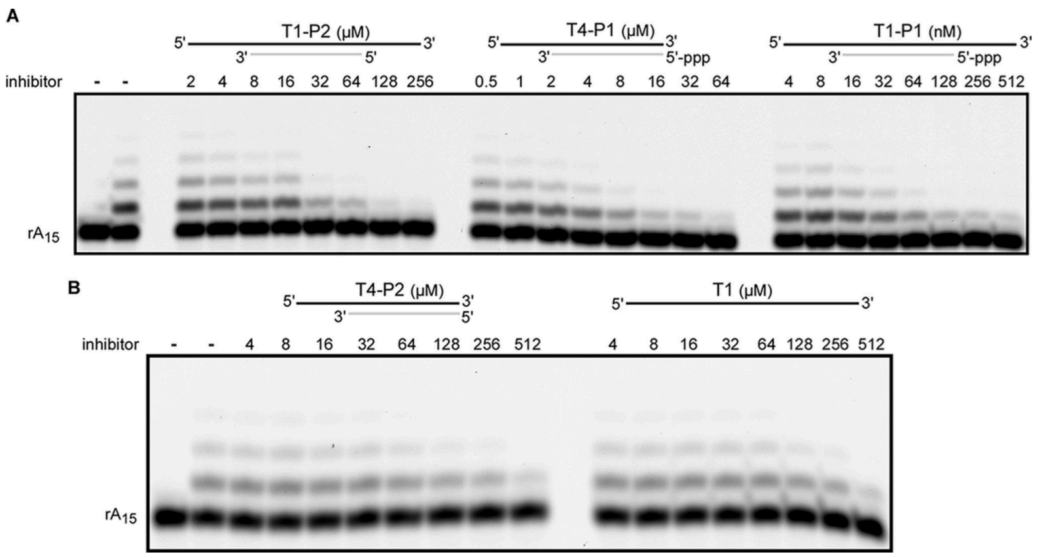

FIGURE 3.11. **Inhibition of rA15 primer extension on dT70 template by substrates with different structures**. Panels A and B correspond to two representative gels. Reactions were conducted for 10 minutes at 30 °C and analyzed by 16% Urea-PAGE. Left lane is control incubation without enzyme. On the top schematics, DNA and RNA strands are shown by black and gray lines, respectively.

To examine the functional consequence of this interaction, the primer extension assay were carried using primers and templates designed with or without the binding elements (provided by laboratory of Dr. Tahirov). Briefly, template 60a7 contains the 3' overhang when it's annealed with the primer 5'-tri-P6 or P6, whereas the shorter 53a1 does not. The 5' sequences for synthesis are identical, with a cytosine in the template after the position annealed with the primer that is supposed to incorporate the 33P-labeled-αGTP by primase. The 6-nt RNA primer 5'-tri-P6 containing the tri-P group was synthesized by T7 RNA polymerase *in vitro* and purified as described (71). The chemically synthesized P6 primer is a control. In order to avoid *de novo* synthesis, the pyrimidines were excluded from the single-stranded (ss) regions of the DNA template. Primase incorporates the first 33P-labeled-αGTP marks the start position of the synthesis (Figure 3.12A, lane 2 and 9). There is a mobility change of the two primers due to the 3 additional negatively charged phosphate groups in the 5'tri-P primer. Combinations of the two primer variants and two template variants were tested (tri-P/60, no-P/60, tri-P/53, no-P/53). The product pattern (lanes 3 and 4) is similar to *de novo* synthesis in the 5' tri-P primer with template with 3'overhang. 5'-triphosphate has stronger impact on primase activity in comparison to the 3'-overhang (comparison of *lanes 7, 8* and *10, 11*, respectively). The absence of tri-P results in an approximately ten-fold activity loss (comparison of *lanes 4* and *10*) and significantly reduces the mobility of RNA primers on the gel (comparison of *lanes 2* and *9*). Primase efficiently counts the primer length on tri-P/overhang substrate: the major products have the length of 8-10 nucleotides independently of reaction time (lanes 3 and 4). The absence of the 3'-overhang or TriP significantly affects this intrinsic primase ability to terminate synthesis, which results in

dramatically raised ratio of products with length >10 nucleotides (*lanes 8* and *11*). The increase of enzyme concentration altering the enzyme to a substrate ratio from 1:20 to 1:2 has little impact on the intrinsic primase ability to terminate synthesis at the defined primer length (Figure 3.12B). The primase activities were estimated and labeled below the figure. The absence of the 3 -overhang results in a 4-fold reduction in activity (comparison of lanes 3 and 7). Tri-P has a stronger impact on the primase activity in comparison to the 3'overhang (comparison of lanes 7 and 10). In the absence of p58C, primase does not sense tri-P and the 3'overhang and cannot count the primer length even on the optimal substrate (Figure 3.12A, lanes 15 and 16). The deletion of p58C dramatically reduces RNA-polymerizing activity to a level close to that for the wild-type primase on the worst substrate, no tri-p or overhang (comparison of lanes 12 and 15). No primase de novo activity was observed on the T6 template in the absence of the primer after 2 min of incubation with a 50 nM enzyme (Figure 3.12A, lane 6), whereas the 8-fold increase of incubation time and the 10-fold increase of enzyme concentration (80-fold total) resulted in a significant level of products synthesized de novo (Figure 3.12A, lane 14). The level of de novo synthesis observed in lane 14 (no primer) is enhanced 2-fold in comparison to lane 13, where approximately half of DNA molecules are primed by RNA and could not serve as templates for dinucleotide synthesis. Taking this into account, we can conclude that most of the products seen in lane 13 (Figure 3.12A) are generated during the extension of a 6-mer primer. These data together with the gel shift result (not shown, (71)) indicate that the 5'tri-P from the RNA primer and the 3'-overhang at the template binding with the p58C is important for primase to extend limited numbers of bases efficiently (Figure 3.11).

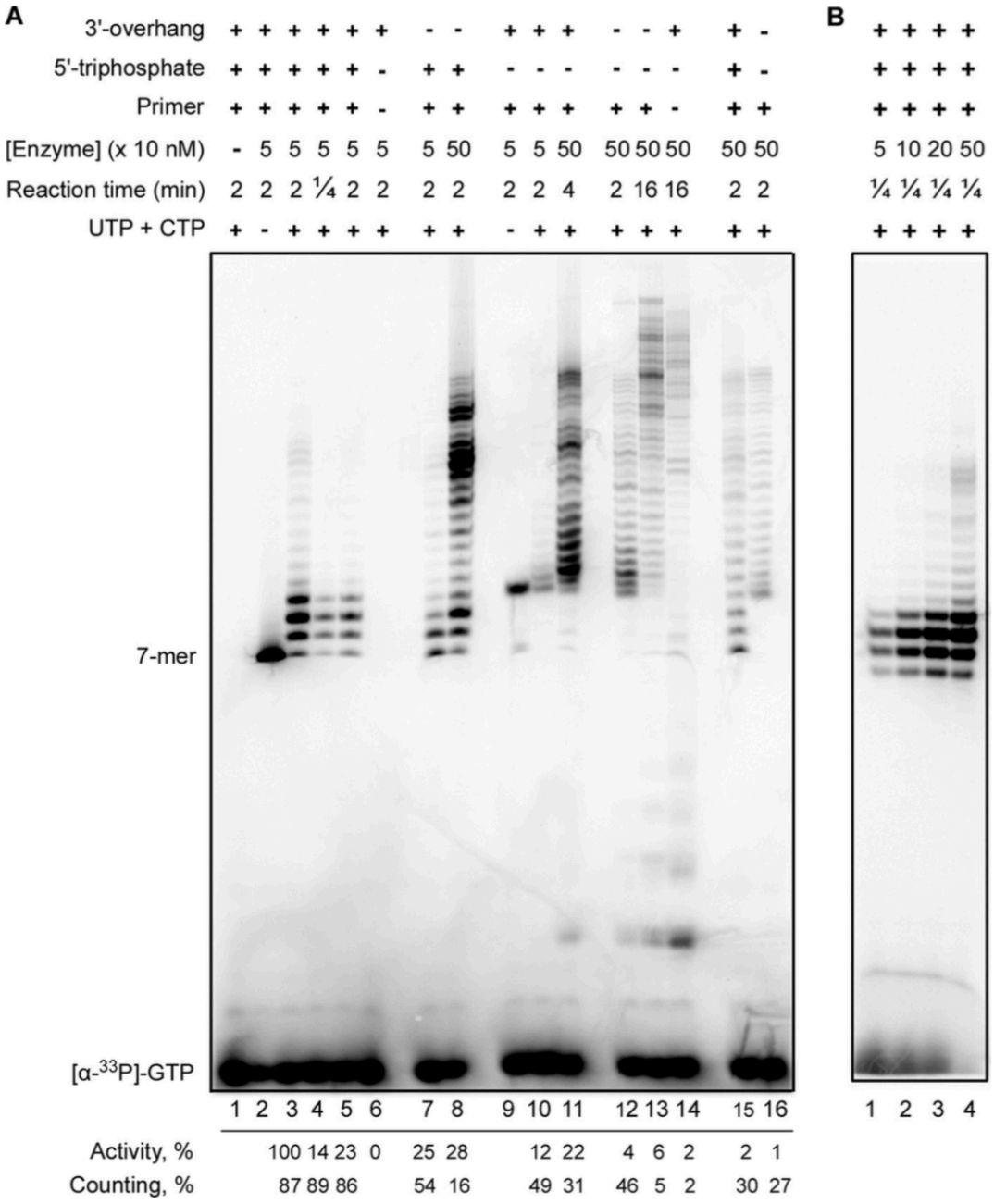
A
3'-overhang + + + + + + - - + + + - - + + -
5'-triphosphate + + + + + - + + - - - - - - + -
Primer + + + + + - + + + + + + + - + +
[Enzyme] (x 10 nM) - 5 5 5 5 5 5 50 5 5 50 50 50 50 50 50
Reaction time (min) 2 2 2 ¼ 2 2 2 2 2 2 4 2 16 16 2 2
UTP + CTP + - + + + + + + - + + + + + + +
7-mer
[α-33P]-GTP
1 2 3 4 5 6 7 8 9 10 11 12 13 14 15 16
Activity, % 100 14 23 0 25 28 12 22 4 6 2 2 1
Counting, % 87 89 86 54 16 49 31 46 5 2 30 27
B
5 10 20 50
¼ ¼ ¼ ¼
+ + + +
1 2 3 4

Figure 3.12 **Effects of the template-primer structure and p58C on primase activity**. Primase activity was analyzed in reactions of extension of 6-mer RNA primers (with or without tri-P) annealed with 53- or 60-mer DNA templates. The products were labeled by incorporation of [α-33P]GTP at the 7th position. Note that the negatively charged tri-P moiety significantly increased the mobility of RNA primers. A, analysis of the primase activity of primase-polαCTD (lanes 1–14) and primaseΔ[Fe-S]-polαCTD (lanes 15 and 16). Lanes 1–5 and 15, tri-P/60; lanes 6 and 14, ss 60a5 template for de novo synthesis; lanes 7 and 8, tri-P/53; lanes 9 –11, no-P/60; lanes 12, 13, and 16, no-P/53. Reactions corresponding to lane 5 contained 10 μM GTP. Quantification of the data is provided under each lane below the gel. The intensity of all bands was determined for estimation of the relative primase activity normalized to the protein concentration (the highest activity level was taken for 100%). The primase counting ability was calculated as the ratio of the combined intensity of the bands corresponding to the 8, 9, and 10-mer primers to the total intensity of all products, multiplied by 100%. B, effect of the enzyme-template ratio on the primase ability to terminate primer synthesis at the defined position. Reactions were run at the same conditions as for lane 4 (panel A) except the concentration of primase-polαCTD was varied.

To further characterize the observed sequence-dependent counting of primase synthesis (Figure 3.9 and 3.10) in *de novo* assay, factors influencing the product's length were analyzed in an extension assay using the natural template/primer contain the tri-phosphate and overhang. One difference between the *de novo* assays and extension were the type of divalent metal used, manganese vs. magnesium, respectively. Primase was inhibited several fold when Mg^{2+} concentration decreased from 5 mM to 0.5 mM (Figure 3.13, lanes 4, 6, and 8), whereas the reduction of the Mn^{2+} concentration enhanced activity (lanes 9, 11, and 13). Moreover, primase demonstrated a different response to monovalent salt (KCl) concentration depending on the type of divalent metal in the reaction. In the presence of Mg^{2+}, primase activity was inhibited almost 4-fold by increasing the salt concentration from 15 mM to 150 mM (lanes 5–7), whereas in the presence of Mn^{2+}, salt stimulated RNA synthesis (lanes 10 –12). We compared primase counting at the previously used conditions (Figure 3.9) and the current ones. At 50 mM KCl, the level of the unit-length primers was lower in the presence of 2 mM Mn^{2+} in comparison to 2 mM Mg^{2+} (lanes 6 and 11). The increase of KCl salt concentration from 50 mM to 150 mM reduced the counting effect in the presence of 2 mM Mg^{2+} (lanes 6 and 7), whereas the opposite effect was observed in the presence of 2 mM Mn^{2+} (lanes 11 and 12). The pronounced ability of primase to count the primer length is not due to peculiarities of the template sequence. Primase demonstrated the same behavior on the heterogeneous template 33a5 (Table 2.3; Figure 3.13, lane 3).

To verify that the primase cannot extend the longer primer with the 5' tri-P group, primase extension activity on 6-, 9-, and 10-mer primers were compared (Figure 3.13). Primase extends a 6-mer primer very efficiently (lanes 2 and 3), whereas extension of 9-

mer (lanes 8 and 9) and especially 10-mer primers (lanes 4–7) is dramatically decreased. The result means that primase not only terminates primer synthesis when its length is nine nucleotides, but also cannot efficiently extend the unit length primers. When compared to the result in Figure 3.12, there are small amount of synthesis beyond the 10 nt point. This suggests that primase has difficulties to transform from the apo-form to the active-form, which the active site in p49 is difficult to reach the 3' end of the primer if the "natural" primer is 9 or 10 nt. When the primase started with a shorter primer (e.g. 6 nt), the continuous mode of synthesis allows primase to make a decision to either dissociate, or continues, which possibility will be lower for the later if the substrate is "natural".

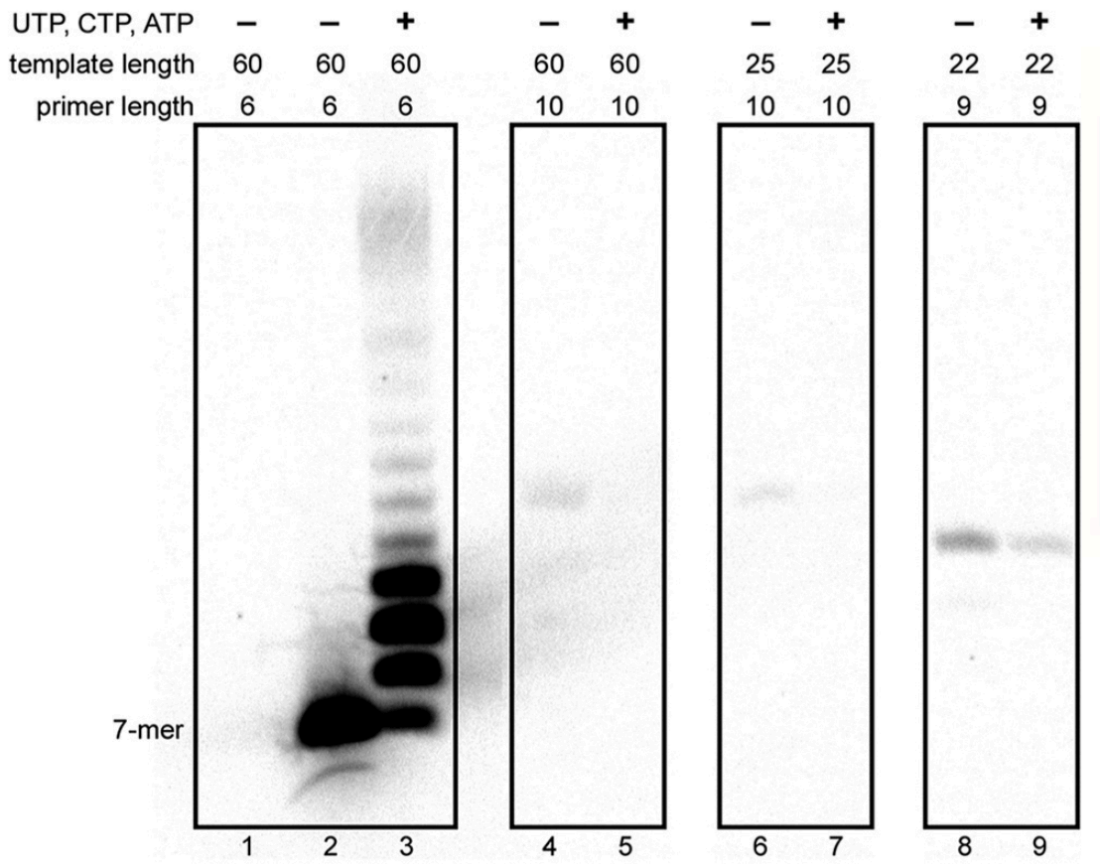

Figure 3.13. Length of the RNA primer affects primase-polαCTD activity. Lanes 1–3, 60a7/5'tri-P6; lanes 4 and 5, 60a10/5'tri-P10; lanes 6 and 7, 25a3/5'tri-P10; lanes 8 and 9, 22a6/5'tri-P9. Reactions corresponding to lanes 2, 4, 6, and 8 were conducted in the presence of [α-33P]-GTP alone to show the position of the first product of primer extension. Reactions corresponding to lanes 3, 5, 7, and 9 were supplemented with 0.1 mM each UTP, CTP, and ATP. Reactions were run for 2 min at 35 °C, and products were resolved by 20% urea-PAGE.

3.2.9. Primase to polα switch in the presence of polα and dNTP

To define the precise position of the switch (i.e. the length of the primer at which the 3' end of RNA primer becomes accessible for the polα catalytic site), we analyzed the products of primase•polα tetramer-catalyzed extension of a 6-mer primer with various composition of the rNTPs/dNTPs pool (Figure 3.14A). The template sequence directs incorporation of UTP/dTTP at the 8 to 10th positions and CTP/dCTP at the 11th position of the primer. The incorporation of dNMPs (versus rNMPs) could be distinguished because of slightly higher mobility of the corresponding products on the gel. In the presence of both ribo- and deoxy-NTPs, the primase incorporates only ribonucleotides (Figure 3.14A, lane 1). Analysis of the products generated by the tetrameric polα reveals that the insertion of dNMPs begins from the 10th position (lanes 2 and 3). This means that Polα can gain access to the 3'-end of the primer when its length is 9 nucleotides or longer. The exclusion of dCTP (lanes 5 and 6) or both CTP/dCTP (lanes 8 and 9) from the reaction, which inhibits the processive primer extension by Polα, demonstrated that 10-mer primers mainly contain the 3'-dTMP. In the absence of dTTP, the primase to Polα switch with a 9-mer primer is abrogated and we can observe the switch with a 10-mer primer (lanes 11 and 12). These results clearly show that the switch mainly happens when the primer length is 9. If Polα is unable to pick up the 9-mer primer, it can easily start with a 10-mer. Incorporation of dTMP was not observed using templates 58a and 59a that were designed to stop both primase and polα synthesis after synthesis of the 8- and 9-mer primers (no CTP/dCTP in reaction), respectively (Figure 3.14B). These results confirm that Polα cannot start extension of primers shorter than 9-mer (when p58C holds them) and sup- port the structural model (Figure 3.13).

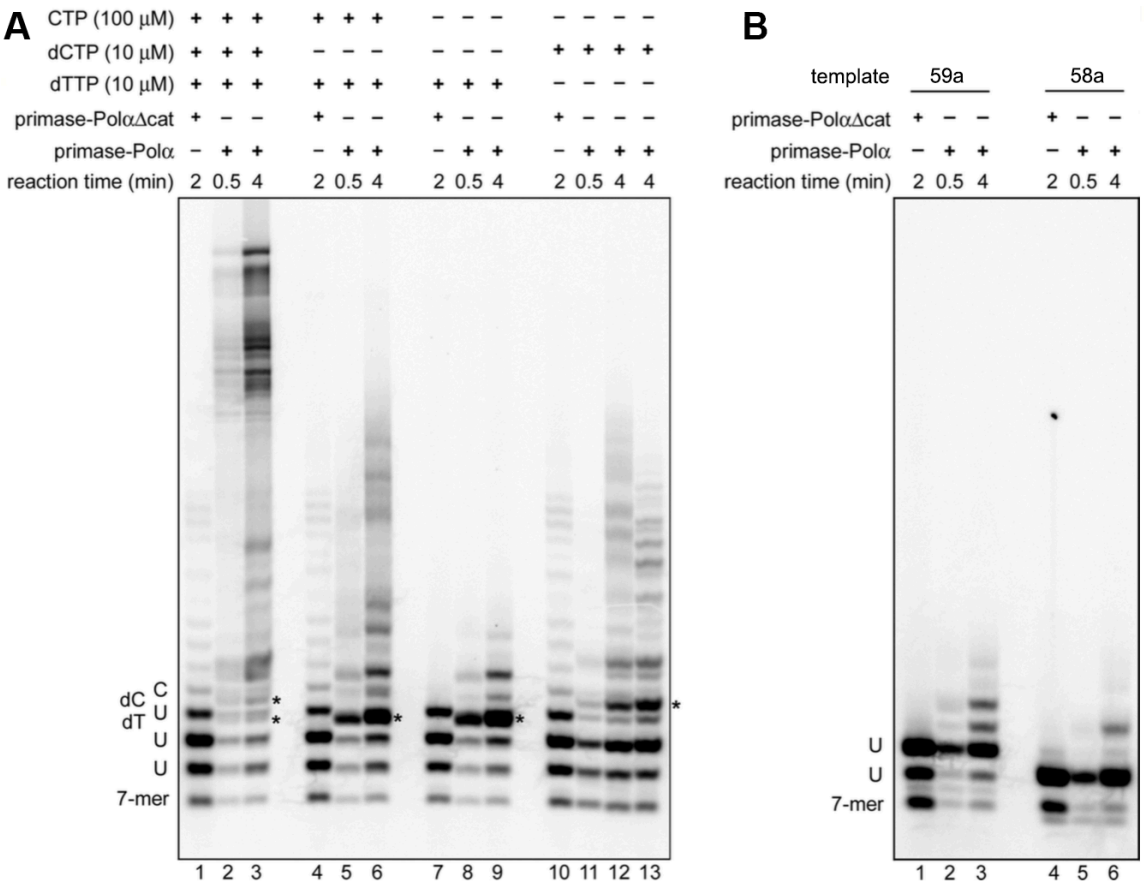

Figure 3.14. **Determination of the start position of polα for RNA primer extension**. A and B, analysis of the ribo- and deoxy-NTPs incorporation using the 6-mer RNA primer 5'tri-P6 annealed to the 60-mer DNA template 60a10 (A) or to the 59-mer and 58-mer DNA templates 59a and 58a, respectively (B). All reactions in panel A contain 100 μM UTP; all reactions in panel B contain 100 μM UTP and 10 μM dTTP.

3.3 Discussion

This chapter describes experiments aimed at the elucidation of the role of the highly conserved polα B subunit (p70) and the C-terminal domain of polα catalytic subunit (p180C). The function of the CTD of the large subunit of primase (p58), necessary for the initial dinucleotide synthesis, is also investigated.

Polα is composed of a large catalytic subunit and a smaller B-subunit. Only the catalytic domain of the large subunit is necessary for the DNA synthesis, however its CTD and B-subunit are required for the replication and cell viability (72,73). The contact between the B-subunit and the CTD with primase is thought to tether primase to the replisomes and origins (36,46,74,75). The exact role of the polα CTD and B-subunit in primer synthesis is unknown. In the SV40 replication system, polα synthesizes the whole viral genome (5.2 kb) in the presence of the viral helicase (large-T antigen) through the helicase interaction with p49, p70, and p180 (48,76,77). The most critical contacts seem to be with the N-terminus of p70 (48). We have found that the presence of p70•p180C sharply increases the lengths of the reaction products, most likely affecting the primase processivity (Figure 3.2). The binding to p180C can stabilize the p58N domain, which is proposed to be involved in the interaction with the DNA-RNA hybrid duplex (78). Furthermore, p180C by itself may participate in stabilizing the primase complex with the RNA-primed template because it is located near p58N. Yeast p70•p180C heterodimer has OB-fold and Zn-finger domains and possesses a micro-molar affinity to dsDNA (36).

The deoxynucleotides act as natural competitive inhibitors of primase during the primer extension reaction (Figure 3.2B, lanes 3-5). Primase inserts first dNTP with the efficiency close to that of rNTPs but slowly extends from them (Figure 3.3). It's probably

due to that primase lacks significant selectivity between ribo- and deoxy-nucleotides and the inhibitory effect of deoxyribonucleotides is mediated by an inefficient extension. Primase has two NTP binding sites: so-called initiation and elongation sites. In the course of dinucleotide synthesis the "initiation" site binds NTP, which becomes the 5'-terminal nucleotide of the primer. Biochemical and structural data accumulated so far indicate that primase uses the same set of functional residues for dinucleotide synthesis and its extension, which means that the 3'-terminal nucleotide of primer is located in the initiation site (65,79,80). Our data indicate that the initiation site is more selective for rNTPs than the elongation site. Primase is known to synthesize the RNA primer 8 to 10 nucleotides long, which is then extended by polα to 30 nucleotides (17,51,70). In vitro biochemical evidence from our study and others suggests that the heterodimeric primase is a low-processivity enzyme, but it is capable of synthesis far beyond 10 nucleotides by iterative cycles of synthesis (41,43). We confirmed that the interaction of primase in a tetrameric complex with polα is mediated by binding of pri2N to p180C (Figure 3.1C). This stabilizes the complex and enhances primase activity (Figure 3.2). The presence of polα inhibited the primase activity in the reactions containing rNTPs but no dNTPs. This suggests that polymerase and primase activities of the complex are competitive in vitro. In the crystal structure, polα establishes an elaborated network of contacts with nine bp of DNA-RNA duplex (52) and should effectively capture an RNA primed template when the primase synthesizes the unit length primer. This reduces the effective amount of primers available for the primase.

The X-ray crystal structures of the p58C and its analog from yeast are available (44,64,81). The folding of the region that binds single-stranded DNA indicates that the N-

terminus of the p58C can adapt to become α-helical or β-sheet structure, which suggests possible conformational change during priming (81). Based on our data that p58C does not interact with the other parts of the polα-prim complex (Figure 3.1C), it is possible that the p58C domain is flexible by itself and in respect to other parts of the complex. This domain may act as an extra finger domain that binds to the first 5' nucleotide for the critical rate-limiting step of di-nucleotide synthesis.

Ribonucleotides at high concentrations inhibit B-family pols in a step preceding base pairing (82). Polα strongly prefers dNTPs over NTPs (83), therefore, in the absence of deoxynucleotides it does not participate significantly in primer extension. We also observed a limited RNA and robust DNA pols activity of the tetrameric complex in reaction with a mixed pool of nucleotides (Figure 3.5). These results demonstrate that the primase is a non-processive enzyme, whose activity is further suppressed in the polα-prim complex. In the presence of primase in the polα complex, the product length increased (Figure 3.5, compare lanes 5-7 to 11-13). Polα-primase complex has two active sites for the primed DNA template, which increases the probability of substrate binding. After initial binding in the primase active site and following extension, the substrate might be translocated to the polα active site without dissociation from the complex (39).

The comparison of the catalytic activity of the polα p180ΔN-core and p70•p180ΔN indicates that the catalytic activity of polα is negatively regulated by p70•p180C. The active conformation of the yeast polα core appears to be in tighter contact with the DNA-RNA duplex (52) in comparison to RB69 polymerase (gp43), a prototype of the eukaryotic B-family pols α, δ, ε, and ζ, which lacks the distinctive C-terminal domain and B-subunit (11,84). The C-terminal domain and the B-subunit of polα are not required for

its catalytic activity. We propose that the p70•p180C in the polα complex interferes with the formation of the ternary complex including the primer/template duplex and deoxynucleotides. The structure showed that the p70•p180C is positioned in the complex in a way that lowers accessibility of the polα active site (40), because entry to the DNA-binding site is blocked by the Zn2 module of p180C and oligonucleotide/ oligosaccharide-binding domain-fold of p70 (40). This structure explains why the p180ΔN-core activity is higher than polα dimer (Figure 3.4, 3.6).

Additional evidence that supports that the C-terminal domain and B-subunit play a role in regulation of polα activity is the suppression of the inhibitory effect of p70•p180C on pol activity by the optimal concentration of DTT (Fig.7 C and D, note that the p180ΔN-core works completely independently of the DTT concentration). It is noticeable that certain concentrations of DTT also result in a change of the distribution of sizes of DNA fragments synthesized by p70•p180ΔN. DTT is a well-known agent modulating DNA polymerases activities in vitro (77). It is thought to reduce the intra-molecular disulfide linkages that may affect p180C folding (85). The p180C contains two highly conserved four-Cys motifs, which bind either two Zn atoms or one Zn and one Fe-S cluster (30,37,52).

Recent X-ray crystallography work from Dr. Tahirov group provided an insight of how primase *de novo* synthesis happens. First, the p58C first binds to the template DNA, which forms 13 hydrogen bonds. The His-300, Arg-302, His-303, Arg-306, Tyr-345 residues of p58C form 6 hydrogen bonds with the β - and γ-phosphates of the triphosphate moiety of the first GTP (40). There is also a divalent Mg (or Mn) ion that further stabilizes the complex. This multi-residue and Me^{2+} enhanced interaction is

unique compare to DNA polymerases, which explains why primase is needed for de novo synthesis.

Based on our biochemical experiments, we propose that the tri-P of the initiating nucleotide, which forms the 5'end of the RNA primer, interacts with p58C during both stages of primer synthesis; therefore, p58C always stays bound to the DNA/RNA junction at the 5'end of the primer, whereas p49-p58N moved away from the p58C as the active site translocates the 3'terminal of the substrate. This mode of template-primer binding predicts the increasing distance between the two functional domains during primer elongation and offers a mechanism for how the primase may count the primer length. Surprisingly, the structure shows that the flexible linker between p58N and p58C domains shortens during the synthesis of the RNA primer. The initial distance between p58C and N is 43 Å. The synthesis and substrate translocation pushes the p58C that bound to the 5' tri-P of the primer and template 3' end towards the p58N, which shortens the distance to 19 Å(40). This observation explains why the artificially shortened linker reduced the primase activity but did not change the size of the products (Figure 3.9, 3.10).

Structural and biochemical data suggest that during RNA primer elongation, p58C moves toward p180core, pushing it to dissociate from the p49. The p58C rotates 100 degrees after p49 releases the primer. Therefore it creates an opportunity for p180core to catch primer conveniently (40). The importance of the p58C is not only in the initiation stage (di-nt synthesis) of the primer synthesis, but also for its ability to coordinate the primase and polα catalytic activity via the binding to the template/primer during RNA primer elongation and switch.

CHAPTER 4: Interplay between divalent metal ions and substrates during DNA synthesis by polymerase α and other DNA polymerases.

Most of the material presented in this chapter is submitted for publication in the following article:

Zhang, Y., Baranovskiy, A.G., Tahirov, E.T., Tahirov, T.H and Pavlov, Y.I. "Divalent ions attenuate DNA synthesis by human DNA polymerase α by changing the structure of the template/primer or by perturbing polymerase reaction itself".

4.1. Introduction

DNA and RNA polymerases (pols) use at least two divalent metal ions (Me^{2+}), called A and B, at the specific positions of the active site during each cycle of polymerization (86). Early studies of several DNA and RNA pols revealed that the relative orientations of two Mg^{2+}, the 3'OH group of primer terminus, and the phosphates of incoming (deoxy)ribonucleoside triphosphate ((d)NTP) are invariant, despite the differences in pol domain structures and in the ways these Mg^{2+} are coordinated (87,88). The metal A increases the nucleophilicity by lowering the pK_a of the 3'-OH of the primer terminus. The metal B coordinates the triphosphate moiety of the incoming nucleotide (nucleotide binding) and subsequently facilitates the release of pyrophosphate. Both metals are required throughout the polymerase reaction: active positioning of the 3'-OH with α-phosphate by rearranging the side chains of carboxylate residues (Asp or Glu); stabilization of the pentacovalent intermediate during the transition state; and substrate translocation (89,90). Recent structural studies of DNA polymerases suggest there might be a third, transient, Me^{2+} in the polymerase active site that participates in the reaction (89,91,92). The newly discovered Mg^{2+}, for example in the polη active site, is seen only transiently after the formation of the pentacovalent intermediate, and probably stabilizes the intermediate and prevents translocation of substrate DNA before the completion of the reaction cycle (89). In addition to active sites, there are Me^{2+} binding sites elsewhere in polymerases with undefined roles. For example, around 20 Mn^{2+} binding sites were identified in *E. coli* DNA polymerase I (DNA pol I) (93).

Besides the role of metals in DNA polymerase reaction itself, divalent ions affect polymerase reaction indirectly, by effects on substrates of DNA polymerase reaction The

formation of unusual structures of DNA has a tremendous impact on DNA and RNA transactions in living organisms (94,95). Interactions of divalent metal ions with nucleic acids play a significant role in changing nucleic acid geometry (96). The severe effects of repeats in template DNA on pol reactions are ubiquitous (97). For example, the Klenow fragment and polα from calf thymus paused on repeats of $d(CT)_{27}$ (98,99); *Xenopus* DNA polγ and human polα stalled on templates containing poly-dT tracts (100,101). The inhibition was likely due to the formation of triplexes by a folded back repeated template DNA strand ahead of synthesized repeated duplex (illustrated in upper part of Figure 4.1), because it was alleviated when the 7-Deaza derivative of dATP, unable to form stable Hoogsteen pairs, was used for synthesis (100,102). High concentrations of Mg^{2+} increase the stability of triplexes and concomitantly impede DNA synthesis by thermostable pols (103).

Manganese (Mn^{2+}) is able to effectively substitute for Mg^{2+} by DNA pols *in vitro*, because of the close chemical properties of these two ions (104-107). Studies *in vitro* have shown that substitution with Mn^{2+} is not benign and increases error rates, drastically increases pol activity or changes the specificity of many pols (108-111), including polα (112). Another divalent ion that has often been found in DNA pols is Zn^{2+}. Purified *E.coli* DNA pol I contains Zn atoms at 0.1 to 2 moles per mole of enzyme, depending on the strain and purification method (113-116). The effects of Zn^{2+} on DNA pols are controversial. Both stimulation and inhibition of polymerase and exonuclease activities have been observed (117-120). A NMR study of polβ revealed that Zn^{2+} not only occupies the active site, but also adopts an active conformation analogous to Mg^{2+} (121).

Zn^{2+} also exhibits a higher affinity to triphosphates comparable to Mg^{2+} and Mn^{2+} (122,123).

The X-ray crystal structure of the catalytic domain of yeast polα with RNA/DNA substrates revealed that the RNA/DNA duplex forms an A-form structure that favors the binding of polα (124). The extension pattern of RNA primer showed a prominent stop as the size of synthesized DNA reaches 20 nt. This led to the hypothesis of the intrinsic mechanism of counting of the number of nucleotides in primer by polα due to a switch from DNA-RNA to DNA-DNA duplex (52). Experimental evidence was consistent with the idea, as yeast polα extended RNA primers much more efficiently compared to DNA primers and stopped after synthesizing no more than 20 nucleotides. However, the only template that has been used was poly-dT.

In this chapter, we show that both preferential use of RNA primers and counting can be observed only on the templates with homopolymeric runs. The pattern of products synthesized by human polα on poly-dT is similar to yeast polα, however, the pol synthesizes much longer products and has the same activity with either DNA or RNA primers on a template with a more natural random sequence. On poly-dT template, the length of DNA fragments synthesized by human polα was inversely correlated with concentration of Mg^{2+}. A systematic investigation of the effects of divalent metal ions on polα activity in comparison to other well-studied DNA pols indicates that the pattern of synthesis on the poly-dT_{70} template is determined by the effect of Mg^{2+} or Mn^{2+} on the formation of an unusual structure of DNA substrates/primers (Figure 4.1, upper part). This is not a general property of divalent ions, and Zn^{2+} disturbed the pol reaction itself

with peculiarities specific to each pol studied, prim·polα and the Klenow fragment (Figure 4.1, lower part).

Effect on DNA structure (triplex)

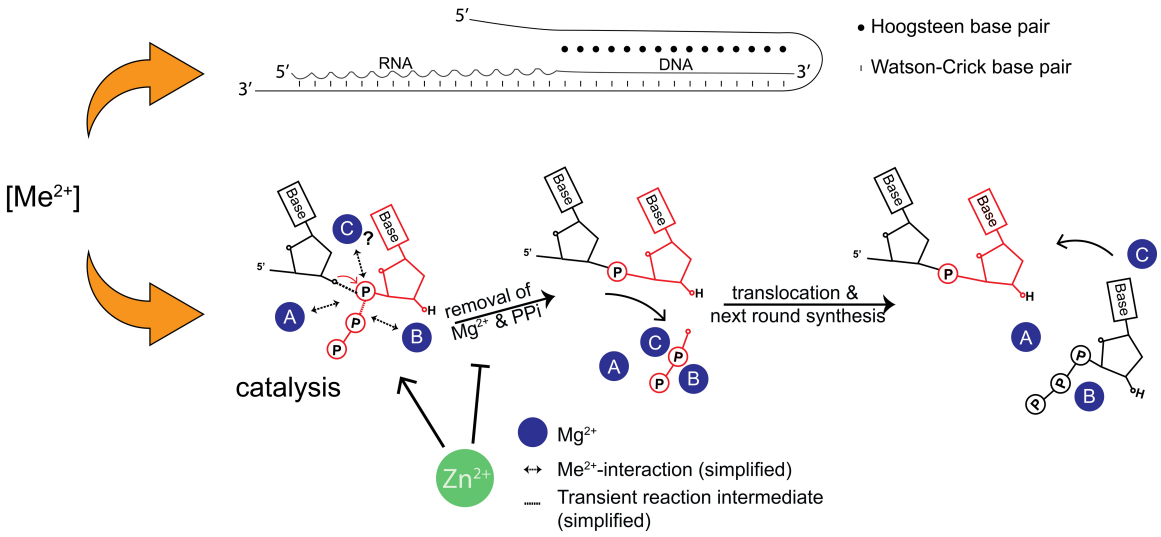

Effect on DNA polymerase active site

Figure 4.1. **Two mechanisms of Me^{2+} induced attenuation of DNA polymerase synthesis.** The *upper arrow* points to a mechanism of Mg^{2+} induced triplex formation the on poly-dT template. Our results indicate that this structure is most readily formed with the DNA•DNA duplex and ssDNA tail, but not the RNA•DNA duplex. Therefore, the rA_{15} primer can be extended by polα at high [Mg^{2+}], but polα is only stalled when a sufficiently long DNA duplex appears and the template DNA is folded back on it. The *lower arrow* points to a mechanisms of Zn^{2+}-dependent catalysis and inhibition. The complete replacement of Mg^{2+} (blue) by Zn^{2+} (green) supports the formation of an intermediate of the reaction, but subsequently inhibits the ion removal (in Klenow). The three-metal ion catalysis model is drawn here (with the metal site C). The transient involvement of the third metal is quite possible for polα, based on the modeling of the yeast polα active site with polδ (124). Generally, the Mg^{2+} occupies this site C after breakage of the bond between α- and β-phosphates of dNTP (89,92). It bridges the leaving pyrophosphate with the non-bridging oxygen of α-phosphate preventing further primer translocation. Then, the bridged reaction intermediates are removed through an unknown mechanism to allow the translocation of the substrate and entry into the next round of reaction.

4.2. Results

4.2.1. Polα preferentially uses RNA primers and synthesizes only around 20 nt on poly-dT_{70} template

We confirmed the observations on pattern of DNA synthesis by yeast polα synthesis on poly-dT70 template with DNA or RNA primers (52) using p180ΔN-core. The efficiency of the extension of the 15-mer DNA primer by p180ΔN-core is much lower in comparison to the 15-mer RNA primer (Figure 4.2A, note the different electrophoretic mobility of DNA vs. RNA). The efficiency of this reaction with both types of primers is increased when the concentration of dATP goes up (Figure 4.2B). However, most products remain short, about 20 nucleotides of newly synthesized DNA, despite overall stimulation. It appears that the addition of 20 nucleotides of DNA attached to 15-mer DNA or RNA is around the upper limit of the synthetic potential of the p180ΔN-core on this template (Figure 4.2B, lane 7, 8). The result is in agreement with the data for yeast polα with the same poly-dT template (124).

To explore whether this "20-mer rule" is a general or template-specific property of polα, we examined DNA synthesis by the same core enzyme in the extension of RNA and DNA 16-mer primers with identical heterogeneous sequences. We designed two different templates with a heterogeneous sequence and a single, fixed site of primer annealing. The first template, 73a, included a 35 homopolymeric-dT run at the 5' end. The second template, 73b, contained all heterogeneous sequences with the 3' 38-mer sequence identical to the template 73a. Surprisingly, the efficiency of the extension of DNA and RNA primers by p180ΔN-core was identical in the matched primer/template pair (Figure 4.3). Interestingly, the synthesis by the p180ΔN-core on template 73a was

prone to termination at positions around 20-nucleotides deep into the 35 homo-dT run. No such pausing was detected on the heteropolymeric 73b template, and polα reached the end of the template, similar to T4 DNA polymerase. We concluded that polα has a limited capacity for DNA synthesis only on the poly-dT template.

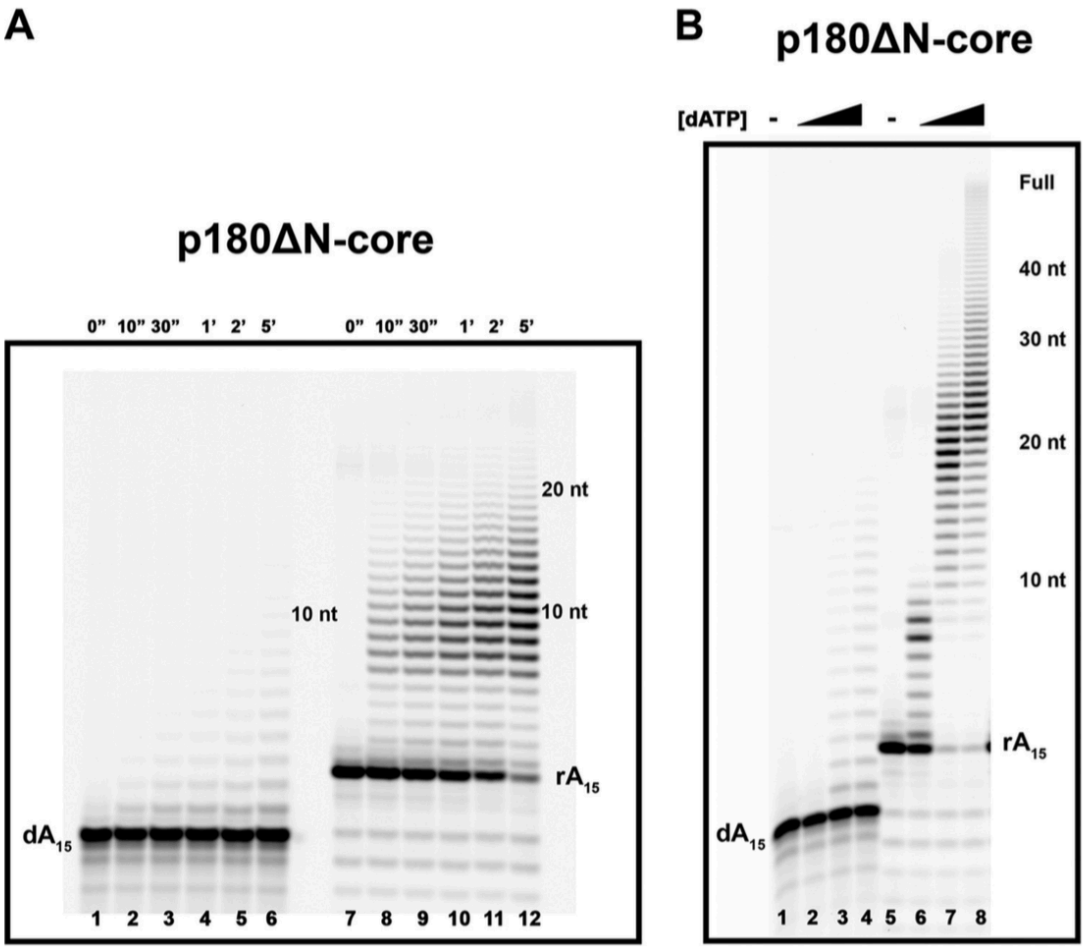
A
p180ΔN-core
0" 10" 30" 1' 2' 5' 0" 10" 30" 1' 2' 5'
20 nt
10 nt
10 nt
rA15
dA15
1 2 3 4 5 6 7 8 9 10 11 12
B
p180ΔN-core
[dATP] - -
Full
40 nt
30 nt
20 nt
10 nt
rA15
dA15
1 2 3 4 5 6 7 8

Figure 4.2 **Preferential RNA primer extension by human polα polymerase domain (p180ΔN-core) on the homopolymeric $(dT)_{70}$ template** . (A) Extension of the poly-dA_{15} and poly-rA15 primers (enzyme: primer/template ratios = 1:50 and 1:80, respectively) in the presence of 0.2 mM dATP. The products of reactions at the indicated time points were analyzed as described in Experimental Procedures. (B) The dependence of the extension of the poly-dA15 and poly-rA15 primers primers (enzyme: primer/template ratios = 1:50 and 1:80, respectively) on the dATP concentration. The black triangle indicates that the reactions were carried out with the increase of dATP concentrations (0.01, 0.1, and 1 mM, respectively). The reaction time was 20 min.

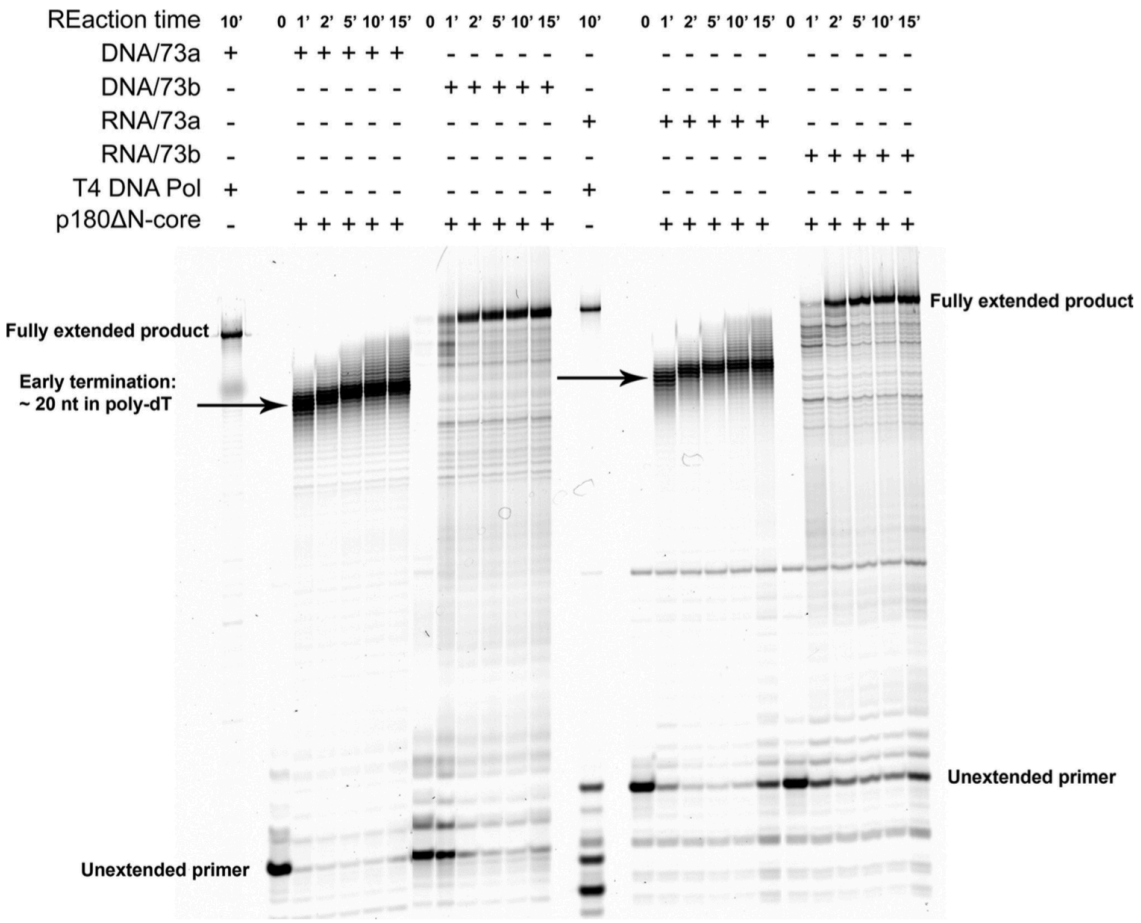

Figure 4.3. **Same efficiency of the extension of DNA and RNA primers on hetero-homopolymeric hybrid and heteropolymeric DNA templates by the p180ΔN-core**. For control of the full extension of the primers we have used reactions with T4 DNA polymerase, which robustly and completely extended DNA as well as RNA primers (left lane in left and right halves of the gel). Arrows show the zones of termination of DNA synthesis. All reactions contain 0.2 mM dNTPs and the enzyme to primer/template ratio was 1: 50, except for the T4 DNA pol (~1:2500).

4.2.2. Mg^{2+} and Mn^{2+} -induced barrier to polα progression simulates the effect of "counting" of the number of nucleotides in the product on the poly-dT_{70}.

The main obstacle for DNA pols on the poly-dT template maybe the formation of triplex DNA (100). To study why polα is virtually inactive on the poly-dT_{70} template with DNA primers but active with RNA primers (101,124), we have used several different assay conditions, varying enzyme/template ratio, temperature, reaction time and dATP concentrations. The DNA pol activity of all polα variants tested, single polypeptide catalytic core (p180ΔN-core), two-subunit polα, and the full four-subunit polα-prim (101), was invariably low at all of those different conditions (data not shown). There was one striking exception. When Mg^{2+} concentration was reduced from typically used 10 mM to 0.2 mM, the activity of the p180ΔN-core with DNA primers was recovered and became identical to its activity with RNA primers (Figure 4.4, lanes 2 and 3, 8 and 9). When the concentration of Mg^{2+} was increased to 0.5 mM, the activity of the p180ΔN-core was sharply reduced in the case of DNA primers (lane 4), in comparison to RNA primers (lane 10). However, the product size with RNA primers was shortened as [Mg^{2+}] increased above 0.5 mM, to less than 20 nt long at 16 mM (lanes 10-15). A similar pattern of synthesis by p180ΔN-core was observed with Mn^{2+} (Figure 4.5). It is noticeable that the high Mg^{2+} and Mn^{2+} concentrations did not inhibit the overall activity of the p180ΔN-core with RNA primers. The results of these experiments suggested a possibility that the formation of inhibitory triplex at high Mg^{2+} occurs right after annealing of the DNA template with the DNA primer and thus there is no synthesis by polα. Apparently, the RNA primer annealed to the DNA template does not promote

triplex formation, and the extension of RNA primer by a certain length of DNA is necessary before the triplex can form (Figure 1, upper part).

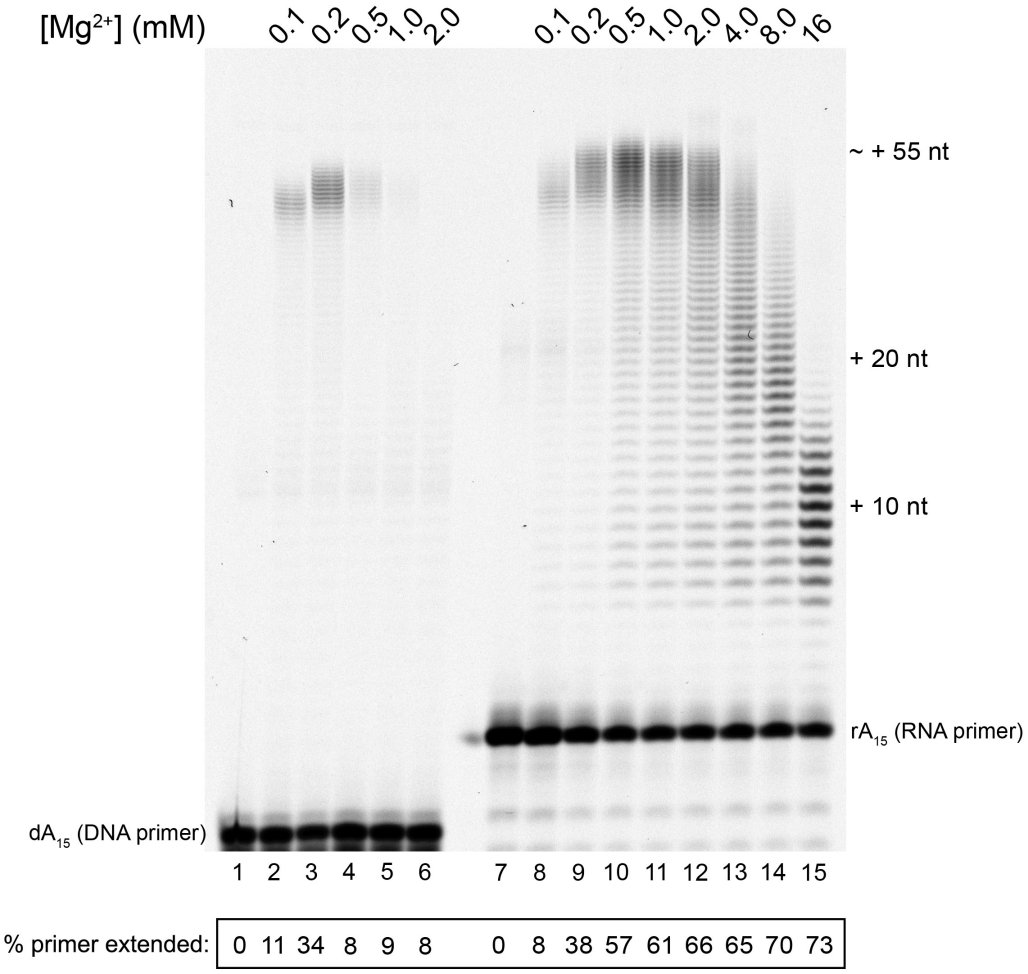

Figure 4.4. **High concentrations of Mg2+ attenuate DNA synthesis by the p180ΔN-core on the poly-dT70 template**. Extension of DNA (poly-dA15) or RNA (poly-rA15) primers was carried out by p180ΔN-core (enzyme to primer/template ratio = 1:15) in the absence of Mg2+ or in the presence of increased concentrations of Mg2+. Reactions were carried out at 35° C for 4 minutes. The efficiency of each reaction (number under each lane) was calculated as the percentage of extended primers.

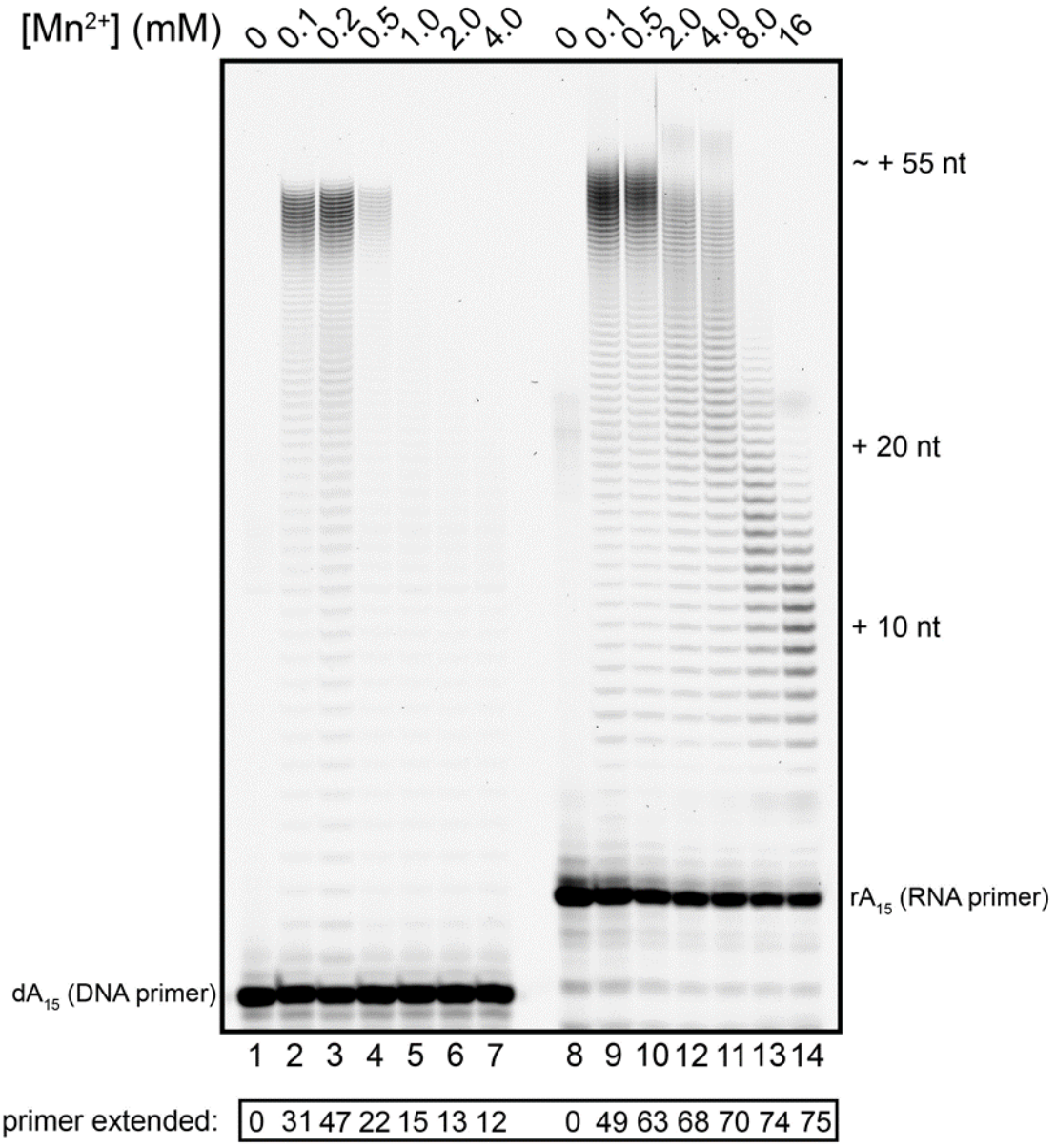

Figure 4.5. **High concentrations of Mn^{2+} attenuate DNA synthesis by the p180ΔN-core on the poly- dT70 template**. Extension of DNA (poly-dA15) or RNA (poly-rA15) primers by p180ΔN-core (enzyme to primer/template ratio = 1:15) in the absence or presence of up to 4.0 mM or up to 16.0 mM Mn2+, respectively. Reactions were carried out at 35 °C for four minutes.

The inability to perform efficient DNA primer extension is specific to the poly-dT template. Polα extends DNA and RNA primers annealed to heterogeneous sequence equally well (101,125). To examine the effects of [Mg^{2+}] on pol stalling on the internal poly-dT run positioned at a distance from primer, we used the hybrid template with 5' 35-nt poly-dT and heterogeneous sequence at 3' as the annealing site of the DNA primer. P180ΔN-core stalling was only observed within the 35-nt poly-dT zone (Figure 4.6). Increasing concentrations of Mg^{2+} moderately increased the usage of the primer and led to a progressive shortage of the length of products synthesized on the poly-dT template, simulating the decreased pol processivity. Apparently, the formation of a barrier for elongation, triplex DNA, occurred within shorter stretches of T/A duplexes with an increase of concentration of Mg^{2+} (Fig. 4.1, upper panel).

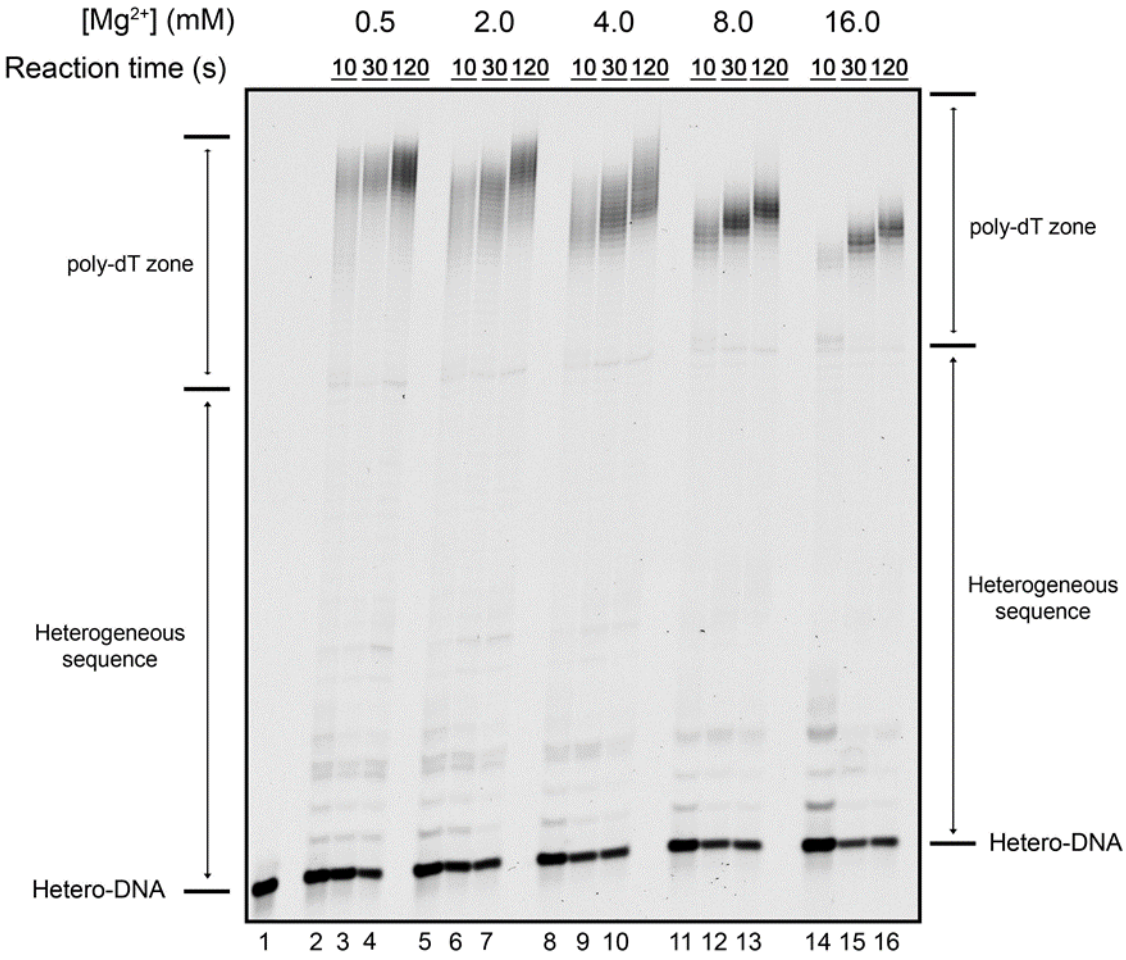

Figure 4.6. **Mg^{2+}-dependent inhibition of DNA synthesis occurs only on homopolymeric runs**. Extension of the hetero-DNA primers annealed to the hybrid poly-dT/hetero template (73a) by polα- core (enzyme to primer/template ratio = 1:20). Reactions were run in the presence of 0.5, 2, 4, 8 and 16 mM Mg^{2+} with three time points of 10, 30 and 120 seconds at 35 °C. The poly-dT zone indicates the 35 nt of the poly-dT sequence at the 5' half of the template.

4.2.3 Mg^{2+}-induced restraining of pol activity is relieved when synthesis occurs in the presence of 7-Deaza-dATP.

DNA pols can use 7-Deaza-dATP (7DdATP) instead of dATP (126). Due to the lack of a N7 atom (substituted by a CH group), 7DdATP does not efficiently participate in the formation of Hoogsteen base pairs in addition to the normal Watson-Crick base pairs. This property can be used in DNA pol reactions to relieve the negative effects of triplex DNA formation on pol synthesis (100). Human polα can utilize 7DdATP, albeit 2.5-fold less efficiently compared to dATP (127). The presence of 7DdATP did not affect the DNA primer usage mediated by Mg^{2+} ions in comparison to dATP, indicating that the Hoogsteen base pair-dependent triplexes were formed before the reaction (Figure 4.7A, and quantification in Figure 4.7C). The reactions with 7DdATP led to the recovery of longer products of extension. This suggested that the incorporation of 7DdATP readily disrupted the triplexes. Similar to the extension of dA_{15} primers, 7DdATP did not significantly affect the overall rA_{15} primer usage, but strongly relieved the premature synthesis termination at high concentrations of Mg^{2+} (Figure 4.7B, it is noticeable that the products with 7DdATP migrate faster than the dATP products). The products at comparable concentrations of Mg^{2+} were always longer with the deaza nucleotide, indicating that the formation of Hoogsteen base pairs in triplexes was impeded in a substantial proportion of DNA substrates. However, at 16 mM Mg^{2+} in reactions with 7DdATP, 50% of the extension products were still terminated around 10 nt. This suggested that high Mg^{2+} ions might stabilize the Hoogsteen base pairing regardless of the N7 atom.

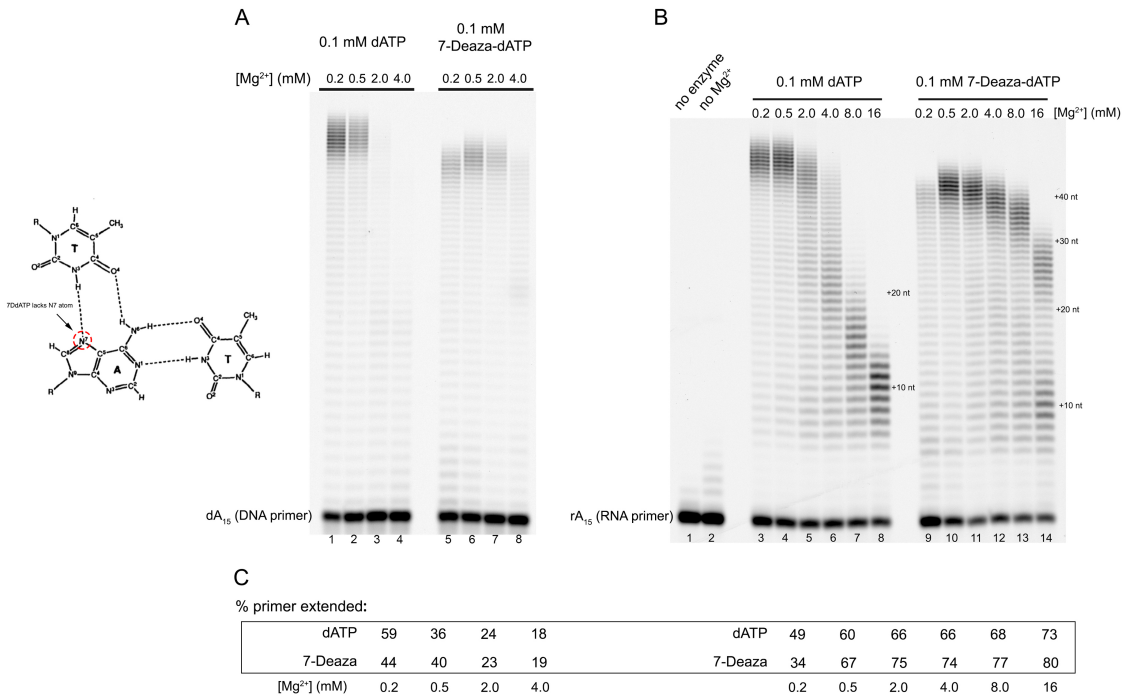

Figure 4.7. **Inclusion of 7-Deaza-dATP into reactions relieves polα pausing on the poly-dT template.** The Hoogsteen T•A•T hydrogen bonding is shown on the left (128). The N7 atom which 7DdATP lacks is highlighted and pointed. (A) Extension of DNA (poly-dA15) primers by human DNA polα core (enzyme to primer/template ratio = 1:5) using dATP (lanes 1-4) or 7DdATP (lanes 5-8) in the presence of 0.2-4 mM Mg2+, respectively. Reactions were carried out at 35 °C for 5 minutes. (B) Extension of RNA (poly-rA15) primers by human DNA polα core (enzyme to primer/template ratio = 1:10) using dATP (lanes 1-4; 1 min reaction at 35 ºC) or 7DdATP (lanes 5-8; 3 min reaction, due to the lower efficiency of 7DdATP incorporation by polα) in the presence of 0.2-4 mM Mg2+. Quantifications of the primer usage are below each panel. (C) Comparison of the efficiency of the pol reactions with dATP vs. 7DdATP.

4.2.4. Mg^{2+}-induced poly-dT template-specific stalling is characteristic of different DNA pols.

Polα-prim possesses two separate active sites responsible for RNA pol and DNA pol activities (101). The inhibitory effects of Mg^{2+} on synthesis on the poly-dT_{70} template with both DNA and RNA primers by the whole complex of polα-prim were similar to the single polypeptide p180ΔN-core possessing DNA pol active site only (Figure 4.8A). It meant that the primase part of the holoenzyme does not affect the parameters of DNA synthesis of poly-dT template. Experiments with different DNA pols, the Klenow fragment (Figure 4.8B) and yeast polδ (WT and exonuclease-deficient variant, Pol3-5DV (a generous gift from Dr. Peter Burgers laboratory at Washington University in St. Louis), 3-subunit complexes; Figures. 4.8 C and D, respectively) showed that the Mg^{2+} induced polymerase stalling on the poly-dT_{70} template was a general phenomenon not specific to polα. It was noticeable that yeast polδ was more resistant to the inhibitory effect of high concentrations of Mg^{2+} than the Klenow fragment and human polα, but still the effect was very clear. Thus, the high Mg^{2+} concentration promoted formation of triplex DNA is a strong barrier for different DNA pols.

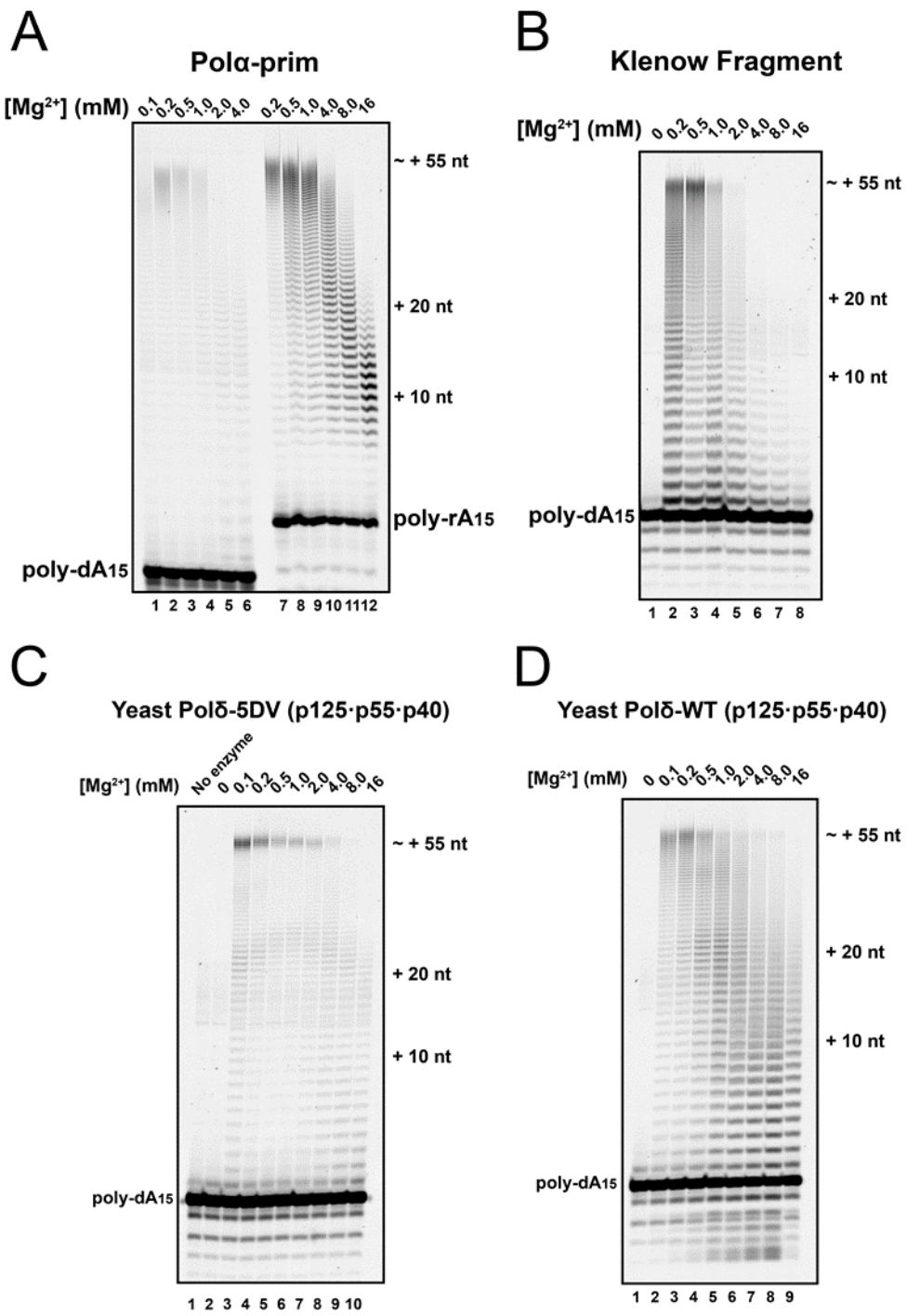

Figure 4.8. **High [Mg2+] stalls polα, the Klenow fragment and polδ**. (A) extension of DNA (poly-dA15) or RNA (poly-rA15) primers by polα- prim (enzyme to primer/template ratio = 1:15) in the presence of 0.1 to 4.0 mM Mg2+ or 0.2-16.0 mM

Mg2+, respectively. (B) Extension of DNA (poly-dA15) primer (0.15 μM) by the Klenow fragment (enzyme to primer/template ratio = 1:15) in the presence of up to 16.0 mM Mg2+. Reactions were carried out at 35° C for four minutes. (C) and (D) extension of DNA (poly-dA15) primers by 3-subunit yeast exonuclease-defective polδ-5DV and wild type polδ (enzyme to primer/template ratio = 1:15) in the presence of 0.1-16 mM Mg2+. Reactions were carried out at 35 °C for 10 minutes.

Next, to get more information on the effects of Mg^{2+}, we directly compared the polα-prim and Klenow fragment on the template with heterogeneous random sequences (73b, Materials and Methods). Polα extended the primer to the full length with an increasing efficiency when the concentration of Mg^{2+} elevated from 0.2 to 4 mM (Figure 4.9, lanes 2-5), then mildly slowed down at 8 mM (lane 6), and stalled more severely at 16 mM (lane 7). The Klenow fragment, on the other hand, reached its activity plateau at 0.2 mM Mg^{2+} (Figure 4.9, right panel), and produced almost the same pattern of elongated product over a range of concentrations of Mg^{2+}. Its activity was only slightly declined when [Mg^{2+}] was increased to 16 mM (lanes 9-14). It was noticeable that the early sites of termination of synthesis by the Klenow fragment were more pronounced at a low [Mg^{2+}] concentration, a mirror-like effect in comparison to polα-prim (lanes 9 and 10). These experiments confirmed that high concentrations of Mg^{2+} were harmful for pol reaction only when abnormal DNA structures could form.

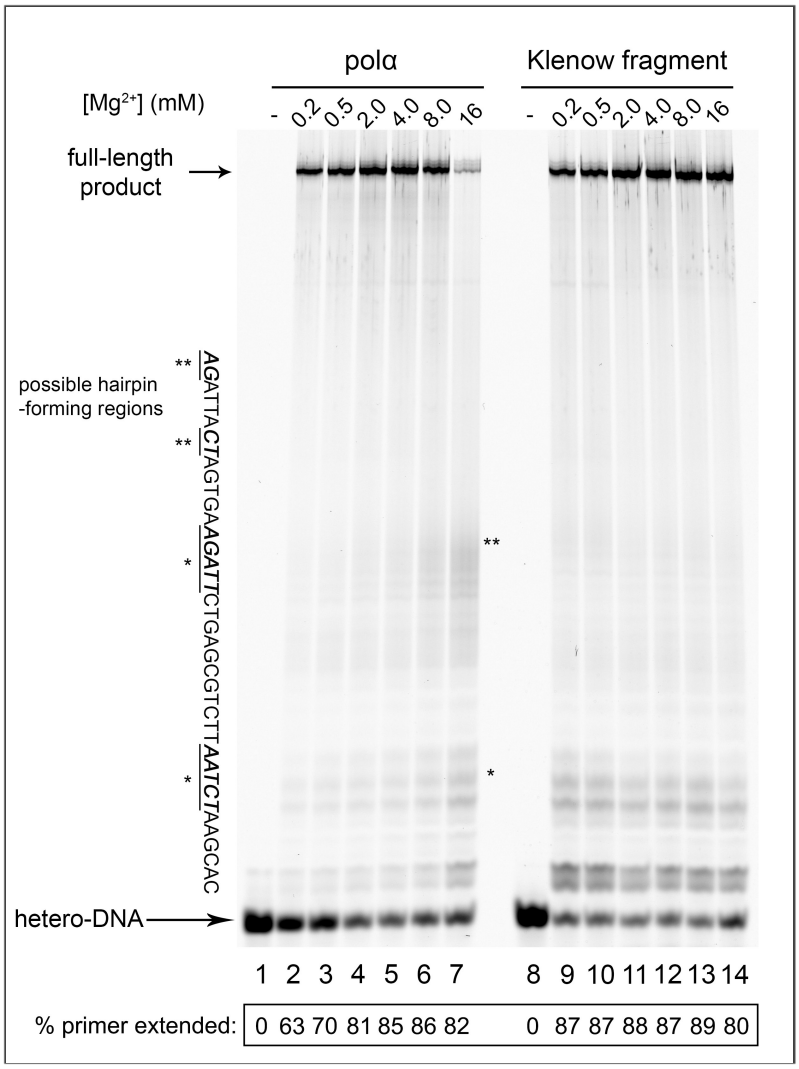

Figure 4.9. **Comparison effects of Mg2+ concentration on the activity of polα-prim and the Klenow fragment on the template with random sequence**. Sequence of the 3' portion of the template 73b (excludes the 5' primer-binding region) that can potentially form two hairpins (marked by * and **) is shown. The extension of hetero-DNA primers annealed with the template contains a heterogeneous sequence (73b) by polα-prim (enzyme to primer/template ratio = 1:15) and the Klenow fragment (enzyme to primer/template ratio = 1: 5) in the absence or presence of 0.2-16.0 mM Mg2+. Reactions were carried out at 35 °C for three minutes (polα-prim) and one minute (Klenow fragment).

4.2.5. Zn^{2+} -catalyzed polymerase reactions.

To explore whether the mechanism of Mg^{2+} effects seen in our experiments is a general feature of divalent metal ions, we studied the effects of Zn^{2+}. Zn^{2+} is not a traditional catalytic metal ion in polymerase reactions, but it could be tightly associated with polymerases. Two zincs are seen in the crystal structure of the C-terminal domain of the catalytic subunit of yeast polα (36). In the structure-based model of the human polα catalytic center (Figure 4.10), the metal site B was occupied by Mg^{2+} whereas the site A was occupied by Zn^{2+}. The Zn^{2+} at the A site showed octahedral metal coordination. The binding of Zn^{2+} in site A indicated that Zn^{2+} has a potential to influence (support or inhibit) the polymerase reaction. It's not well known how Zn^{2+} behaves in the DNA pol cycle. DNA synthesis by *E.coli* DNA pol I proceeds with Zn^{2+}, but at lower rate than with Mg^{2+} (114,117,118). In these earlier studies, only bulk incorporation was measured, which did not provide information on the sizes of reaction products. Zn^{2+} in fact forms a more stable complex with carboxylate residues as well as the triphosphate group of nucleotides than Mn^{2+} and Mg^{2+} (122,123).

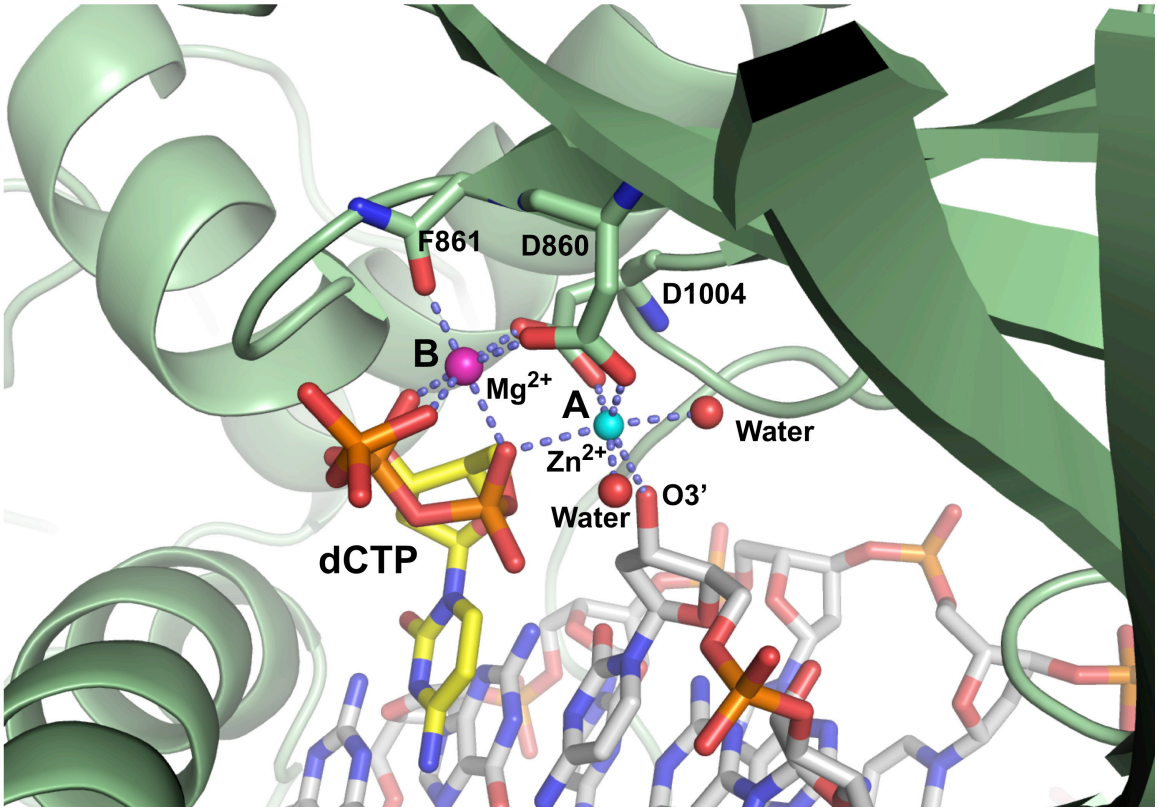

Figure 4.10. **The model explaining the dual effects of Zn2+ in polymerase reaction**. The structure of the active site of the human polα in the ternary complex with RNA primed the DNA template and incoming dCTP. Polα is represented as schematic and appears as green. The DNA, RNA, and dCTP as well as polα residues involved in the coordination of divalent metal ions are shown as sticks and appear blue for nitrogen, red for oxygen, and grey, yellow and green for the carbons of DNA/RNA, dCTP and polα, respectively. The Mg2+, Zn2+ and water molecules are shown as spheres and appear magenta, cyan and red, respectively. The potential coordinate covalent bonds are depicted as blue dashed lines. The model is based on the coordinates of the structure with PDB ID 4QCL. The image and the modeling of the 3'-OH group of the RNA primer were performed with the PyMOL Molecular Graphics System, Version 1.3, Schrodinger, LLC.

On the heterogeneous 73b template with DNA primer, 10 to 50 μM Zn^{2+} supported DNA synthesis by both the polα (tetramer) and the Klenow fragment (Figure 4.11). The increase of Zn^{2+}concentration led to longer products, but the total amount of extended primers was increased insignificantly (Figure 4.11A, lanes 4-6 and 12-14; quantification is below the gel). The activity of the polα with 50 μM Zn^{2+} was, on average, 2.5-fold less than with 8 mM Mg^{2+} (Figure 4.11A, compare lanes 4-6 to lane 3, lanes 12-14 to lane 11 and quantification below the gel image). The Klenow fragment extended more than 80% of primers to the end of the template within a 1 min reaction with 8 mM Mg^{2+} (Figure 4.11B, lane 19). Strikingly, when 10-50 μM Zn^{2+} was used alone, an average of 60% of the primers were extended, but the reaction primarily stopped after incorporation of the first nucleotide (Figure 4.11B, lanes 20-22).

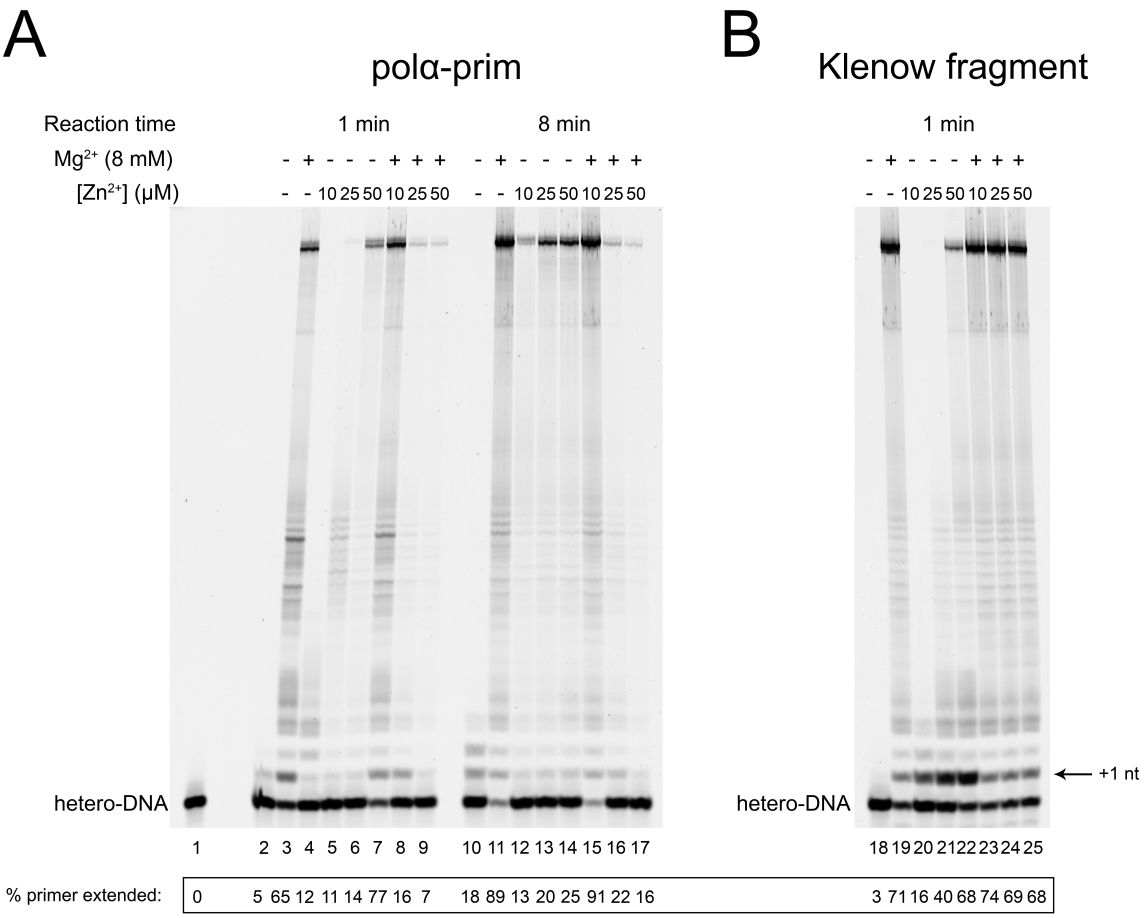

Figure 4.11. **Comparison of the effects of Zn^{2+} alone and in combination with Mg^{2+} on DNA synthesis by polα-prim and the Klenow fragment. (A)** Extension of hetero-DNA primers annealed with heterogeneous 73b template by polα-prim (enzyme to primer/template ratio = 1:10) and **(B)** the Klenow fragment. (enzyme to primer/template ratio = 1:5). Lanes 2-9, reactions by the polα-prim for one minute; Lanes 10-17, reactions by polα-prim for eight minutes; Lanes 18-25, reactions by the Klenow fragment for one minute; all with 100 μM dNTP at 35 °C. Reactions contain no enzyme (lane 1), no additional Me^{2+} (lanes 2, 10, 18), 8 mM Mg^{2+} (lanes 3, 11, 19), 10 to 50 μM Zn^{2+} (lanes 4-6, 12-14, 20-22), and 8 mM Mg^{2+} with 10 to 50 μM Zn^{2+} (lanes 7-9, 15-17, 23-25).

Zn^{2+} became sharply inhibitory to polα when Mg^{2+} (8 mM) was also present in the reactions. The activity of the polα was unaffected at 10 μM Zn^{2+} (Figure 4.11A, comparing lanes 7 and 15 to 3 and 11, respectively), inhibited by four-fold at 25 μM Zn^{2+} (Figure 4.11A, lanes 8 and 16), then by six-fold at 50 μM Zn^{2+}. The template sequence-independent stimulatory and inhibitory effects of Zn^{2+} at micro-molar concentrations suggested that these effects could be related to binding of metals at the A and B sites in the catalytic center (see Introduction). The addition of Zn^{2+} to reactions containing 8 mM Mg^{2+} did not result in inhibition of the Klenow fragment to the same extent as the polα (Figure 4.11B, lanes 23-25). This suggests that the Klenow fragment strongly preferred Mg^{2+} to Zn^{2+} for catalysis, whereas the reactions in the active site of the polα was easily perturbed with Zn^{2+}.

On the poly-dT_{70} template with RNA primers, Zn^{2+} also inhibited polα reaction sharply (about two-fold at 25 μM and four-fold at 50 μM), compare to 1 mM Mg^{2+} alone and with 10 μM Zn^{2+} (Figure 4.12A, compare lanes 6 and 7 with lane 4 and 5; quantification is below the gel). Similar effects were also observed with Mn^{2+} (Figure 4.12A, lanes 8-11). The Klenow fragment was mildly inhibited by Zn^{2+} (at 10-50 μM) in the presence of 0.2 mM Mg^{2+} (Figure 4.12B). Zn^{2+} did not cause the same premature termination on the poly-dT template as did the Mg^{2+} and Mn^{2+}, suggesting that the inhibition is not likely due to the formation of an unusual DNA structure. Note that the concentrations when Zn^{2+} supported and inhibited pol reaction were in the micro-molar range. This may explained why we did not see its effects on the structure of the template, which was seen at millimolar concentrations of Mg^{2+}.

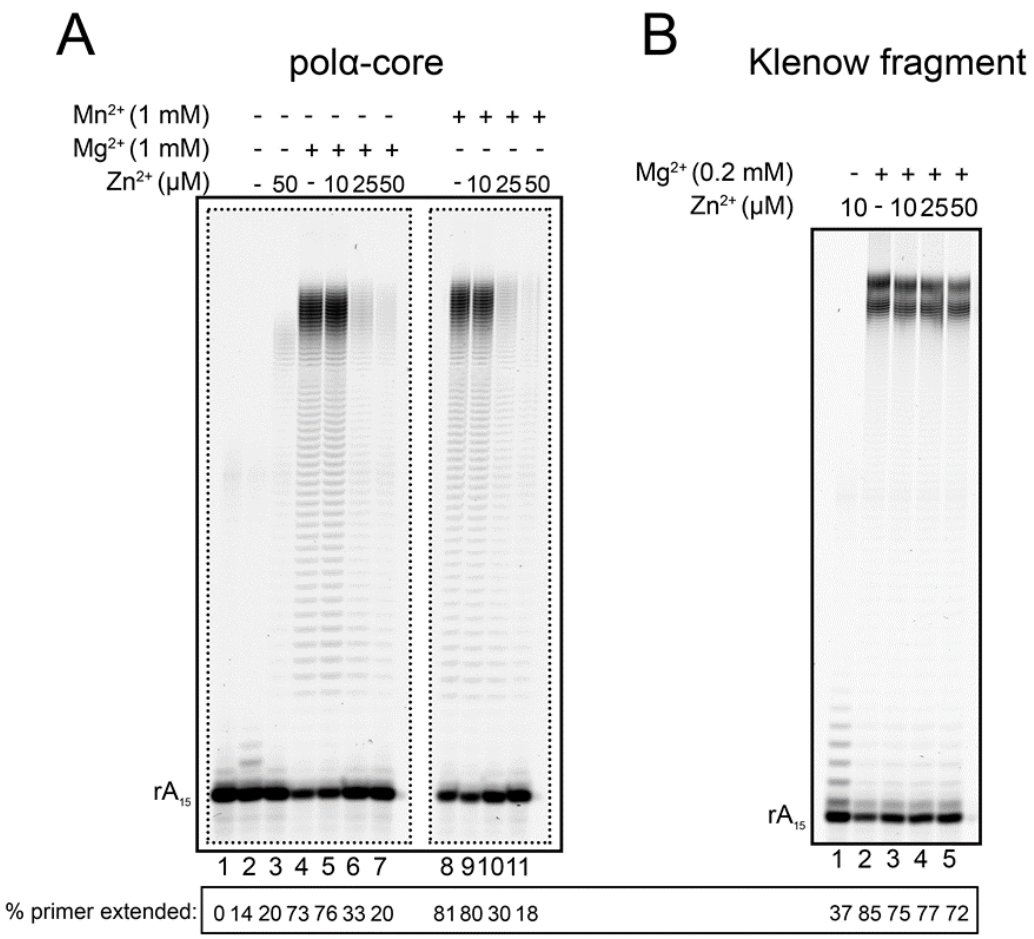
A
polα-core
B
Klenow fragment
Mn2+ (1 mM) - - - - - - + + + +
Mg2+ (1 mM) - - + + + + - - - -
Zn2+ (μM) - 50 - 10 25 50 - 10 25 50
Mg2+ (0.2 mM) - + + + +
Zn2+ (μM) 10 - 10 25 50
rA15
rA15
1 2 3 4 5 6 7 8 9 10 11
1 2 3 4 5
% primer extended: 0 14 20 73 76 33 20 81 80 30 18 37 85 75 77 72

Figure 4.12. **Inhibitory effect of Zn^{2+} on Mg^{2+} or Mn^{2+}-dependent catalysis by p180ΔN-core and the Klenow fragment on the poly-dT70 template with the poly-rA15 primer**. (A) Extension of poly-rA15 primers by p180ΔN-core (enzyme to primer/template ratio = 1:15) in reactions with 100 μM dATP at 35° C for five minutes. Reactions contain no enzyme (lane 1), no additional Me2+ ion (lane 2), additional 50 μM Zn^{2+} (lane 3), 1.0 mM Mg^{2+} with titration of Zn^{2+} from 0 to 50 μM (lane 4-7), and 1.0 mM Mn^{2+} with titration of Zn2+ from 0 to 50 μM (lane 8-11). (B) Extension of poly-rA15 primers by the Klenow fragment (enzyme to primer/template ratio = 1:5) with 100 μM dATP at 35 °C for two minutes. Reactions contain 10 μM Zn^{2+} (lane 1), and 0.2 mM Mg^{2+} with titration of Zn^{2+} from 0 to 50 μM (lanes 2-5). The efficiency of each reaction was calculated as the percent of extended primers and is written under each lane.

To further understand the inhibition of polα activity in the presence of both Zn^{2+} and Mg^{2+}, the usage of Zn^{2+} as catalytic Me^{2+} by polα core was studied in more depth. It is likely that this inhibition on polα was mainly driven by the concentration of Zn^{2+} reaching a certain threshold, because the dramatic effects were caused by tiny changes in [Zn^{2+}] (Figure 4.11 and 12). Polα reactions proceeded with 10-50 μM Zn^{2+} in the presence of a standard concentration of nucleotide triphosphates (100 μM). Nucleotide triphosphates are able to chelate the positively charged Zn^{2+} at the reaction conditions. It was possible that the ratio of [dNTP]/[Zn^{2+}] affects pol activity stimulation by Zn^{2+}. The range of [Zn^{2+}] supporting the polα reaction shifted from 5 to 80 μM when the concentration of dATP was increased from 10 to 160 μM, respectively (Figure 4.13; lanes 3, 7, 11, and 15). As predicted, once [Zn^{2+}] exceeded [dATP], polymerase activity decreased (Figure 4.13; lanes 4-5, 8-9, 12-13, and 16-17). Reactions with 160 μM of all dNTPs were generally similar to 160 μM dATP at the same [Zn^{2+}] (Figure 4.13, lanes 11-13, 15-17). We noticed that the overall product sizes at 80 μM Zn^{2+} were slightly smaller with dNTPs (Figure 4.13, compare lane 15 to lane 11). This was probably due to the slowed polymerase reaction in the presence of the non-cognate nucleotides and Zn^{2+}. It was noticeable that traces of Me^{2+} were present in the purified human polα samples that supported the polymerase reactions (Figure 4.13, lanes 2, 6, 10, and 14). This residual synthesis was more prominent at lower [dATP] (10 and 40 μM; Figure 4.13, lanes 2 and 6). Since these reactions reflected unusual conditions with a limited quantity of trace metal ions, it was possible that higher [dATP] chelated these trace metal ions that decreased the probability of available Me^{2+}-dATP at the active site.

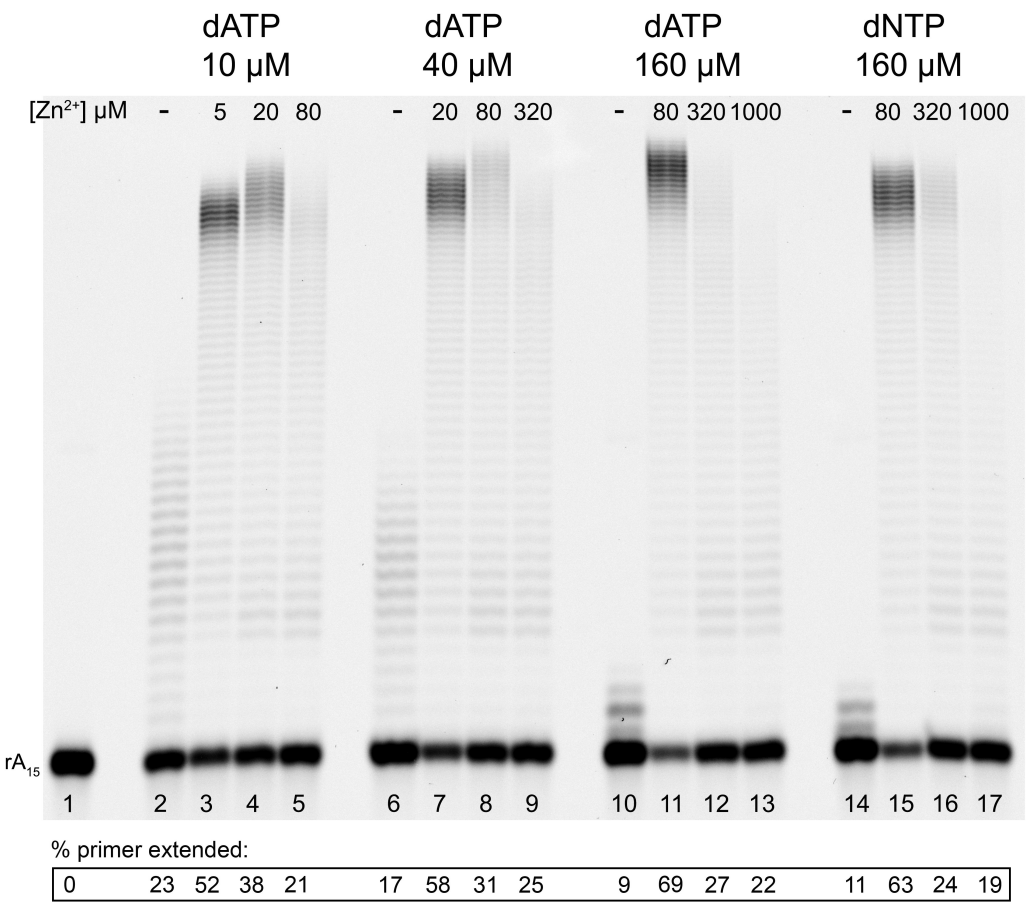

Figure 4.13. **The optimum zinc concentration supportive for DNA synthesis is determined by the availability of the nucleotide substrates**. Extension of the RNA (poly-rA15) primer (0.15 µM) by human polα (enzyme to primer/template ratio = 1:15) in reactions at 35 °C for five minutes. Lane 1, no enzyme; lanes 2-5 reactions with 0, 5, 20, 80 µM Zn2+ in the presence of 10 µM dATP; lanes 6-9 reactions with 0, 20, 80, 320 µM Zn2+ in the presence of 40 µM dATP; lanes 10-13 reactions with 0, 80, 320, 1000 µM Zn2+ in the presence of 160 µM dATP; and lanes 14-17 reactions with 0, 80, 320, 1000 µM Zn2+ in the presence of 160 µM dNTP.

The concentration-dependent effect of nucleotides on the pol reaction in the presence of Zn^{2+} was further explored by varying concentration of Zn^{2+} in reactions with 160 μM dATP at three time points. At 40 μM Zn^{2+}, polα extended more and more primer as reaction time increased from 0.5 to 8 minutes (Figure 4.14; lanes 4-6), similar to reactions with Mg^{2+} (lanes 16-18). At 80 μM Zn^{2+}, polα extended the primer faster at 0.5 minutes (lane 7) than at 40 μM Zn^{2+}, and reached the maximum primer usage at 2 minutes (lane 8). There was almost no increase in primer usage when reaction time was 8 minutes (compare lane 9 to lane 8). At 160 and 320 μM Zn^{2+}, the activity of polα decreased 2- and 4-fold, respectively, in comparison to at 80 μM Zn^{2+} (lanes 10-12 and 13-15). Moreover, the extent of primer usage was unchanged throughout all three reaction time points. The reactions with 160 μM Mg^{2+} showed a slower synthesis at 0.5 minutes in comparison to all reactions with Zn^{2+} at this time point (lane 16 compare to lanes 4, 7, 10, and 13). Thus, the concentration of nucleotides differently affected pol reactions in the presence of the two metals.

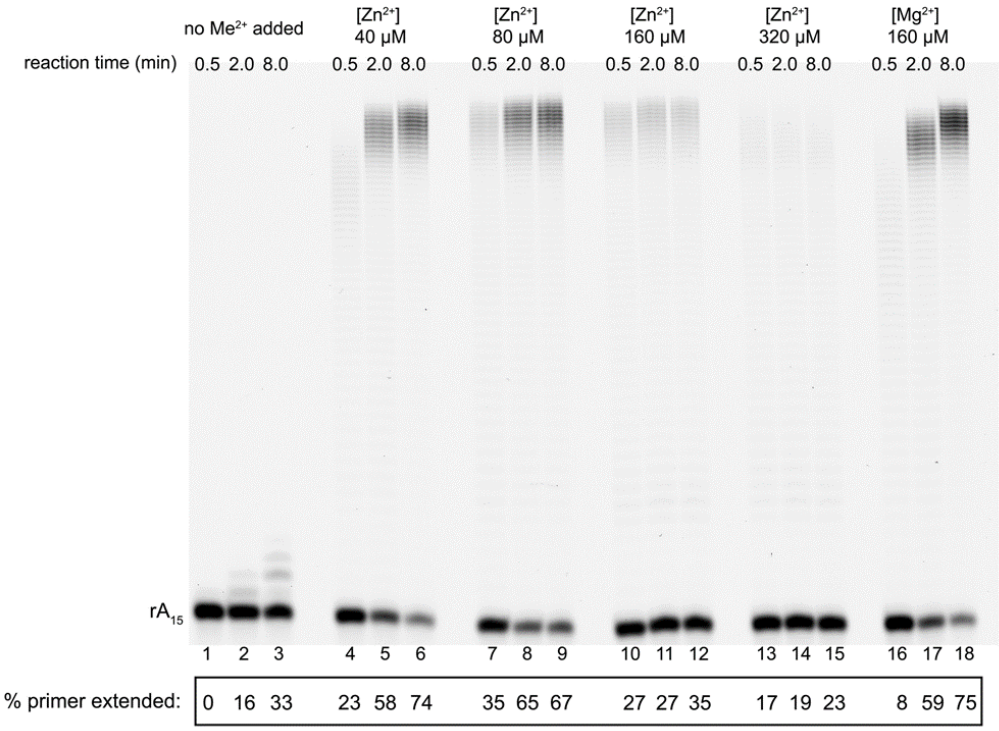

Figure 4.14. **Balance between nucleotide and Zn^{2+} concentrations is required for support of DNA synthesis by the p180ΔN-core**. Extension of poly-rA15/poly-dT70 by p180ΔN-core (enzyme to primer/template ratio = 1:10) in 0.5-, 2-, and 8-minute reactions containing 160 µM dATP at 35 °C. Lanes 1-3, no additional Me2+ in reactions; lanes 4-6, reactions with 40 µM Zn2+; lanes 7-9, reactions with 80 µM Zn^{2+}; lanes 10-12, reactions with 160 µM Zn^{2+}; lanes 13-15, reactions with 320 µM Zn^{2+}; and lanes 16-18 reactions with 160 µM Mg^{2+}.

4.3. Discussion

4.3.1. Structure of DNA polymerase substrates, metal ions and pol reactions.

Our novel finding described in this Chapter is that, with our experimental setup, the formation of triplexes impeding the advancement of DNA polymerases is much more efficient with DNA primers, than with RNA primers. This is supported by the observation that the pattern of usage of the dA_{15} primers was similar with dATP or 7DdATP, therefore, DNA primer was unavailable for pol at a higher [Mg^{2+}] prior to the start of DNA synthesis (Figure 4.7A). It is interesting that the threshold when severe inhibition occurred was shifted to 4 mM Mg^{2+} for reactions with 7DdATP, suggesting that the triplexes are dynamic and start to melt when destabilizing nucleotides are incorporated. When polα extends the RNA (rA_{15}) primer, the formation of triplex with the growing DNA part causes pausing and dissociation of the polymerase, which is also dependent on the concentration of Mg^{2+}.

We observed some peculiarities in how different DNA pols handle poly-dT templates (Figure 4.8). Yeast polδ was more robust than DNA polα and *E.coli* pol I, even with functional proofreading exonuclease (Fig. 4.8, panels C and D). The roles of the DNA polα and *E.coli* pol I in replication are limited to the synthesis of relatively short starts of Okazaki fragments (polα) and short patches of DNA after removal of RNA primer during Okazaki fragment maturation (pol I) (129). Polδ, on the other hand, is one of the major replicative pols in eukaryotes that synthesize the majority of the genome (17,27,130-132). It looks rational that it evolved to tolerate the inhibitory effects of certain templates/conditions better than polα and the Klenow fragment.

It is interesting that the threshold for pol stalling with both DNA and RNA primer is the same, 0.5 mM Mg^{2+} (Figure 4.4). Both primers were extended equally well at concentrations below this threshold. Magnesium in mammalian tissue is present at a typical concentration of 30 mM, but most of it (more than 95%) is bound to proteins, NTPs, or phospholipids (133). The concentration of free Mg^{2+} in nuclei, however, varies between cell cycle phases from 3 to 11 mM (134), and it was assumed that the physiological concentration of Mg^{2+} available for DNA binding is 10 mM (135). The Mg^{2+} is capable of coordinating six water molecules forming its first octahedral solvation shell. The hydrated Mg^{2+} interact with DNA molecules via water-mediated hydrogen bonds. Primary DNA interaction sites include the phosphodiester backbone, the guanine base in the major groove and the A-T pair in the minor groove (136). Moreover, two additional solvation shells can be built upon the first that helps interaction with different DNA molecules (137). Therefore, the potential of Mg^{2+} mediated intra- and inter- strand interactions other than Watson-Crick base pairing is very high, and it is sequence-dependent. It is known that Mg^{2+} and other Me^{2+} stabilize H-DNA structures (reviewed in (128)). Mg^{2+} induces bending of nucleosomal linker DNA (up to 80 bp repetitive sequence (138)), which contributes to folding of nucleosomal arrays (139).The RNA-Mg^{2+} interactions, on the other hand, are direct in the majority and are not mediated by water molecules (140). This may explain the reason for the better extension of the poly-rA_{15} primer on templates with polynucleotide runs. In conclusion, the poly-dT template is a very specific substrate for polymerases and should be used with caution to obtain general conclusions on the mechanisms of pol reactions.

Both polα and the Klenow fragment utilized the hetero-DNA primer well throughout the wide concentration range of Mg^{2+}. On the hybrid poly-dT_{35}-hetero template (73a), Mg^{2+} created a barrier for polα between 10 to 20 nt within the poly-dT zone, without affecting the stimulation of the utilization of the primers (Figure 4.6). On the template with a totally scrambled sequence (73b), polα (p180ΔN-core) showed a slow-down at a high 16 mM of Mg^{2+} around 20 nt synthesis, whereas the Klenow fragment did not (Figure 4.9). Secondary DNA structural prediction analysis revealed several potential hairpin sites in this template. Mg^{2+} is known to increase the stability of the secondary structures of DNA and RNA (141). It looks like polα is more sensitive to irregularities in the template than the Klenow fragment. The latter is known to be able to synthesize over some hairpins (142).

4.3.2. Dynamics of metals in the polymerase active site and the effect of Zn^{2+}.

Zn^{2+} differs from Mg^{2+} in certain interactions with DNA components and proteins. It has a higher affinity toward triphosphates and the Asp/Glu residues (122,123) and directly binds to the N7 position on the adenine ring (143). The stop after the first incorporated nucleotide by the Klenow fragment in the presence of Zn^{2+} suggests that the reaction mediated by Zn^{2+} freezes at the translocation stage after the first reaction cycle (Figure 4.11B). The translocation is critical for the growth of the DNA chain as the prerequisite step for the release of pyrophosphate and bound Mg^{2+} (90). A recent single molecule-based kinetic study with bacteriophage Phi29 DNA polymerase showed that the translocation happens after the release of the pyrophosphate and before the binding of the incoming dNTP, along the DNA template, one nucleotide at a time (144). DNA polymerase at the dNTP/pyrophosphate-free translocation state can thermally diffuse

between the pre- and post-translocation state. The binding of the correct dNTP stabilizes the post-translocation stage with the finger domain closure. It is possible that because of the higher affinity of Zn^{2+} toward the nucleotides, phosphates, or catalytic carboxylates, the pyrophosphate bound to Zn^{2+} in the position of metal B could not be easily released by the Klenow fragment, preventing the translocation (Figure 4.11B). Alternatively, the open finger cannot switch back to the post-translocation confirmation in the presence of Zn^{2+}. On the other hand, human polα behaves differently. Zn^{2+} supports full reaction cycles, but only when there are excessive nucleotide triphosphates to help overcome the negative effects of Zn^{2+}. Our results show that the optimum Zn^{2+} concentrations for the reaction are always less than the concentration of the nucleotides (Figures 4.13 and 14). When [Zn^{2+}] exceeded the concentration of nucleotides, the activity of polα was low and the primer usage and product length remained constant over time (Figure 4.14). This suggests that polα at these conditions was not able to dissociate from the extended primer and/or re-bind. The drastic inhibition of polα by Zn^{2+} in the presence of Mg^{2+} could be explained by the idea that the Zn^{2+} binds to site A only after Mg^{2+} occupies site B (Figure 4.10). The configuration of the active site with the two different ions in sites A and B in polα is apparently improper for a polymerase reaction. In the absence of Mg^{2+}, both A and B sites are occupied by Zn^{2+}, which allows a reaction to proceed when dNTPs are in excess.

The effects of Zn^{2+} on the pol activities of the Klenow fragment and polα might also be explained by the appearance of a third Me^{2+} binding site after breaking the bond between the α- and β-phosphates of dNTP and before the dissociation of the pyrophosphate (89), Fig. 4.1. As was seen in Polη, the third Mg^{2+} transiently stabilizes

the leaving group. At the reaction site of the Klenow fragment, Zn^{2+} might have a much stronger affinity to this site in comparison to Mg^{2+}, which complicates the release of pyrophosphate. Therefore, the translocation is blocked. In polα, Zn^{2+} binding at the third Me^{2+}-binding site apparently does not cause a hindrance of the product release. It is possible that, during evolution, polα acquired an alternative mechanism to release the Zn^{2+}-bound pyrophosphates in comparison to the Klenow fragment. It will be interesting to directly compare the structure basis of Zn^{2+}- and Mg^{2+}- catalyzed DNA polymerase reactions (i.e. how differ are these two ions in binding with catalytic residues, primer 3'end, and incoming nucleotide; metal ions position and hydrogen bonding at active site post reaction; or possible conformational changes).

In summary, in the first part of this Chapter we describe the analysis of the mechanisms of inhibitory effects of high concentration of Mg^{2+} on DNA polymerase (pol) alpha synthesizing DNA on the poly-dT template with DNA or RNA primers. This is important because homopolymeric runs are present in abundance in human genome. In addition, the work has methidologila aspect, because this template is still popular for studies of DNA polymerases. DNA pol stalling at poly-dT runs is attributed to the formation of triplex DNA. Our novel finding in the current work is that the effect is very different for reactions with DNA versus RNA initial primers. Low level DNA synthesis with DNA primers is only observed at the standard concentration of Mg ions. A mere decrease of the concentration by 10-fold completely rescues robust synthesis. We propose that the inhibitory effect of high Mg^{2+} concentrations on DNA pols on templates with repeated sequences is due to the stimulation of formation of unconventional DNA structure(s).

In the second part of this work we did a systematic evaluation of the effects of several single Me^{2+} as well as their combinations putatively disturbing catalysis by human polα and compared it with polδ, the Klenow fragment of polI and human primase. This analysis allowes for better understanding of replication in vivo, which occurs in complex mixtures of metal ions. We found that Zn ions differentially support or inhibit pol reactions depending on the particular DNA pols and the presene of Mg or Mn ions.

CHAPTER 5: Polα integration into replication fork: preliminary results and future directions.

This chapter describes results relevant to polα counting and polα fidelity. We describe how a defect of primase affects genome stability. We discuss a model of the additional role of primase•polα in DNA repair and possible future experiments stemming from our work.

5.1. How does polα stop synthesis?

5.1.1. Background

In the current model of replication polα extends the RNA primer synthesized by primase to a 35 to 40 nt RNA•DNA hybrid (10,17,23,145). This number was derived from experiments *in vitro* and, to our knowledge, has never been measured *in vivo*. Nethanel et al. (146) found a population of aphidicolin-insensitive short RNA-DNA hybrids in a SV40 DNA replication system using isolated monkey kidney cell (CV-1) nuclei or cell extracts. The products were labeled by [α-^{32}P]-NTPs or [α-^{32}P]-dNTPs, separated and visualized on gel. Despite that the authors were aware of the inhibitory effect of aphidicolin on all three B-family pols (polα, δ, and ε), they concluded that the short RNA-DNA hybrids were made by primase•polα, as the primer for Okazaki fragments. This paper has been cited ever since by many reviews, which are in their own turn cited by most current publications. *In vitro*, purified eukaryotic polα produces various sizes of products (39,67,101,147), up to 3kb (148), depending on conditions of the reaction. The 20 nt size of polα synthesized product on poly-dT template was an artifact due to formation of the triplex structure of the template induced by Mg^{2+} ions (chapter 4) (52,101). The distribution of sizes of fragments synthesized by polα *in vitro* under physiological conditions and *in vivo* has to be carefully reinvestigated.

The RNA-DNA primer synthesized by primase•polα on the lagging strand is extended by another B-family DNA polymerase, polδ, which is probably recruited after the loading of PCNA by the eukaryotic clamp loader RF-C (149). RF-C recognizes the 3' primer/template junction, and loads the PCNA to the duplex DNA on the 5' side of the primer (149). RF-C minimal recognition zone is 15 bases of the DNA duplex and 20 bases of the single-stranded template side (150). RF-C alone stimulates DNA polymerases activities in both archaeal and bacterial system (151,152). There is also evidence that RF-C can displace polα from the primer/template substrate, ie. participate in regulation of Okazaki fragment sizes, but the effect was only observed on short template (88 nt) embedded with poly-$(dA)_{18}$ sequence (153), and not on the longer SV40 plasmid, where the addition of RF-C stops polα synthesis approximately at 1 kb after start (154).

5.1.2 Exploration of the self-counting by polα.

We used "natural" template/primer combination that contains 3'overhangs and 5' tri-P, (chapter 3) to test if the binding of the primase part (p58C) or any other elements of the complex to the 5'tri-P and overhang template contributes to the polα counting. The four-subunit primase•polα possesses less polymerase activity that the catalytic core of polα with 10-nt RNA primer in "natural" conditions (Figure 5.1, lanes 1- 4; note the decreased usage of primer). The removal of either 5'tri-P or 3'overhang partially restored the activity of primase•polα, and the 3'overhang in the template apparently had more impact (compare lanes 6 and 9). The "natural" substrate seems slowed down the polα core too, causing a minor premature stop at first one or two nucleotides (lanes 3-4, compare to 7-8, and 10). This result suggests the binding of primase part to the 5' end of

primer with template junction does not necessarily alter the product length synthesized by polα, it rather changes the polymerase activity.

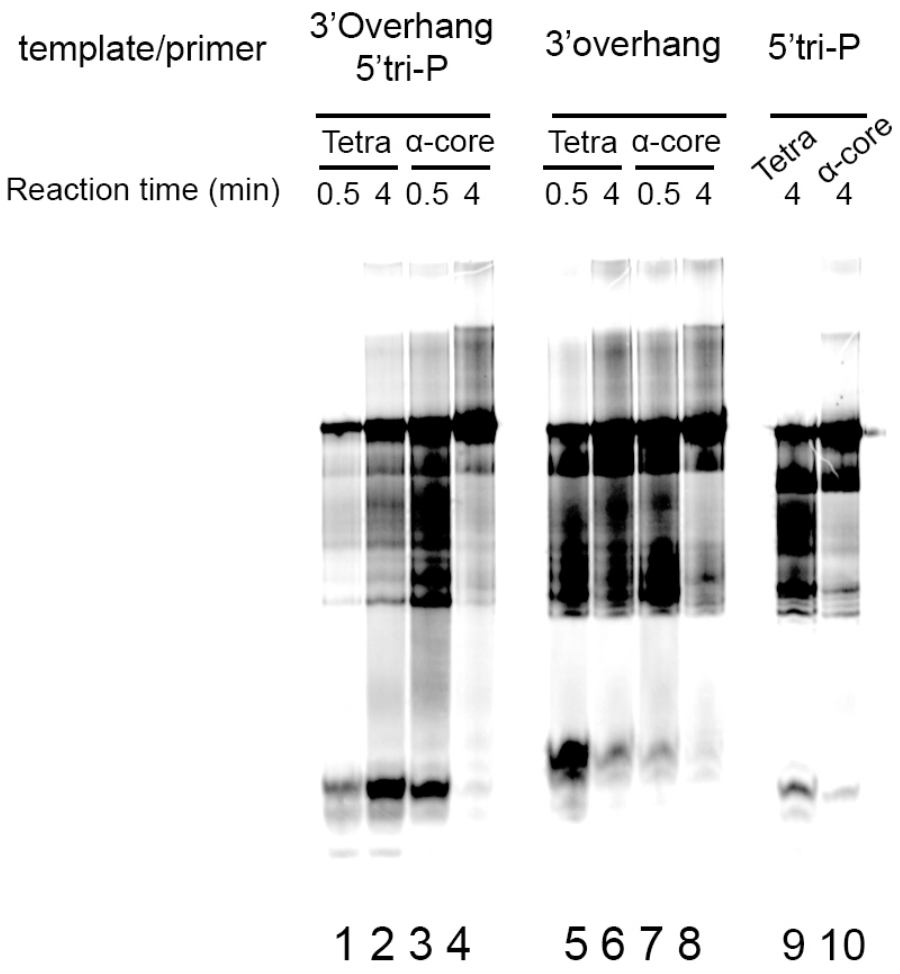

Figure 5.1. **Extension of unlabeled 10-nt RNA primer (5'GGCUGGUCGG) with or without 5' tri-P by tetrameric polα (lanes 1, 2, 5, 6, and 9) and polα-core (3, 4, 7, 8, and 10).** Reactions contain 0.5 μM [^{33}P-α]-dATP (3000 Ci/mmol) with 10 μM cold dTTP, dCTP, dGTP. Lanes 1-4, 60a9 template with 5'tri-P10 primer; lanes 5-7, 60a9 template with P10 primer; Lanes 9 and 10, 53a2 template with 5'tri-P10 primer (tables 2.3 and 2.4). Reactions were carried out in 0.5 and 4 minutes at 35 ºC as depicted in label.

To confirm this result, activities of polα tetramer and dimer (p180•p70) were compared in the two extreme situations, with "natural" primers and templates, with both binding elements, or without any of them. Direct comparison of the p180ΔN-core with the tetramer in Fig. 5.1 without taking the regulatory part of polα (i.e. p70 and p180C) into account was because that the situation was simplified to test if the p58C in primase was responsible for polα counting. Using of the dimeric polα instead of p180ΔN-core should be able to explore whether the inhibition site(s) is(are) located on the regulatory part of polα. The polα dimer was similarly inhibited on the "natural" template/primer, but slightly less than the tetramer (Figure 5.2, lanes 2-4 and 5-7). The DNA polymerase activity of the both complexes was substantially unleashed when both of the binding elements were removed (lanes 9-14). There is no substantial difference in the synthesis pattern (length of the products) between the templates/primers with or without the binding elements (compare lanes 2-4 to 9-11, 5-7 to 12-14). This result suggests that there might be some anchoring of the 5'tri-P and 3' overhang by both polα catalytic domain and the C-terminal domain or the B-subunit. It seems that the C-terminal domain and B-subunit have a major roles on this binding and contribute at the most on slowdown of polα. On the other hand, the binding element has no impact on the synthesis pattern by tetrameric or dimeric polα.

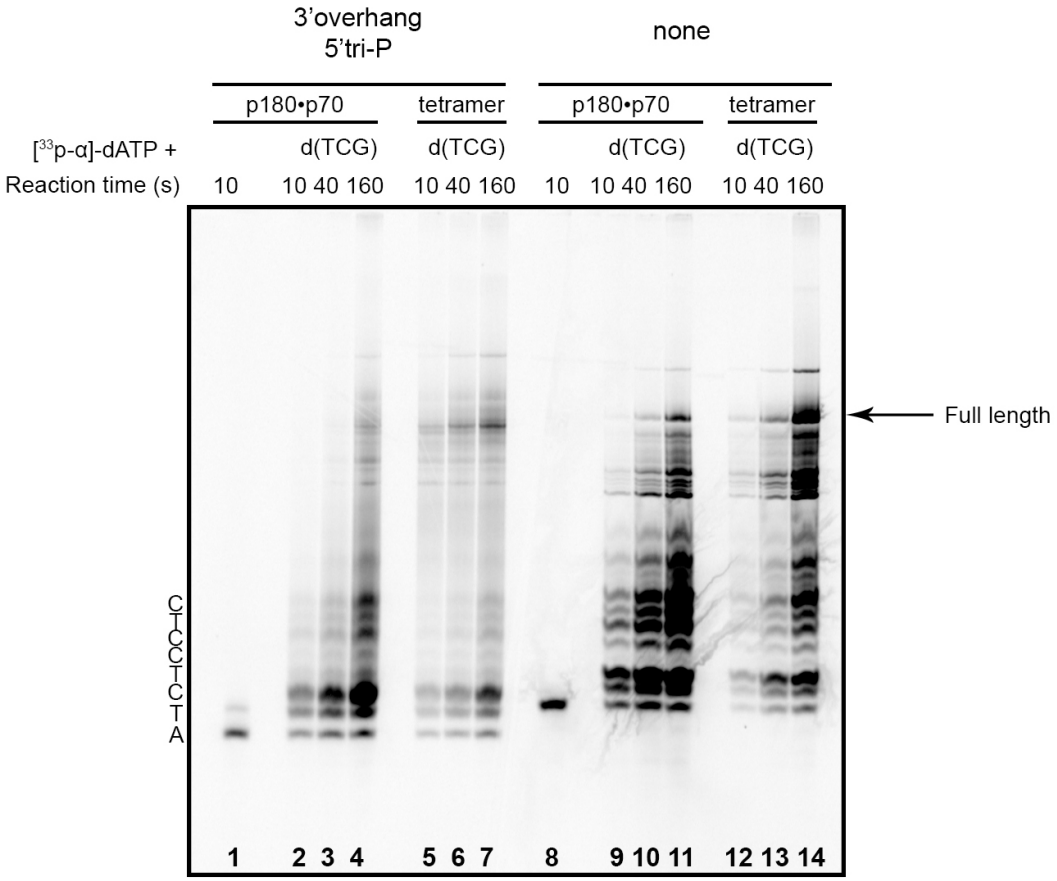

Figure 5.2. **Extension of 60a9 template paired with 5' tri-P10 primer or 53a2 template paired with P10 primer by polα dimer and tetramer**. Reactions contain 0.5 μM [^{33}P-α]-dATP (3000 Ci/mmol) with 10μM cold dTTP, dCTP, dGTP. Reactions were carried out in 10, 40, and 160 seconds at 35 ºC as depicted in label.

To further illustrate that the impact is purely on pol activity, but not on extent of the synthesis, 10 μM cold dATP was added to each reaction to decrease the amount of recovered products. In theory the non-labeled products are 20-fold more than labeled products. Besides, 10 μM of each dNTPs is a more physiological relevant condition for DNA polymerase reactions (83). It will eliminate the possible artifact with the 20-fold lower concentration of dATP might be a rate-limiting factor. The activity of the polα tetramer was lowest when both binding elements were present, with no indication of premature stop of synthesis (Figure 5.3, lanes 1 and 2). The synthesis patterns of polα dimer on primers with or without the 5' tri-P are identical (Figure 5.3, lanes 3,4 and 5, 6). This is consistent with the idea that the binding elements only affect polα activity.

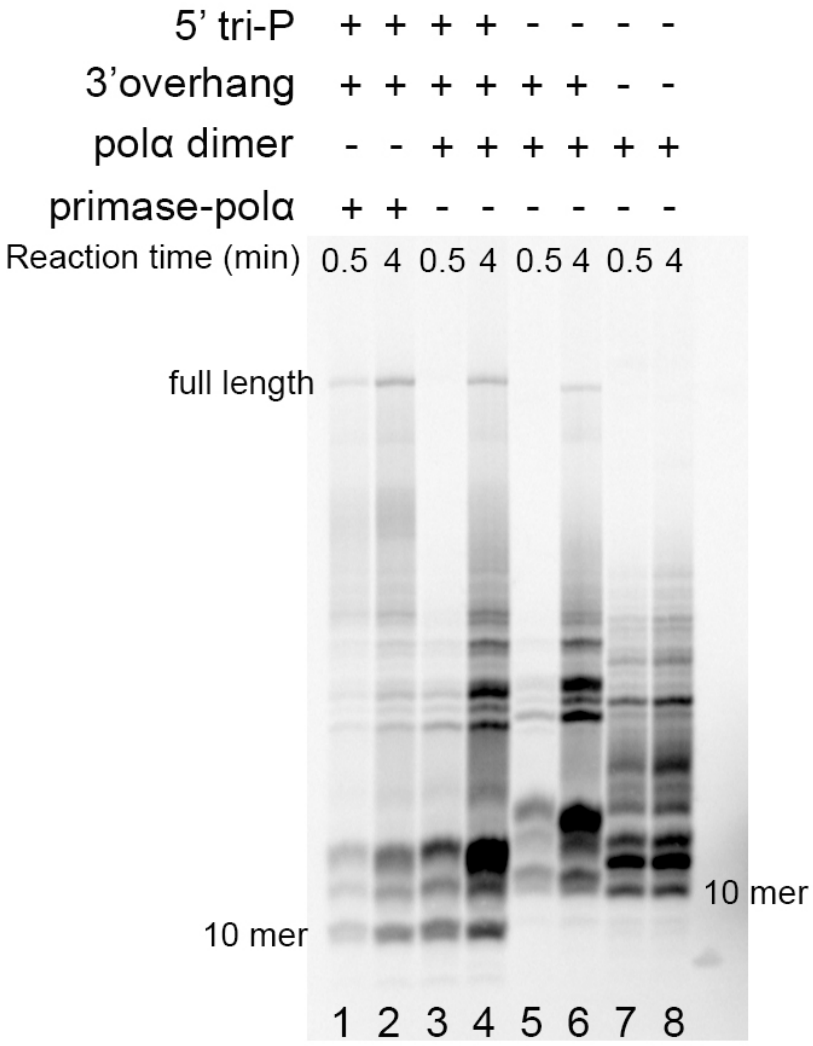

Figure 5.3. **Extension of 59a2 template paired with 5' tri-P9 (lanes 1-4), or P9 (5, and 6), or 52a2 template with P9 (Table 2.3 and 2.4) by polα dimer and tetramer**.

Reactions contain 0.5 μM [^{33}P-α]-dATP (3000 Ci/mmol) with 10 μM cold dNTPs.

Reactions were carried out for 0.5 and 4 minutes at 35 ºC as depicted in label.

The only biochemical data suggesting that RF-C loading of PCNA knocks polα off the template were obtained with the use of ssDNA template (88 nt long, containing a repetitive poly-$(dA)_{18}$ sequence embedded in the middle) with a 18 nt long DNA primer (153). As predicted (150), the RF-C/PCNA was loaded to the primer/template in the presence of RPA. The pre-loading of PCNA by RF-C did not inhibit polα synthesis initially. Instead, polα synthesized exactly 20 nt and stopped within the poly-dA sequence. To test the idea that polα synthesis can be stopped at defined point after the loading of RFC-PCNA, a 9 nt-long RNA primer with 5'tri-P group was used to mimic the primer synthesis situation by prim•polα, without pre-loading of RF-C/PCNA. In one expected outcome, RF-C will replace polα once the DNA synthesized by polα reaches certain length (above 15 nt). The presence of RF-C/PCNA, regardless of ATP hydrolysis, did not affect polα synthesis pattern (Figure 5.4). There is a minor activity change in the reaction without ATP (lane 2). We conclude that in this system RF-C/PCNA do not alter synthesis pattern by polα.

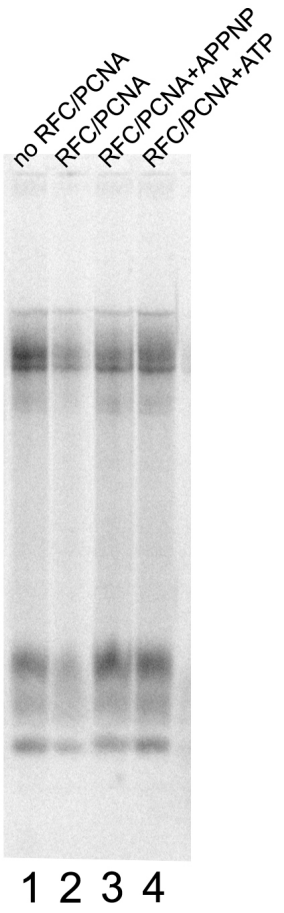

Figure 5.4. **Extension of 5'tri-P9 primer on 59a2 template (50 nM) by polα tetramer (50 nM).** Reactions contain [^{33}P-α]-dATP with 10 μM cold dNTPs. Lane 2, reaction contain additional 50 nM RF-C/PCNA; lane 3 and 4, reaction contain 100 μM AppNp (a non-hydrolysable ATP analog) and ATP in addition to lane 2, respectively.

Biochemical studies of polα switch is challenging because *in vitro*, polα is a very efficient DNA polymerase, whose synthesis rate is even faster than the synthesis by polε (155). The PCNA loading causing polα pausing within the poly-dA observed by Mossi et al. (153) is probably an artifact of high Mg^{2+} ions concentration (10 mM) in reactions (the control experiment in the paper showed a prominent stop at poly-dA too). Also the PCNA-binding sites were not defined, because the substrate used was linear and PCNA can easily slide off it. Bumpers at both ends are usually needed to study effects of PCNA on linear substrates (156). We show here that short linear templates, especially with repetitive sequence, are not ideal for studies polymerase reactions with additional DNA binding proteins. RPA, which has been shown to stimulate polα (157), in reactions with 7 mM Mg^{2+} on poly-dT template attenuated the synthesis by polα (Figure 5.5). The inhibitory effect was more pronounced with polα tetramer than with the catalytic polα-core (lanes 7 and 8 compare to 5 and 6). This is consistent with our prediction that the RF-C effect observed in (153) was a Mg^{2+}-induced artifact on poly-dA sequence. It would be interesting to perform these experiments on circular DNA, with real active loading of PCNA to primer/temple at 3' end and in the presence of varying concentrations of Mg^{2+}.

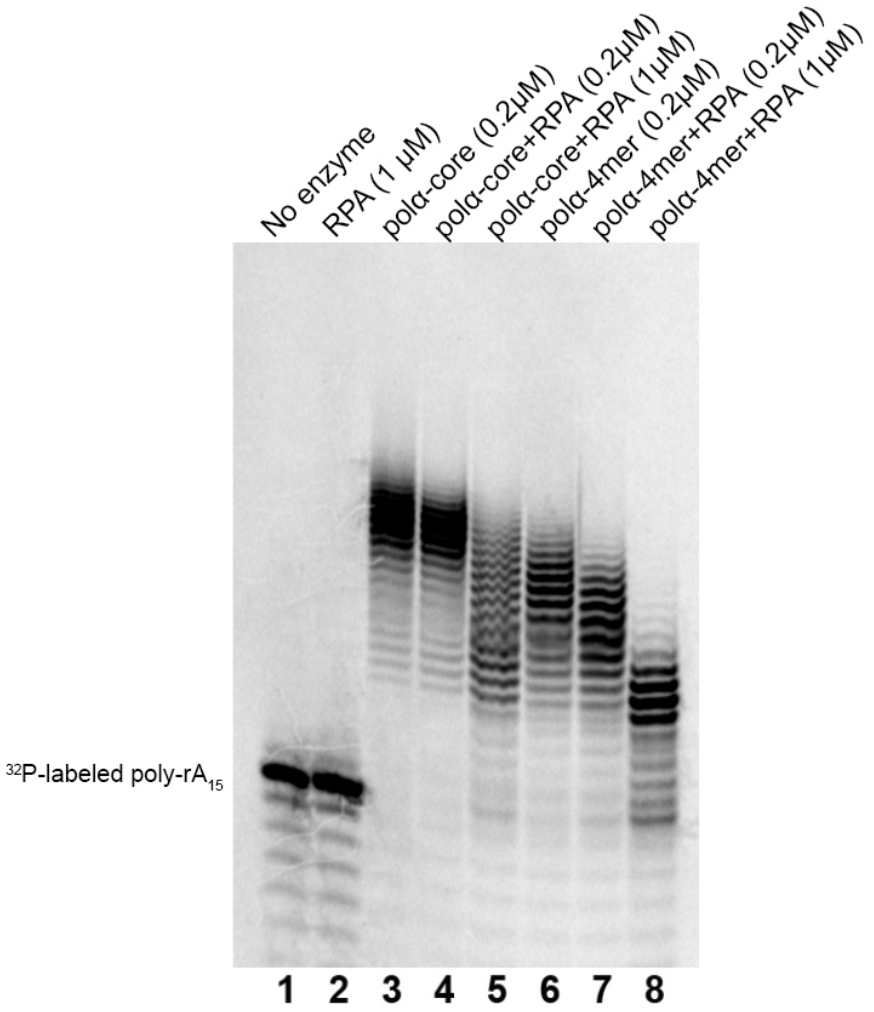

Figure 5.5. **Effect of purified human RPA (3-subunit RPA 70, 32, and 14; was a generous gift from Dr. Gloria Borgstahl lab) on polα extension of ^{32}P-labeled poly-rA15 primer on poly-dT$_{70}$ template (approximately 0.5 to 1 μM).** Lane 1, no enzyme control; lane 2, 1 μM of RPA only (control); lane 3-5 and 6-8, 0.2 μM polα-core and polα-tetramer with no RPA, 0.2 μM RPA, and 1 μM RPA, respectively.

5.1.3. Approaches to delineate the size of primers synthesized by polα and examine the switch to main replicative pols.

Studies of the polα synthesis switch to another DNA pols (i.e. δ and ε) *in vitro* require a second pol to be present in the reactions. However, then it is necessary to distinguish the synthesis performed by the two different DNA polymerases of the same B-family. Yeast polα, δ and ε mutants (*pol1-L868M*, and exonuclease deficient *pol3-5DV* and *pol2-4,* and altered base-selectivity *pol3-L612M, pol2-M644G*) make elevated levels of base substitution and insertion/deletion mutations in *lacZ* gap-filling assay (158-162). The combination of exo- with altered base selectivity further increases enzyme inaccuracy, as seen *in vivo* by skyrocketed mutation rates in corresponding double mutants (Liston and Pavlov, unpublished results). Therefore, these pol variants can be used to trace DNA synthesis by individual pols in vitro. The biochemical reconstitution of replication fork with purified polα, polε or polδ showed complete synthesis on a linear 3 kb substrate in both *de novo* and primer extension conditions (155,163). Inaccurate DNA pols will synthesize the products with many nucleotide changes. Therefore, we propose in future studies to examine the polymerase switch between polα and polδ or polε as follows (Fig. 5.6). First a DNA template will be designed to possess a unique annealing site to an RNA primer, which can only be efficiently extended by polα, but not δ or ε. We will also design primers for deep sequencing of DNA synthesis products. The region immediately after the RNA primer binding is supposed to be extended exclusively by polα for at least 20 nucleotides, even if other pols are present. Therefore this region is a must to sequence and design of amplification of pol synthesis products should allow that. An adapter sequence can be chosen at the 5' end of the template (3' end of DNA synthesis product).

There are several options to amplify the product strand using this single adapter sequence. One example is T7-based linear amplification that has been shown to reliably amplify DNA for deep sequencing (164). The size of the amplified region could be made variable by selecting different 5' adapters from 0.5 to 2 or even 3 kb to calibrate the system. It would be imperative to carefully determine optimal concentrations of DNA pols and accessory factors for robust synthesis. The combination of polα variants with either polδ or ε variants will be used for DNA synthesis. The reaction products will be purified afterward and amplified for deep sequencing with 10,000 - 100,000 x coverage that will allow for detection of pol errors.

We expect to see various outcomes, depending on combination of DNA pols (Figure 5.6). There will be very rare mutations in reaction products with wild-type pols. The combination of wild-type polα with inaccurate Pol2 or Pol3 variants will result in more errors in the 3' portion of the product, if the switch successfully happens at the same place of the template. When both inaccurate polα and polδ or ε variants are added to reactions, the mutations will be across the whole product. But this variant of experiment could be informative also, because the sequence-specificity of and types of mutations are different for different pol variants. One caveat in this approach is the inevitable use of pol variants that can change pol behavior and the "zone" of synthesis by wild-type pol and inaccurate variant will be different. Therefore it is important to characterize all pol variants biochemically and include all possible combinations of wild-type and mutant pols, as well as compare the signatures of mutant pols.

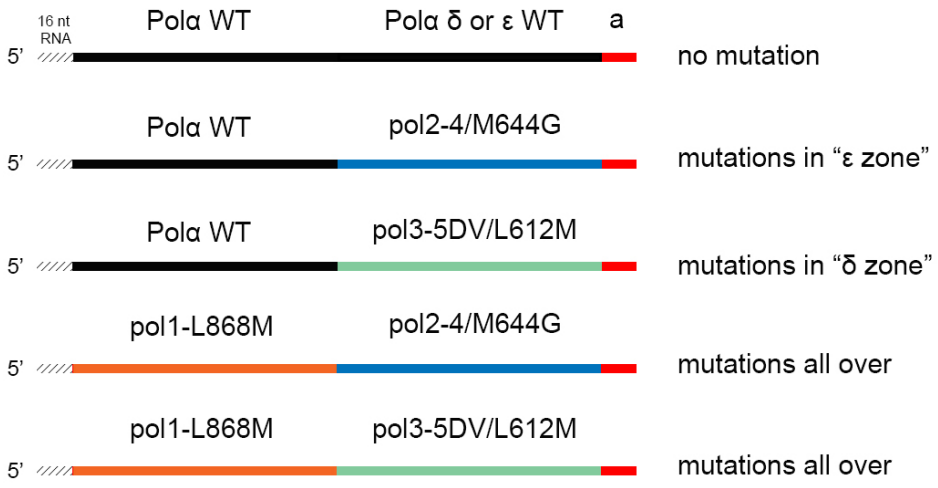

Figure 5.6**. Illustration of the deep-sequencing results of DNA synthesis by various combinations of polymerases**. Grey shade box, the RNA primer for polα-only extension (not present in sequencing result). Red box, the adapter at 3' end for product strand designed for amplification by a T7-based linear method. Black box, sequence contains no mutations. Orange box, sequence contains mutations, made by the pol1-L868M variant of polα. Blue box, sequence contains mutations, made by pol2-4 M644G mutant of polε. Green box, sequence contains mutations, made by pol3-5DV L612M mutant of polδ.

5.2 Genome instability induced by defect of prim•polα and proposed function of prim•polα in double-strand break repair

5.2.1. Background

Eukaryotic polα has an inactivated exonuclease, where the critical catalytic residues for exonuclease activity are substituted for non-catalytic residues, therefore it has lower fidelity in comparison to the proofreading-proficient B-family pols but can efficiently extend RNA primers (18). Study of yeast polα mutant allele *pol1-L868M* (lower fidelity 5.3 and 6.6 fold *in vitro* for base substitutions and frameshifts, respectively) suggested that the mutations made by polα are corrected by polδ proofreading activity and mismatch repair (158). Thompson and Kuchta (147) showed that the calf prim•polα is able to utilize the 9-β-D-Arabinofuranosyladenosine triphosphate (araATP) normally, a strong chain terminator to many DNA polymerases, in *de novo* synthesis condition but not in elongation of a RNA primer (10 mer) with 5' triphosphate. From our data (Figure 3.13) it is evident that the 10-mer RNA primer containing 5' triphosphate is an optimal substrate for polα, but not for primase, because of the binding of the tri-P to p58C does not allow primase to further translocate the substrate due to the clash made with the p58N (40). This suggests that the araATP in Kuchta's experiments was most likely incorporated by polα. Polα can also incorporate 8-doxoGTP and regular ribonucleotides (83). Moreover, polα can perform synthesis across templates containing non-conventional dNMP, 8-oxoguanine (8-oxoG) (127), or even ribonucleotides (165).

There are several observations suggesting that polα together with primase has additional roles, other than priming normal Okazaki fragments at the replication fork. First, both budding yeast (166) and fission yeast (167) catalytic subunit of polα interact

with proteins involved in telomere maintenance. The fission yeast Pol1p directly interacts with the Trt1, the catalytic subunit of telomerase and regulates the length of the telomere *in vitro* and *in vivo* (167). The *pol12-216* allele affecting the B-subunit of polα in budding yeast does not affect polα function in replication, but it is synthetically lethal with the telomere end-binding and capping protein Stn1. The change also disrupts their physical interaction and leads to the loss of telomere capping (168). A study in *Arabidopsis* showed that defects in Stn1 or polα lead to identical dysfunction of telomeres (169). The eukaryotic telomere G-tail is a long 3' overhang located at the end of the chromosomes, which is reverse-transcriptionally synthesized by telomerase (170-172). The 5' part of the G-tail is thought to serve as a template for the opposite C-strand synthesis, which is a lagging strand by definition. But in reality the situation is more complex because the "leading strand" is already synthesized by telomerase and at least partially to be used as a template. Besides, the synthesis of the telomere occurs in late S and G2-M phase (173,174), where standard replisomes are supposed to be inactive (175,176).

Nakamura et al. (177) showed that a temperature–sensitive variant of murine polα possesses a rear centric fusion of two acrocentric chromosomes at semi-permissive temperature, but does not stimulate other types of chromosomal aberrations. An engineered budding yeast strain that has inducible expression of Pol1 gene showed that polα plays an anti-recombination role in ribosomal DNA cluster, a 9-kb 150-200 tandem repeat region of rRNA genes (178). The decreased Pol1 expression level led to increase of both mitotic and meiotic recombination within the rDNA cluster, suggesting two distinct mechanisms of both replication -dependent or -independent double strand breaks.

Several observations suggest that archaeal primase is involved in double strand break repair. The archaeo-eukaryotic primase (AEP) family Mpa (Methanocella paludicola) polymerase incorporates ribonucleotides during non-homologous end joining (NHEJ) repair of double strand breaks, which serves a "flagged" signal for later repair (179,180). Archaeal primases have versatile nucleotidyl polymerization activities using both rNTPs and dNTPs, and can synthesize in both template-dependent and independent ways (3,181). Hu et al. (182) showed biochemically that the archaeon *Sulfolobus solfataricus* primase (SsoPriSL) can synthesis across discontinuous template, which resembles the broken strand. On the other hand, in budding yeast, polα mutant *pol1-L868M* induces mutagenesis in starved non-dividing cells, suggesting polα performs DNA synthesis during DNA repair (183).

5.2.2. Preliminary results: Malfunction of primase induces genome instability in yeast

5.2.2.1 CAN1 forward mutagenesis assay

To investigate the role of primase in maintaining genome stability, we re-constituted the temperature-sensitive *pri2-2* (C434Y) allele (184) in diploid yeast strain YPOM258 using a two-step integration method (Chapter 2.3.1). The residue 434 is one of the cysteines that coordinate the [4Fe-4S] cluster. Its change to alanine does not affect the primase *de novo* activity (41). The Pri2-C434Y mutant has never been biochemically characterized. From our biochemical study, the C-terminal domain is important in primase counting and switching to polα. It is possible that this mutation affects some properties of the complex and ultimately affects the priming of Okazaki fragments. The delay in switching from the RNA primer will slow down the synthesis since primase is slower than polα and takes longer to remove. Yeast carrying this mutation grow slowly

at 30 ^{o}C, and very slowly at 37ºC indicating an abnormality in genome replication (184). After tetrad dissection the *pri2-2* mutation in the isolated spores are immediately distinguishable, as a 2:2 segregation of normal versus small sized colonies (Figure 5.7).

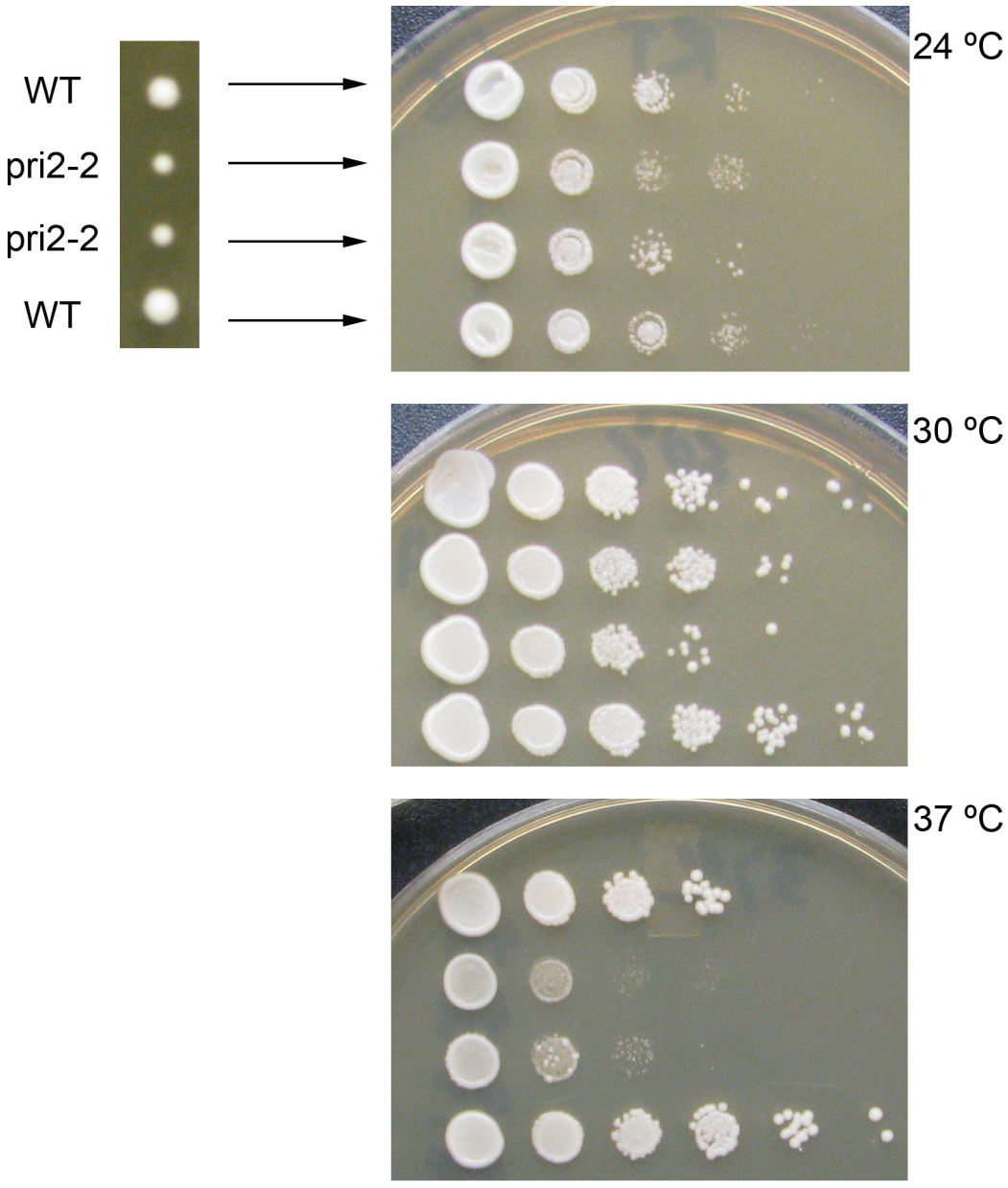
WT
pri2-2
pri2-2
WT
24 ºC
30 ºC
37 ºC

Figure 5.7. **Tetrad analysis of the diploid yeast strain YPOM258 containing heterozygous *pri2-2* mutation and temperature sensitivity at 37 ºC**. The tetrad-dissected spores were isolated (at 24 ºC) and plated on three YPDAU complete media with serial dilution factor of 20, and grow at 24, 30, 37 ºC for one day.

Genome instability was measured by *CAN1* forward mutation assay (Chapter 2.3.2). Comparing to wild type, the *pri2-2* strain has about 10-fold elevated mutation rate (first shown in Longhese et al. (184) with 4.3-fold). Cadmium ions (Cd^{2+}) are known to inhibit mismatch repair (MMR) in yeast (185). Cd^{2+} by itself increased mutation rate in our strain about 2 to 3 fold (Figure 5.8). The combination of Cd^{2+} with *pri2-2* elevated the mutation rate at least 50-fold in comparison to the wild type. The synergistically increased mutation rate typically indicates that errors made by the primase variant could be corrected by MMR system. Analysis of the mutation spectrum at *can1* locus showed that 65% of the mutations were base substitutions (Figure 5.9). 35% mutations are frameshifts, including insertions, deletions, and sequence duplications. There are rare events of large duplication (insertion of identical sequence of 27 bases) and deletions up to 39 bases (Figure 5.10).

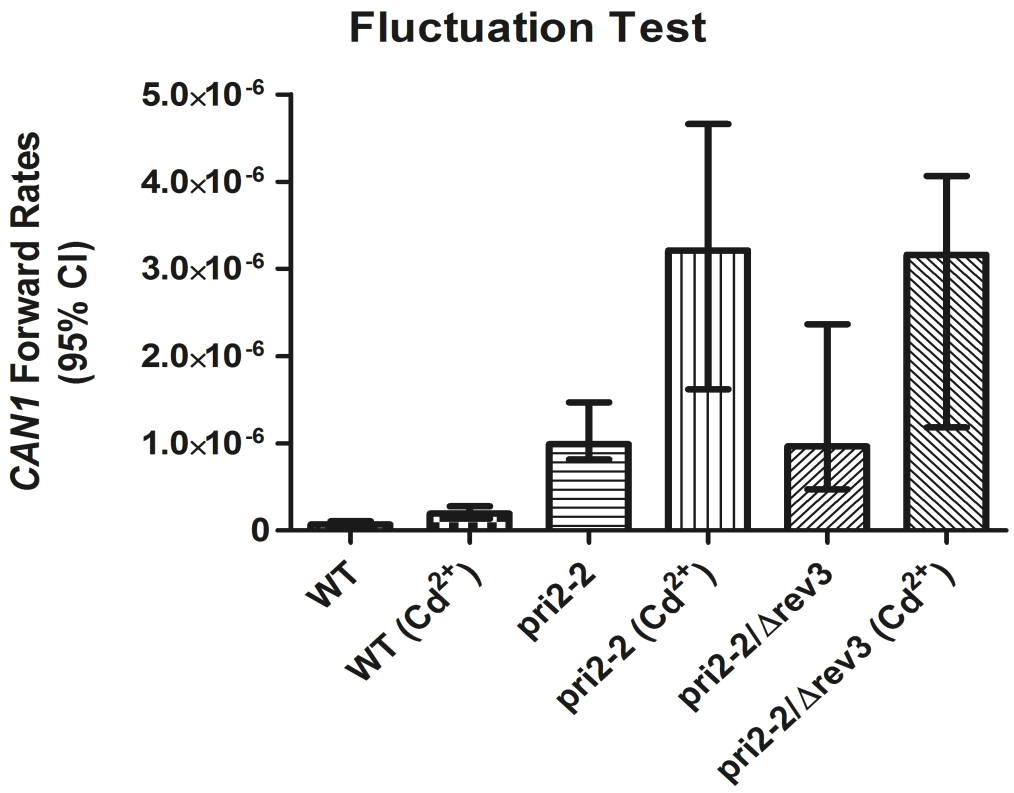

Figure 5.8. **Forward mutation rate at *CAN1* locus of WT, *pri2-2*, *pri2-2* Δ*rev3* strains, with or without Cadmium in the media measured by fluctuation test**. Error bars denote 95% confidence intervals.

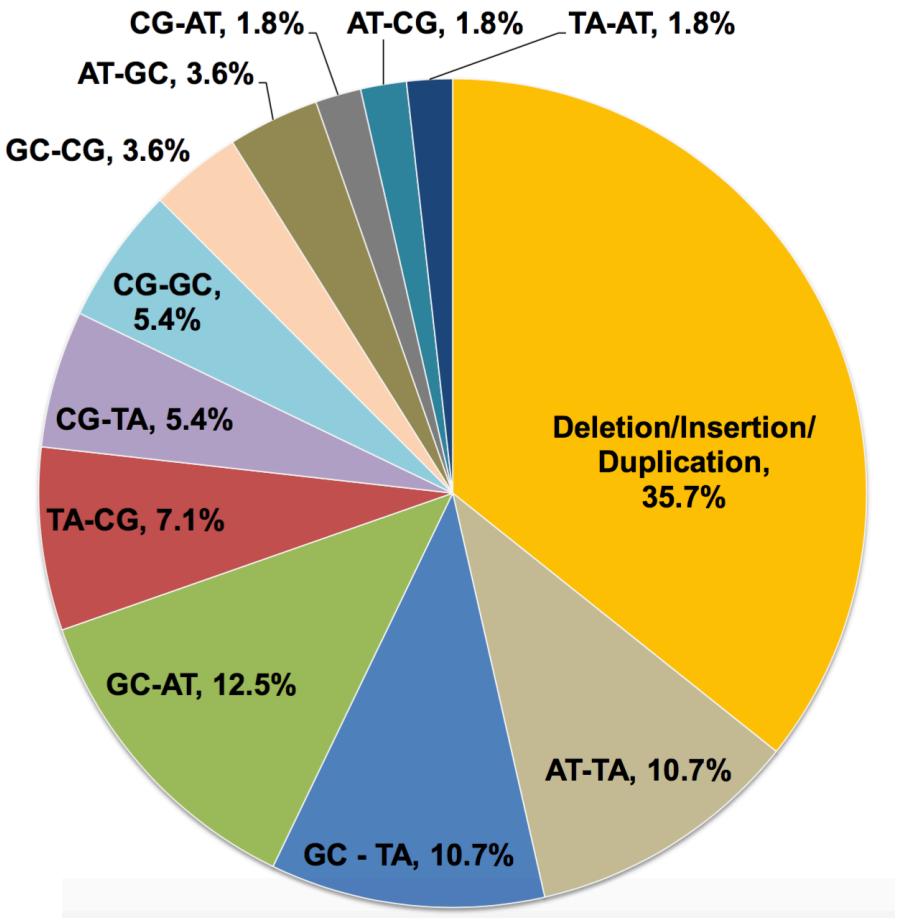

Figure 5.9. **The spectrum of spontaneous base substitutions and complex mutations in the *CAN1* gene of the *pri2-2* strain**. The proportions of individual mutations were calculated from sequencing data shown in Figure 5.10.

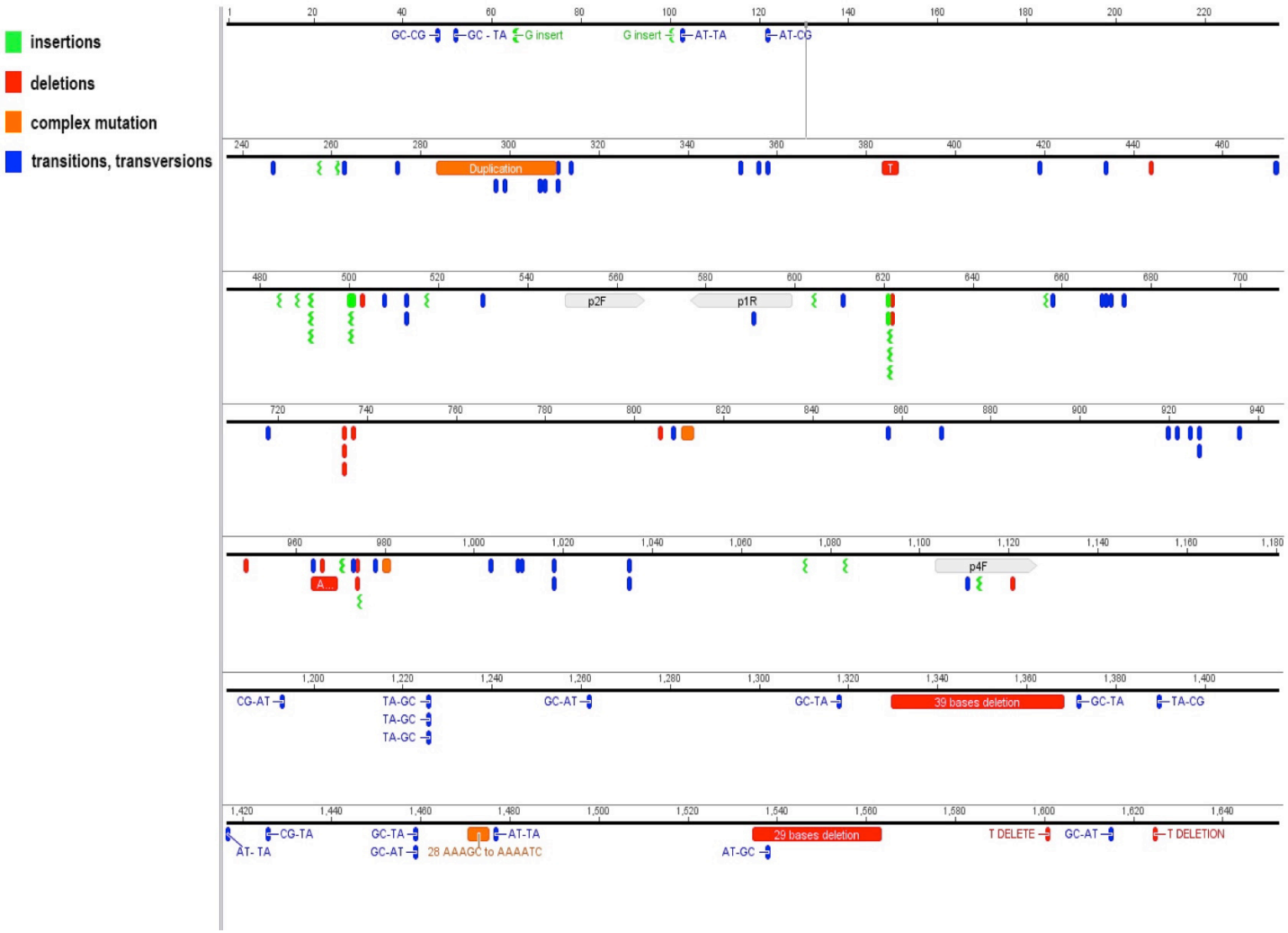
insertions
deletions
complex mutation
transitions, transversions
GC-CG
GC - TA
G insert
G insert
AT-TA
AT-CG
Duplication
T
p2F
p1R
p4F
A...
CG-AT
TA-GC
TA-GC
TA-GC
GC-AT
GC-TA
39 bases deletion
GC-TA
TA-CG
CG-TA
AT- TA
GC-TA
GC-AT
AT-TA
28 AAAGC to AAAATC
29 bases deletion
AT-GC
T DELETE
GC-AT
T DELETION

Figure 5.10. **Distribution of spontaneous- and Cd^{2+}- induced *can1* mutations in the *pri2-2* strain from 116 sequenced clones.** Insertions, deletions, complex mutation (including large duplication of repetitive sequence, both deletion/insertion and base substitution occur together), and base substitutions are annotated by green, red, orange, and blue boxes below the sequence, respectively. The width of the boxes represents the number of bases involved.

The *pri2-2 rev3* strain showed no UV mutability (not shown), but did not show decrease of spontaneous or Cd^{2+} -induced mutagenesis at *CAN1* locus (Figure 5.8). Thus, mutations in the *pri2-2* background arise by a mechanism independent of polζ. It's consistent with the result shown as the spectrum of *can1* mutations made in *pri2-2* strain do not have the characters of polζ-dependent defective-replisome-induced mutagenesis (DRIM) (29), which are primarily GC to CG transversions and complex mutations. The mechanism of *pri2-2* induced mutagenesis is still to be determined in future studies.

5.2.2.2 Tri-nucleotide expansion in pri2-2 cells

Tri-nucleotide repeats (TNR) are tandem repetition of three nucleotides and are the largest class of microsatellites, which abnormally expanded that associates with many disease (186). Shah et al. (63) showed that the defect of replicative DNA polymerases leads to the increasing the rate of TNR expansions. The proposed model is that the destabilization of the replication fork increases the probability of template switching, which polymerase uses the nascent strand as a template. Defect in polα (pol1-L868F) leads to an even larger expansion of the TNR compare to polδ and ε mutants, probably due to an increased average size of Okazaki fragments (187). The phenotypic differences between *pol1-L868F* used in this study and the L868M are that the F mutant yeast grow slowly and are temperature-sensitive and has higher mutation rate at both *CAN1* and *his7* loci (188).

The *pri2-2* effect on TNR expansion was tested using a $(GAA)_{100}$ cassette ((63); a generous gift from Dr. Mirkin lab at Tufts University; chapter 2.3.3). The cassette is imbedded in the intron of the *URA3* gene (Figure 2.1). The expansion of the repeat

increases the size of the intron that affect the splicing in the mRNA maturation, which leads to Ura$^-$ phenotype of the cells. In *pri2-2* strain, the $(GAA)_{100}$ TNR can be expanded up to about 110 more repeats (rarely can be 160 repeats; Figure 5.11). The problem is that there are populations of ura$^-$ cells that carry unexpanded repeats. Therefore it's not applicable to measure the rate of the expansion. In the future this experiment needs to be done in a different strain or using different cassette (i.e. *CAN1*). It might be interesting to sequence the unexpanded *ura3* gene to see what types of mutation are generated.

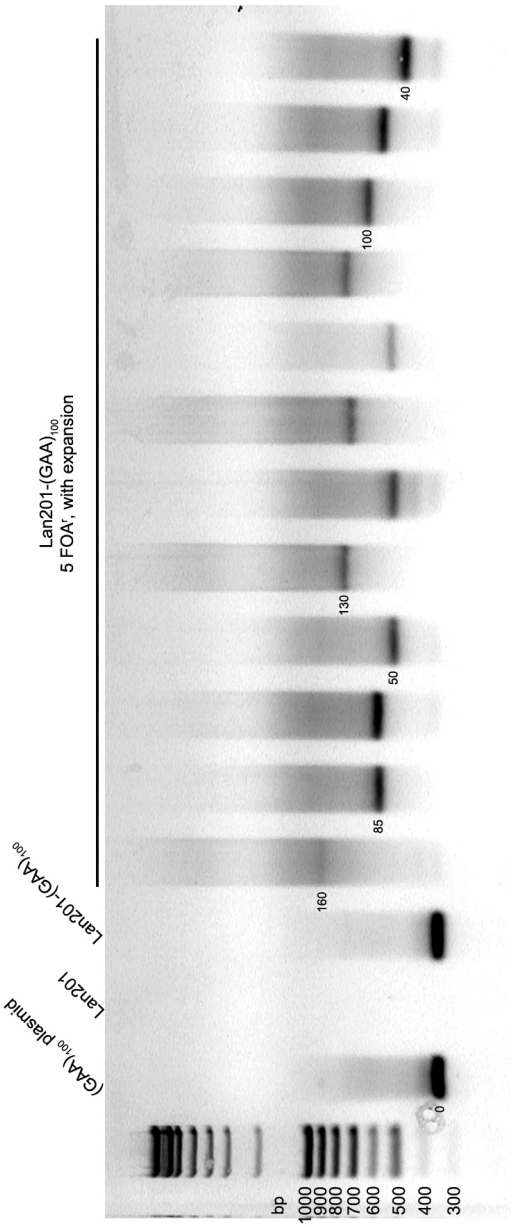

Figure 5.11. **Illustration of variations in sizes of spontaneous expansions of $(GAA)_{100}$ repeats in *pri2-2* strain by PCR**.

5.2.3. Proposed mechanism for pri2-2 induced genome instability

Based on the observations from our preliminary work with *CAN1* mutagenesis assay and TNR expansions and the literature, we propose a possible mechanism for *pri2-2* induced genome instability (Figure 5.12). The *pri2-2* mutation likely causes the delay of priming in each Okazaki fragment synthesis due to the disrupted switches from primase to polα synthesis, since the mutation is at the Fe-S domain. The delay of priming as the replication fork progresses may result in shifts of priming positions and increases the distance between two initiation sites. According to the current model of Okazaki fragment maturation, when polδ encounters the primer of the earlier Okazaki fragment, it displaces the primer for further processing (Figure 1.8; (189)). The aberrant priming in *pri2-2* may have several consequences. First, the mutation may affect the switching from RNA synthesis to DNA, which will further delay the switch to polδ. In addition, the distance for polδ to travel is longer, which may delay polδ approach to the previously made Okazaki fragment for displacement synthesis. The delayed displacement may result an alternative processing of the RNA-DNA primer made in the previous Okazaki fragment. The nucleosome assembles at the matured Okazaki fragment ends (54), but it is unknown if the maturation dictates the nucleosome assembly or *vice versa*. The RNA part could be processed by RNase H. For the polα product, one possibility is that if the nucleosome assembles at certain location regardless of the Okazaki fragment processing, the polα product could be packed into nucleosome right away without displacement by polδ due to the delay. Another possibility is that the delayed seal between two Okazaki fragments may affect the nucleosome assembly, which leaves a non-stable DNA and rarely leads to breaks. This could potentially explain why some of the *pri2-2* cells are

extremely sick (smaller colonies and higher mutation rates). Another possibility is that prim•polα normally participates in repair of the DSB and defective primase abolishes this additional function.

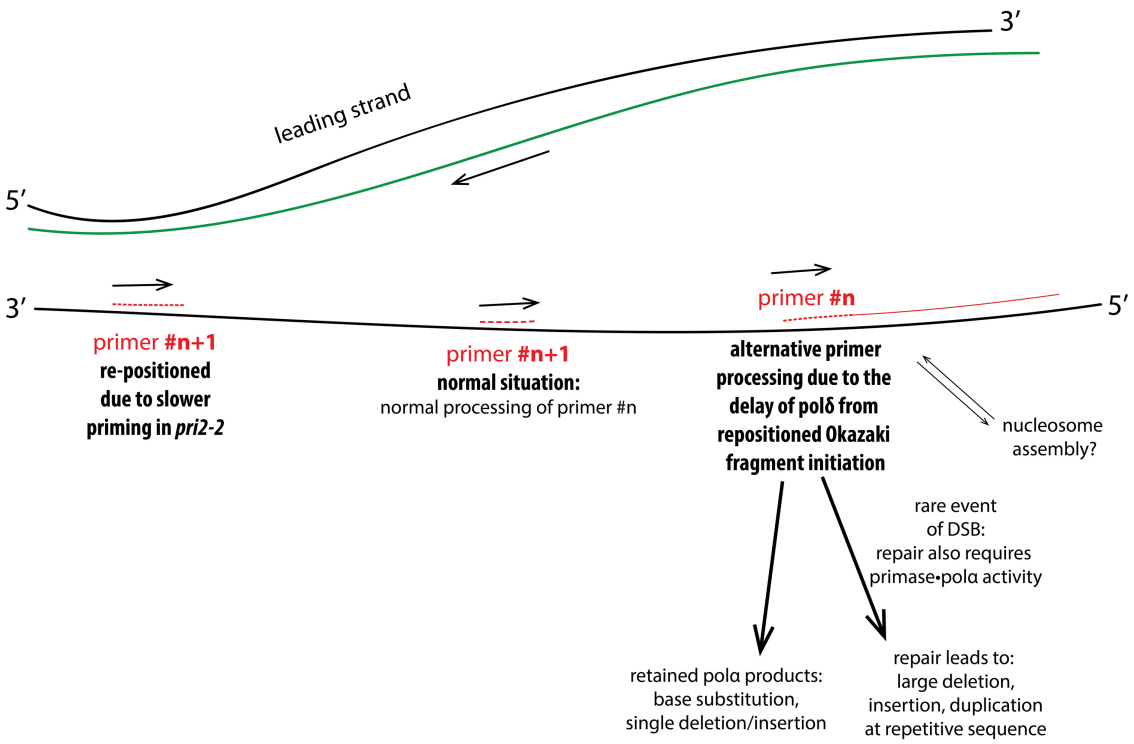

Figure 5.12. **Model explains the observed *pri2-2* genome instability**. The template DNA is in black lines with labeled ends. The leading strand is in green, lagging strand is in red. The dashed lines represent the RNA primers made by primase. The solid red line represents the Okazaki fragment.

To test the idea that *pri2-2* leads to abnormal Okazaki fragment maturation, a defect of the factor that affects this processing can be used. Fen1 and Dna2 endo- and exo-nucleases process the short and long flaps during Okazaki fragment maturation (17). Normally Fen1 and Dna2 can compensate for each other if one is defected (189). If *pri2-2* has a defect in normal primer removal, the mutations in either *FEN1* or *DNA2* can cause more severe damage to the genome.

5.2.4 Polα fidelity depends on the presence of free hydroxyl group at the 2' carbon (deoxyribose vs ribose) of the nucleoside monophosphate

There are several interesting biochemical properties of eukaryotic prim•polα that are worth further exploration. Prokaryotic and archaeal primases are known to synthesize products longer than the template (3,182). This property, however, has never been studied in human primase. During my study, I found that human primase is able to synthesize products twice as large as the templates (which were carefully purified by ion-exchange chromatography or UREA-PAGE to eliminate the impurity). Archaeal primase can perform the synthesis independent of template through its terminal nucleotidyl-transferase activity (181), or across discontinued templates (182). It is likely that human enzyme can use the second mechanism. This property would give primase•polα a unique advantage to repair breaks, but the process is likely to generate DNA rearrangements.

Another property of polα worth further analysis is its relatively low fidelity. As we discussed above polα can use many nucleotides analogs (83,127,147), and even bypass templates containing RNA (165). Preliminary study shows that human polα can misincorporate only when it extends DNA primer (Figure 5.13). The errors with RNA

primer start to occur only after the first nucleotide incorporated is a dNMP (Figure 5.13B, lanes 2, 9, 12, 15). The most efficient mismatches are G-G, G-T, A-A, T-C, T-G, and C-A pairs. The less efficient but still doable mismatches are A-C, A-G, T-T, and C-T pairs. Insertion of G across A and C across C are almost impossible.

To summarize this Chapter, it is highly likely that, despite amazing progress in studies of prim•polα, future studies might still discover novel functions and additional mechanisms attributable to this unique enzyme.

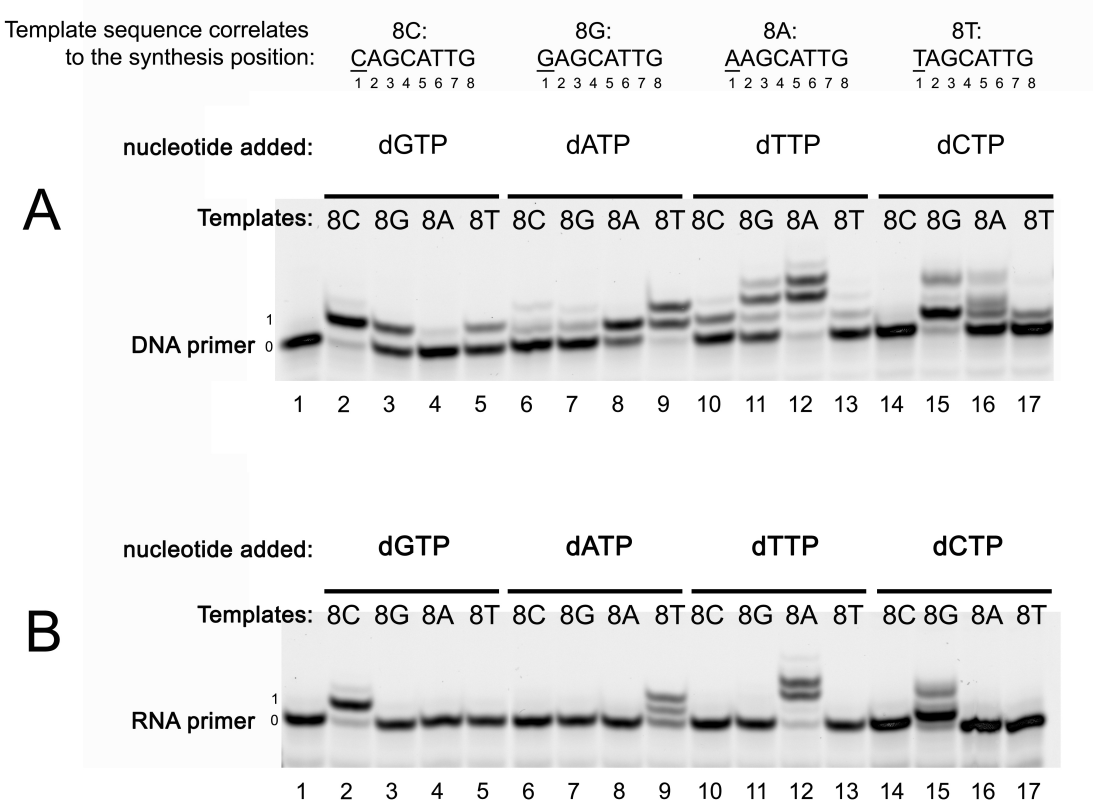

Figure 5.13. **Misincorporation of each dNTP by polα-core on templates annealed with hetero-DNA (panel A) or hetero-RNA (panel B) primers**.

Reference List

1. Watson, J. D., and Crick, F. H. (1953) Genetical implications of the structure of deoxyribonucleic acid. *Nature* **171**, 964-967
2. Meselson, M., and Stahl, F. W. (1958) THE REPLICATION OF DNA IN ESCHERICHIA COLI. *Proceedings of the National Academy of Sciences of the United States of America* **44**, 671-682
3. Lao-Sirieix, S. H., and Bell, S. D. (2004) The heterodimeric primase of the hyperthermophilic archaeon Sulfolobus solfataricus possesses DNA and RNA primase, polymerase and 3'-terminal nucleotidyl transferase activities. *J Mol Biol* **344**, 1251-1263
4. García-Gómez, S., Reyes, A., Martínez-Jiménez, María I., Chocrón, E. S., Mourón, S., Terrados, G., Powell, C., Salido, E., Méndez, J., Holt, Ian J., and Blanco, L. (2013) PrimPol, an Archaic Primase/Polymerase Operating in Human Cells. *Mol Cell*
5. Bianchi, J., Rudd, S. G., Jozwiakowski, S. K., Bailey, L. J., Soura, V., Taylor, E., Stevanovic, I., Green, A. J., Stracker, T. H., Lindsay, H. D., and Doherty, A. J. (2013) PrimPol Bypasses UV Photoproducts during Eukaryotic Chromosomal DNA Replication. *Mol Cell* **52**, 566-573
6. Zuo, Z., Rodgers, C. J., Mikheikin, A. L., and Trakselis, M. A. (2010) Characterization of a Functional DnaG-Type Primase in Archaea: Implications for a Dual-Primase System. *J Mol Biol* **397**, 664-676
7. Le Breton, M., Henneke, G., Norais, C., Flament, D., Myllykallio, H., Querellou, J., and Raffin, J. P. (2007) The heterodimeric primase from the euryarchaeon Pyrococcus abyssi: a multifunctional enzyme for initiation and repair? *J Mol Biol* **374**, 1172-1185
8. Finnegan, D. J. (2012) Retrotransposons. *Current Biology* **22**, R432-R437
9. Steitz, T. A. (1993) DNA- and RNA-dependent DNA polymerases. *Curr Opin Struct Biol* **3**, 31-38
10. Johansson, E., and Dixon, N. (2013) Replicative DNA polymerases. *Cold Spring Harb Perspect Biol* **5**
11. Franklin, M. C., Wang, J., and Steitz, T. A. (2001) Structure of the replicating complex of a pol alpha family DNA polymerase. *Cell* **105**, 657-667
12. Hogg, M., Osterman, P., Bylund, G. O., Ganai, R. A., Lundstrom, E. B., Sauer-Eriksson, A. E., and Johansson, E. (2014) Structural basis for processive DNA synthesis by yeast DNA polymerase varepsilon. *Nat Struct Mol Biol* **21**, 49-55
13. Zenkin, N., and Severinov, K. (2008) RNA polymerase -the third class of primases. *Cell Mol Life Sci* **65**, 2280-2288
14. Rodina, A., and Godson, G. N. (2006) Role of conserved amino acids in the catalytic activity of Escherichia coli primase. *J Bacteriol* **188**, 3614-3621
15. Hauschka, P. V. (1973) Analysis of nucleotide pools in animal cells. *Methods Cell Biol* **7**, 361-462

16. Sheaff, R. J., and Kuchta, R. D. (1993) Mechanism of calf thymus DNA primase: slow initiation, rapid polymerization, and intelligent termination. *Biochemistry* **32**, 3027-3037
17. Garg, P., and Burgers, P. M. (2005) DNA polymerases that propagate the eukaryotic DNA replication fork. *Crit Rev Biochem Mol Biol* **40**, 115-128
18. Pavlov, Y. I., Shcherbakova, P. V., and Rogozin, I. B. (2006) Roles of DNA polymerases in replication, repair, and recombination in eukaryotes. *Int Rev Cytol* **255**, 41-132
19. Kunkel, T. A. (2009) Evolving views of DNA replication (in)fidelity. *Cold Spring Harb Symp Quant Biol* **74**, 91-101
20. MacNeill, S. (2012) Composition and dynamics of the eukaryotic replisome: a brief overview. *Subcell Biochem* **62**, 1-17
21. Waisertreiger, I. S., Liston, V. G., Menezes, M. R., Kim, H. M., Lobachev, K. S., Stepchenkova, E. I., Tahirov, T. H., Rogozin, I. B., and Pavlov, Y. I. (2012) Modulation of mutagenesis in eukaryotes by DNA replication fork dynamics and quality of nucleotide pools. *Environ Mol Mutagen* **53**, 699-724
22. Tanaka, S., and Araki, H. (2013) Helicase Activation and Establishment of Replication Forks at Chromosomal Origins of Replication. *Cold Spring Harb Perspect Biol*
23. Pellegrini, L. (2012) The Pol alpha-Primase Complex. *Subcell Biochem* **62**, 157-169
24. Tahirov, T. H. (2012) Structure and function of eukaryotic DNA polymerase delta. *Subcell Biochem* **62**, 217-236
25. Hogg, M., and Johansson, E. (2012) DNA Polymerase epsilon. *Subcell Biochem* **62**, 237-257
26. Kunkel, T. A., and Burgers, P. M. (2008) Dividing the workload at a eukaryotic replication fork. *Trends Cell Biol* **18**, 521-527
27. Pavlov, Y. I., and Shcherbakova, P. V. (2010) DNA polymerases at the eukaryotic fork-20 years later. *Mutat Res* **685**, 45-53
28. Lawrence, C. W., and Hinkle, D. C. (1996) DNA polymerase zeta and the control of DNA damage induced mutagenesis in eukaryotes. *Cancer Surv* **28**, 21-31
29. Northam, M. R., Robinson, H. A., Kochenova, O. V., and Shcherbakova, P. V. (2010) Participation of DNA polymerase zeta in replication of undamaged DNA in Saccharomyces cerevisiae. *Genetics* **184**, 27-42
30. Baranovskiy, A. G., Lada, A. G., Siebler, H. M., Zhang, Y., Pavlov, Y. I., and Tahirov, T. H. (2012) DNA polymerase delta and zeta switch by sharing accessory subunits of DNA polymerase delta. *J Biol Chem* **287**, 17281-17287
31. Johnson, R. E., Prakash, L., and Prakash, S. (2012) Pol31 and Pol32 subunits of yeast DNA polymerase delta are also essential subunits of DNA polymerase zeta. *Proc Natl Acad Sci U S A* **109**, 12455-12460
32. Makarova, A. V., Stodola, J. L., and Burgers, P. M. (2012) A four-subunit DNA polymerase zeta complex containing Pol delta accessory subunits is essential for PCNA-mediated mutagenesis. *Nucleic Acids Res* **40**, 11618-11626

33. Gomez-Llorente, Y., Malik, R., Jain, R., Choudhury, J. R., Johnson, R. E., Prakash, L., Prakash, S., Ubarretxena-Belandia, I., and Aggarwal, A. K. (2013) The Architecture of Yeast DNA Polymerase zeta. *Cell Rep* **5**, 79-86
34. Lee, M., Lee, C. H., Demin, A. A., Munashingha, P. R., Amangyeld, T., Kwon, B., Formosa, T., and Seo, Y. S. (2014) Rad52/Rad59-dependent recombination as a means to rectify faulty Okazaki fragment processing. *J Biol Chem* **289**, 15064-15079
35. Dua, R., Levy, D. L., and Campbell, J. L. (1998) Role of the putative zinc finger domain of Saccharomyces cerevisiae DNA polymerase epsilon in DNA replication and the S/M checkpoint pathway. *J Biol Chem* **273**, 30046-30055
36. Klinge, S., Nunez-Ramirez, R., Llorca, O., and Pellegrini, L. (2009) 3D architecture of DNA Pol alpha reveals the functional core of multi-subunit replicative polymerases. *EMBO J* **28**, 1978-1987
37. Netz, D. J., Stith, C. M., Stumpfig, M., Kopf, G., Vogel, D., Genau, H. M., Stodola, J. L., Lill, R., Burgers, P. M., and Pierik, A. J. (2012) Eukaryotic DNA polymerases require an iron-sulfur cluster for the formation of active complexes. *Nat Chem Biol* **8**, 125-132
38. Tahirov, T. H., Makarova, K. S., Rogozin, I. B., Pavlov, Y. I., and Koonin, E. V. (2009) Evolution of DNA polymerases: an inactivated polymerase-exonuclease module in Pol epsilon and a chimeric origin of eukaryotic polymerases from two classes of archaeal ancestors. *Biol Direct* **4**, 11
39. Copeland, W. C., and Wang, T. S. (1993) Enzymatic characterization of the individual mammalian primase subunits reveals a biphasic mechanism for initiation of DNA replication. *J Biol Chem* **268**, 26179-26189
40. Baranovskiy, A. G., Babayeva, N. D., Zhang, Y., Gu, J., Suwa, Y., Pavlov, Y. I., and Tahirov, T. H. (2016) MECHANISM OF CONCERTED RNA-DNA PRIMER SYNTHESIS BY THE HUMAN PRIMOSOME. *J Biol Chem*
41. Klinge, S., Hirst, J., Maman, J. D., Krude, T., and Pellegrini, L. (2007) An iron-sulfur domain of the eukaryotic primase is essential for RNA primer synthesis. *Nat Struct Mol Biol* **14**, 875-877
42. Carr, A. M., Paek, A. L., and Weinert, T. (2011) DNA replication: failures and inverted fusions. *Semin Cell Dev Biol* **22**, 866-874
43. Weiner, B. E., Huang, H., Dattilo, B. M., Nilges, M. J., Fanning, E., and Chazin, W. J. (2007) An iron-sulfur cluster in the C-terminal domain of the p58 subunit of human DNA primase. *J Biol Chem* **282**, 33444-33451
44. Vaithiyalingam, S., Warren, E. M., Eichman, B. F., and Chazin, W. J. (2010) Insights into eukaryotic DNA priming from the structure and functional interactions of the 4Fe-4S cluster domain of human DNA primase. *Proc Natl Acad Sci U S A* **107**, 13684-13689
45. Kilkenny, M. L., De Piccoli, G., Perera, R. L., Labib, K., and Pellegrini, L. (2012) A conserved motif in the C-terminal tail of DNA polymerase alpha tethers primase to the eukaryotic replisome. *J Biol Chem* **287**, 23740-23747
46. Mizuno, T., Yamagishi, K., Miyazawa, H., and Hanaoka, F. (1999) Molecular architecture of the mouse DNA polymerase alpha-primase complex. *Mol Cell Biol* **19**, 7886-7896

47. Huang, H., Weiner, B. E., Zhang, H., Fuller, B. E., Gao, Y., Wile, B. M., Zhao, K., Arnett, D. R., Chazin, W. J., and Fanning, E. (2010) Structure of a DNA polymerase alpha-primase domain that docks on the SV40 helicase and activates the viral primosome. *J Biol Chem* **285**, 17112-17122
48. Zhou, B., Arnett, D. R., Yu, X., Brewster, A., Sowd, G. A., Xie, C. L., Vila, S., Gai, D., Fanning, E., and Chen, X. S. (2012) Structural Basis for the Interaction of a Hexameric Replicative Helicase with the Regulatory Subunit of Human DNA Polymerase alpha-Primase. *J Biol Chem* **287**, 26854-26866
49. Baranovskiy, A. G., Babayeva, N. D., Liston, V. G., Rogozin, I. B., Koonin, E. V., Pavlov, Y. I., Vassylyev, D. G., and Tahirov, T. H. (2008) X-ray structure of the complex of regulatory subunits of human DNA polymerase delta. *Cell Cycle* **7**, 3026-3036
50. Suwa, Y., Gu, J., Baranovskiy, A. G., Babayeva, N. D., Pavlov, Y. I., and Tahirov, T. H. (2015) Crystal Structure of the Human Pol alpha B Subunit in Complex with the C-terminal Domain of the Catalytic Subunit. *J Biol Chem* **290**, 14328-14337
51. Kuchta, R. D., and Stengel, G. (2010) Mechanism and evolution of DNA primases. *Biochim Biophys Acta* **1804**, 1180-1189
52. Perera, R. L., Torella, R., Klinge, S., Kilkenny, M. L., Maman, J. D., and Pellegrini, L. (2013) Mechanism for priming DNA synthesis by yeast DNA Polymerase α. *eLife Sciences* **2**
53. Zerbe, L. K., and Kuchta, R. D. (2002) The p58 subunit of human DNA primase is important for primer initiation, elongation, and counting. *Biochemistry* **41**, 4891-4900
54. Smith, D. J., and Whitehouse, I. (2012) Intrinsic coupling of lagging-strand synthesis to chromatin assembly. *Nature* **483**, 434-438
55. Morrison, A., Araki, H., Clark, A. B., Hamatake, R. K., and Sugino, A. (1990) A third essential DNA polymerase in S. cerevisiae. *Cell* **62**, 1143-1151
56. Stodola, J. L., and Burgers, P. M. (2016) Resolving individual steps of Okazaki-fragment maturation at a millisecond timescale. *Nat Struct Mol Biol* **advance online publication**
57. Reijns, M. A., Kemp, H., Ding, J., de Proce, S. M., Jackson, A. P., and Taylor, M. S. (2015) Lagging-strand replication shapes the mutational landscape of the genome. *Nature*
58. Baranovskiy, A. G., Gu, J., Babayeva, N. D., Agarkar, V. B., Suwa, Y., and Tahirov, T. H. (2014) Crystallization and preliminary X-ray diffraction analysis of human DNA primase. *Acta Crystallogr Sect F* **70**, 206-210
59. Lada, A. G., Stepchenkova, E. I., Waisertreiger, I. S. R., Noskov, V. N., Dhar, A., Eudy, J. D., Boissy, R. J., Hirano, M., Rogozin, I. B., and Pavlov, Y. I. (2013) Genome-Wide Mutation Avalanches Induced in Diploid Yeast Cells by a Base Analog or an APOBEC Deaminase. *PLoS Genet* **9**, e1003736
60. Liu, H., and Naismith, J. H. (2008) An efficient one-step site-directed deletion, insertion, single and multiple-site plasmid mutagenesis protocol. *BMC Biotechnol* **8**, 91

61. Kozmin, S. G., Pavlov, Y. I., Kunkel, T. A., and Sage, E. (2003) Roles of Saccharomyces cerevisiae DNA polymerases Poleta and Polzeta in response to irradiation by simulated sunlight. *Nucleic Acids Res* **31**, 4541-4552
62. Drake, J. W. (1991) A constant rate of spontaneous mutation in DNA-based microbes. *Proceedings of the National Academy of Sciences* **88**, 7160-7164
63. Shah, Kartik A., Shishkin, Alexander A., Voineagu, I., Pavlov, Youri I., Shcherbakova, Polina V., and Mirkin, Sergei M. (2012) Role of DNA Polymerases in Repeat-Mediated Genome Instability. *Cell Reports*
64. Sauguet, L., Klinge, S., Perera, R. L., Maman, J. D., and Pellegrini, L. (2010) Shared active site architecture between the large subunit of eukaryotic primase and DNA photolyase. *PLoS One* **5**, e10083
65. Kilkenny, M. L., Longo, M. A., Perera, R. L., and Pellegrini, L. (2013) Structures of human primase reveal design of nucleotide elongation site and mode of Pol α tethering. *Proceedings of the National Academy of Sciences*
66. Simon, A. C., Zhou, J. C., Perera, R. L., van Deursen, F., Evrin, C., Ivanova, M. E., Kilkenny, M. L., Renault, L., Kjaer, S., Matak-Vinkovic, D., Labib, K., Costa, A., and Pellegrini, L. (2014) A Ctf4 trimer couples the CMG helicase to DNA polymerase alpha in the eukaryotic replisome. *Nature*
67. Sheaff, R. J., Kuchta, R. D., and Ilsley, D. (1994) Calf thymus DNA polymerase alpha-primase: "communication" and primer-template movement between the two active sites. *Biochemistry* **33**, 2247-2254
68. Baranovskiy, A. G., Zhang, Y., Suwa, Y., Babayeva, N. D., Gu, J., Pavlov, Y. I., and Tahirov, T. H. (2015) Crystal Structure of the Human Primase. *J Biol Chem* **290**, 5635-5646
69. Copeland, W. C. (1997) Expression, purification, and characterization of the two human primase subunits and truncated complexes from Escherichia coli. *Protein Expr Purif* **9**, 1-9
70. Frick, D. N., and Richardson, C. C. (2001) DNA primases. *Annu Rev Biochem* **70**, 39-80
71. Baranovskiy, A. G., Zhang, Y., Suwa, Y., Gu, J., Babayeva, N. D., Pavlov, Y. I., and Tahirov, T. H. (2016) Insight into the Human DNA Primase Interaction with Template-Primer. *J Biol Chem* **291**, 4793-4802
72. Mizuno, T., Ito, N., Yokoi, M., Kobayashi, A., Tamai, K., Miyazawa, H., and Hanaoka, F. (1998) The second-largest subunit of the mouse DNA polymerase alpha-primase complex facilitates both production and nuclear translocation of the catalytic subunit of DNA polymerase alpha. *Mol Cell Biol* **18**, 3552-3562
73. Feng, W., and D'Urso, G. (2001) Schizosaccharomyces pombe cells lacking the amino-terminal catalytic domains of DNA polymerase epsilon are viable but require the DNA damage checkpoint control. *Mol Cell Biol* **21**, 4495-4504
74. Makiniemi, M., Pospiech, H., Kilpelainen, S., Jokela, M., Vihinen, M., and Syvaoja, J. E. (1999) A novel family of DNA-polymerase-associated B subunits. *Trends Biochem Sci* **24**, 14-16
75. Gambus, A., van Deursen, F., Polychronopoulos, D., Foltman, M., Jones, R. C., Edmondson, R. D., Calzada, A., and Labib, K. (2009) A key role for Ctf4 in

coupling the MCM2-7 helicase to DNA polymerase alpha within the eukaryotic replisome. *EMBO J* **28**, 2992-3004
76. Huang, S. G., Weisshart, K., Gilbert, I., and Fanning, E. (1998) Stoichiometry and mechanism of assembly of SV40 T antigen complexes with the viral origin of DNA replication and DNA polymerase alpha-primase. *Biochemistry* **37**, 15345-15352
77. Bohn, E. W., and Wilson, S. H. (1974) Studies on the Activity of the A Particle-associated DNA Polymerase. *Cancer Research* **34**, 1977-1981
78. Lao-Sirieix, S. H., Nookala, R. K., Roversi, P., Bell, S. D., and Pellegrini, L. (2005) Structure of the heterodimeric core primase. *Nat Struct Mol Biol* **12**, 1137-1144
79. Copeland, W. C., and Tan, X. (1995) Active site mapping of the catalytic mouse primase subunit by alanine scanning mutagenesis. *J Biol Chem* **270**, 3905-3913
80. Vaithiyalingam, S., Arnett, D. R., Aggarwal, A., Eichman, B. F., Fanning, E., and Chazin, W. J. (2014) Insights into eukaryotic primer synthesis from structures of the p48 subunit of human DNA primase. *J Mol Biol*
81. Agarkar, V. B., Babayeva, N. D., Pavlov, Y. I., and Tahirov, T. H. (2011) Crystal structure of the C-terminal domain of human DNA primase large subunit: Implications for the mechanism of the primase-polymerase α switch. *Cell Cycle* **10**, 926-931
82. Yao, N. Y., Schroeder, J. W., Yurieva, O., Simmons, L. A., and O'Donnell, M. E. (2013) Cost of rNTP/dNTP pool imbalance at the replication fork. *Proceedings of the National Academy of Sciences*
83. Nick McElhinny, S. A., Watts, B. E., Kumar, D., Watt, D. L., Lundström, E.-B., Burgers, P. M. J., Johansson, E., Chabes, A., and Kunkel, T. A. (2010) Abundant ribonucleotide incorporation into DNA by yeast replicative polymerases. *Proceedings of the National Academy of Sciences* **107**, 4949-4954
84. Bebenek, A., Carver, G. T., Dressman, H. K., Kadyrov, F. A., Haseman, J. K., Petrov, V., Konigsberg, W. H., Karam, J. D., and Drake, J. W. (2002) Dissecting the fidelity of bacteriophage RB69 DNA polymerase: site-specific modulation of fidelity by polymerase accessory proteins. *Genetics* **162**, 1003-1018
85. Aguirre, J. D., Chifotides, H. T., Angeles-Boza, A. M., Chouai, A., Turro, C., and Dunbar, K. R. (2009) Redox-regulated Inhibition of T7 RNA polymerase via establishment of disulfide linkages by substituted Dppz dirhodium(II,II) complexes. *Inorg Chem* **48**, 4435-4444
86. Steitz, T. A. (1998) A mechanism for all polymerases. *Nature* **391**, 231-232
87. Pelletier, H., Sawaya, M. R., Kumar, A., Wilson, S. H., and Kraut, J. (1994) Structures of ternary complexes of rat DNA polymerase beta, a DNA template-primer, and ddCTP. *Science* **264**, 1891-1903
88. Steitz, T. A., Smerdon, S. J., Jager, J., and Joyce, C. M. (1994) A unified polymerase mechanism for nonhomologous DNA and RNA polymerases. *Science* **266**, 2022-2025
89. Nakamura, T., Zhao, Y., Yamagata, Y., Hua, Y.-j., and Yang, W. (2012) Watching DNA polymerase η make a phosphodiester bond. *Nature* **487**, 196-201

90. Golosov, A. A., Warren, J. J., Beese, L. S., and Karplus, M. (2010) The mechanism of the translocation step in DNA replication by DNA polymerase I: a computer simulation analysis. *Structure* **18**, 83-93
91. Swan, M. K., Johnson, R. E., Prakash, L., Prakash, S., and Aggarwal, A. K. (2009) Structural basis of high-fidelity DNA synthesis by yeast DNA polymerase delta. *Nat Struct Mol Biol* **16**, 979-986
92. Freudenthal, B. D., Beard, W. A., Perera, L., Shock, D. D., Kim, T., Schlick, T., and Wilson, S. H. (2015) Uncovering the polymerase-induced cytotoxicity of an oxidized nucleotide. *Nature* **517**, 635-639
93. Mullen, G. P., Serpersu, E. H., Ferrin, L. J., Loeb, L. A., and Mildvan, A. S. (1990) Metal binding to DNA polymerase I, its large fragment, and two 3',5'-exonuclease mutants of the large fragment. *J Biol Chem* **265**, 14327-14334
94. Frank-Kamenetskii, M. D., and Mirkin, S. M. (1995) Triplex DNA structures. *Annu Rev Biochem* **64**, 65-95
95. Bacolla, A., Wang, G., and Vasquez, K. M. (2015) New Perspectives on DNA and RNA Triplexes As Effectors of Biological Activity. *PLoS Genet* **11**, e1005696
96. Gueroult, M., Boittin, O., Mauffret, O., Etchebest, C., and Hartmann, B. (2012) Mg2+ in the major groove modulates B-DNA structure and dynamics. *PLoS One* **7**, e41704
97. Boyer, A. S., Grgurevic, S., Cazaux, C., and Hoffmann, J. S. (2013) The human specialized DNA polymerases and non-B DNA: vital relationships to preserve genome integrity. *J Mol Biol* **425**, 4767-4781
98. Lapidot, A., Baran, N., and Manor, H. (1989) (dT-dC)n and (dG-dA)n tracts arrest single stranded DNA replication in vitro. *Nucleic Acids Res* **17**, 883-900
99. Hile, S. E., and Eckert, K. A. (2004) Positive correlation between DNA polymerase alpha-primase pausing and mutagenesis within polypyrimidine/polypurine microsatellite sequences. *J Mol Biol* **335**, 745-759
100. Mikhailov, V. S., and Bogenhagen, D. F. (1996) Termination within oligo(dT) tracts in template DNA by DNA polymerase gamma occurs with formation of a DNA triplex structure and is relieved by mitochondrial single-stranded DNA-binding protein. *J Biol Chem* **271**, 30774-30780
101. Zhang, Y., Baranovskiy, A. G., Tahirov, T. H., and Pavlov, Y. I. (2014) The C-terminal Domain of the DNA Polymerase Catalytic Subunit Regulates the Primase and Polymerase Activities of the Human DNA Polymerase α-Primase Complex. *J Biol Chem* **289**, 22021-22034
102. Baran, N., Lapidot, A., and Manor, H. (1991) Formation of DNA triplexes accounts for arrests of DNA synthesis at d(TC)n and d(GA)n tracts. *Proc Natl Acad Sci U S A* **88**, 507-511
103. Krasilnikov, A. S., Panyutin, I. G., Samadashwily, G. M., Cox, R., Lazurkin, Y. S., and Mirkin, S. M. (1997) Mechanisms of triplex-caused polymerization arrest. *Nucleic Acids Res* **25**, 1339-1346
104. Blanca, G., Shevelev, I., Ramadan, K., Villani, G., Spadari, S., Hubscher, U., and Maga, G. (2003) Human DNA polymerase lambda diverged in evolution from DNA polymerase beta toward specific Mn(++) dependence: a kinetic and thermodynamic study. *Biochemistry* **42**, 7467-7476

105. Tabor, S., and Richardson, C. C. (1989) Effect of manganese ions on the incorporation of dideoxynucleotides by bacteriophage T7 DNA polymerase and Escherichia coli DNA polymerase I. *Proc Natl Acad Sci U S A* **86**, 4076-4080
106. Beckman, R. A., Mildvan, A. S., and Loeb, L. A. (1985) On the fidelity of DNA replication: manganese mutagenesis in vitro. *Biochemistry* **24**, 5810-5817
107. Kunkel, T. A., and Loeb, L. A. (1979) On the fidelity of DNA replication. Effect of divalent metal ion activators and deoxyrionucleoside triphosphate pools on in vitro mutagenesis. *J Biol Chem* **254**, 5718-5725
108. Zakour, R. A., Kunkel, T. A., and Loeb, L. A. (1981) Metal-induced infidelity of DNA synthesis. *Environ Health Perspect* **40**, 197-205
109. Frank, E. G., and Woodgate, R. (2007) Increased catalytic activity and altered fidelity of human DNA polymerase iota in the presence of manganese. *J Biol Chem* **282**, 24689-24696
110. Batra, V. K., Beard, W. A., Shock, D. D., Pedersen, L. C., and Wilson, S. H. (2008) Structures of DNA polymerase beta with active-site mismatches suggest a transient abasic site intermediate during misincorporation. *Mol Cell* **30**, 315-324
111. Makarova, A. V., Grabow, C., Gening, L. V., Tarantul, V. Z., Tahirov, T. H., Bessho, T., and Pavlov, Y. I. (2011) Inaccurate DNA synthesis in cell extracts of yeast producing active human DNA polymerase iota. *PLoS One* **6**, e16612
112. Copeland, W. C., Lam, N. K., and Wang, T. S. (1993) Fidelity studies of the human DNA polymerase alpha. The most conserved region among alpha-like DNA polymerases is responsible for metal-induced infidelity in DNA synthesis. *J Biol Chem* **268**, 11041-11049
113. Slater, J. P., Mildvan, A. S., and Loeb, L. A. (1971) Zinc in DNA polymerases. *Biochem Biophys Res Commun* **44**, 37-43
114. Springgate, C. F., Mildvan, A. S., Abramson, R., Engle, J. L., and Loeb, L. A. (1973) Escherichia coli Deoxyribonucleic Acid Polymerase I, a Zinc Metalloenzyme : NUCLEAR QUADRUPOLAR RELAXATION STUDIES OF THE ROLE OF BOUND ZINC. *J Biol Chem* **248**, 5987-5993
115. Ferrin, L. J., Mildvan, A. S., and Loeb, L. A. (1983) Metal content of DNA polymerase I purified from overproducing and wild type Escherichia coli. *Biochem Biophys Res Commun* **112**, 723-728
116. Walton, K. E., FitzGerald, P. C., Herrmann, M. S., and Behnke, W. D. (1982) A fully active DNA polymerase I from Escherichia coli lacking stoichiometric zinc. *Biochem Biophys Res Commun* **108**, 1353-1361
117. Sirover, M. A., and Loeb, L. A. (1976) Metal activation of DNA synthesis. *Biochem Biophys Res Commun* **70**, 812-817
118. Burgers, P. M., and Eckstein, F. (1979) A study of the mechanism of DNA polymerase I from Escherichia coli with diastereomeric phosphorothioate analogs of deoxyadenosine triphosphate. *J Biol Chem* **254**, 6889-6893
119. Slaby, I., Lind, B., and Holmgren, A. (1984) T7 DNA polymerase is not a zinc-metalloenzyme and the polymerase and exonuclease activities are inhibited by zinc ions. *Biochem Biophys Res Commun* **122**, 1410-1417

120. Fridlender, B., Chejanovsky, N., and Becker, Y. (1978) Selective inhibition of herpes simplex virus type 1 DNA polymerase by zinc ions. *Virology* **84**, 551-554
121. Kirby, T. W., DeRose, E. F., Cavanaugh, N. A., Beard, W. A., Shock, D. D., Mueller, G. A., Wilson, S. H., and London, R. E. (2012) Metal-induced DNA translocation leads to DNA polymerase conformational activation. *Nucleic Acids Res* **40**, 2974-2983
122. Smith, R. M., Martell, A. E., and Chen, Y. (1991) Critical evaluation of stability constants for nucleotide complexes with protons and metal ions and the accompanying enthalpy changes. *Pure Appl Chem* **63**, 1015-1080
123. Dawson, R. M. C., Elliott, D. C., Elliott, W. H., and Jones, K. M. (1986) Stability Constants for Metal Complexes. in *Data for biochemical research*, Third Ed., Oxford Science Publications, OUP, Oxford. pp 399-415
124. Perera, R. L., Torella, R., Klinge, S., Kilkenny, M. L., Maman, J. D., and Pellegrini, L. (2013) Mechanism for priming DNA synthesis by yeast DNA Polymerase α. *eLife Sciences* **2**, e00482
125. Thompson, H. C., Sheaff, R. J., and Kuchta, R. D. (1995) Interactions of calf thymus DNA polymerase alpha with primer/templates. *Nucleic Acids Res* **23**, 4109-4115
126. Seela, F., and Roling, A. (1992) 7-Deazapurine containing DNA: efficiency of c7GdTP, c7AdTP and c7IdTP incorporation during PCR-amplification and protection from endodeoxyribonuclease hydrolysis. *Nucleic Acids Res* **20**, 55-61
127. Patro, J. N., Urban, M., and Kuchta, R. D. (2009) Interaction of human DNA polymerase alpha and DNA polymerase I from Bacillus stearothermophilus with hypoxanthine and 8-oxoguanine nucleotides. *Biochemistry* **48**, 8271-8278
128. Mirkin, S. M., and Frank-Kamenetskii, M. D. (1994) H-DNA and related structures. *Annu Rev Biophys Biomol Struct* **23**, 541-576
129. Balakrishnan, L., and Bambara, R. A. (2013) Okazaki fragment metabolism. *Cold Spring Harb Perspect Biol* **5**, pii. a010173
130. Prindle, M. J., and Loeb, L. A. (2012) DNA polymerase delta in DNA replication and genome maintenance. *Environ Mol Mutagen* **53**, 666-682
131. Tahirov, T. H. (2012) Structure and function of eukaryotic DNA polymerase delta. *Subcell Biochem* **62**, 217-236
132. Stillman, B. (2015) Reconsidering DNA Polymerases at the Replication Fork in Eukaryotes. *Mol Cell* **59**, 139-141
133. Wolf, F. I., and Cittadini, A. (2003) Chemistry and biochemistry of magnesium. *Molecular Aspects of Medicine* **24**, 3-9
134. Strick, R., Strissel, P. L., Gavrilov, K., and Levi-Setti, R. (2001) Cation-chromatin binding as shown by ion microscopy is essential for the structural integrity of chromosomes. *J Cell Biol* **155**, 899-910
135. Brukner, I., Susic, S., Dlakic, M., Savic, A., and Pongor, S. (1994) Physiological concentration of magnesium ions induces a strong macroscopic curvature in GGGCCC-containing DNA. *J Mol Biol* **236**, 26-32

136. Lavery, R., and Pullman, B. (1981) Molecular electrostatic potential on the surface envelopes of macromolecules: B-DNA. *Int J Quant Chem* **20**, 259-272
137. Subirana, J. A., and Soler-Lopez, M. (2003) Cations as hydrogen bond donors: a view of electrostatic interactions in DNA. *Annu Rev Biophys Biomol Struct* **32**, 27-45
138. Routh, A., Sandin, S., and Rhodes, D. (2008) Nucleosome repeat length and linker histone stoichiometry determine chromatin fiber structure. *Proc Natl Acad Sci U S A* **105**, 8872-8877
139. Grigoryev, S. A., Arya, G., Correll, S., Woodcock, C. L., and Schlick, T. (2009) Evidence for heteromorphic chromatin fibers from analysis of nucleosome interactions. *Proc Natl Acad Sci U S A* **106**, 13317-13322
140. Juneau, K., Podell, E., Harrington, D. J., and Cech, T. R. (2001) Structural basis of the enhanced stability of a mutant ribozyme domain and a detailed view of RNA--solvent interactions. *Structure* **9**, 221-231
141. Ottová, P., Espinoza-Herrera, S. J., and Štěpánek, J. (2011) Magnesium effect on premelting transitions in nucleic acids: DNA duplex and RNA hairpin models. *Journal of Molecular Structure* **993**, 324-327
142. Ohashi, E., Bebenek, K., Matsuda, T., Feaver, W. J., Gerlach, V. L., Friedberg, E. C., Ohmori, H., and Kunkel, T. A. (2000) Fidelity and Processivity of DNA Synthesis by DNA Polymerase κ, the Product of the Human DINB1 Gene. *Journal of Biological Chemistry* **275**, 39678-39684
143. Bock, J. L. (1980) The binding of metal ions to ATP: A proton and phosphorus nmr investigation of diamagnetic metal-ATP complexes. *Journal of Inorganic Biochemistry* **12**, 119-130
144. Morin, J. A., Cao, F. J., Lazaro, J. M., Arias-Gonzalez, J. R., Valpuesta, J. M., Carrascosa, J. L., Salas, M., and Ibarra, B. (2015) Mechano-chemical kinetics of DNA replication: identification of the translocation step of a replicative DNA polymerase. *Nucleic Acids Res* **43**, 3643-3652
145. Waga, S., and Stillman, B. (1998) The DNA replication fork in eukaryotic cells. *Annu Rev Biochem* **67**, 721-751
146. Nethanel, T., Reisfeld, S., Dinter-Gottlieb, G., and Kaufmann, G. (1988) An Okazaki piece of simian virus 40 may be synthesized by ligation of shorter precursor chains. *J Virol* **62**, 2867-2873
147. Thompson, H. C., and Kuchta, R. D. (1995) Arabinofuranosyl nucleotides are not chain-terminators during initiation of new strands of DNA by DNA polymerase alpha-primase. *Biochemistry* **34**, 11198-11203
148. Huang, H., Zhao, K., Arnett, D. R., and Fanning, E. (2010) A specific docking site for DNA polymerase {alpha}-primase on the SV40 helicase is required for viral primosome activity, but helicase activity is dispensable. *J Biol Chem* **285**, 33475-33484
149. Hedglin, M., Kumar, R., and Benkovic, S. J. (2013) Replication clamps and clamp loaders. *Cold Spring Harb Perspect Biol* **5**, a010165
150. Tsurimoto, T., and Stillman, B. (1991) Replication factors required for SV40 DNA replication in vitro. II. Switching of DNA polymerase alpha and delta during initiation of leading and lagging strand synthesis. *J Biol Chem* **266**, 1961-1968

151. Xing, X., Zhang, L., Guo, L., She, Q., and Huang, L. (2014) Sulfolobus Replication Factor C Stimulates the Activity of DNA Polymerase B1. *Journal of Bacteriology* **196**, 2367-2375
152. Imamura, K., Fukunaga, K., Kawarabayasi, Y., and Ishino, Y. (2007) Specific interactions of three proliferating cell nuclear antigens with replication-related proteins in Aeropyrum pernix. *Mol Microbiol* **64**, 308-318
153. Mossi, R., Keller, R. C., Ferrari, E., and Hubscher, U. (2000) DNA polymerase switching: II. Replication factor C abrogates primer synthesis by DNA polymerase alpha at a critical length. *J Mol Biol* **295**, 803-814
154. Maga, G., Stucki, M., Spadari, S., and Hubscher, U. (2000) DNA polymerase switching: I. Replication factor C displaces DNA polymerase alpha prior to PCNA loading. *J Mol Biol* **295**, 791-801
155. Georgescu, R. E., Schauer, G. D., Yao, N. Y., Langston, L. D., Yurieva, O., Zhang, D., Finkelstein, J., and O'Donnell, M. E. (2015) *Reconstitution of a eukaryotic replisome reveals suppression mechanisms that define leading/lagging strand operation*,
156. Dovrat, D., Stodola, J. L., Burgers, P. M., and Aharoni, A. (2014) Sequential switching of binding partners on PCNA during in vitro Okazaki fragment maturation. *Proc Natl Acad Sci U S A* **111**, 14118-14123
157. Braun, K. A., Lao, Y., He, Z., Ingles, C. J., and Wold, M. S. (1997) Role of protein-protein interactions in the function of replication protein A (RPA): RPA modulates the activity of DNA polymerase alpha by multiple mechanisms. *Biochemistry* **36**, 8443-8454
158. Pavlov, Y. I., Frahm, C., Nick McElhinny, S. A., Niimi, A., Suzuki, M., and Kunkel, T. A. (2006) Evidence that errors made by DNA polymerase alpha are corrected by DNA polymerase delta. *Curr Biol* **16**, 202-207
159. Shcherbakova, P. V., Pavlov, Y. I., Chilkova, O., Rogozin, I. B., Johansson, E., and Kunkel, T. A. (2003) Unique error signature of the four-subunit yeast DNA polymerase epsilon. *J Biol Chem* **278**, 43770-43780
160. Fortune, J. M., Stith, C. M., Kissling, G. E., Burgers, P. M. J., and Kunkel, T. A. (2006) RPA and PCNA suppress formation of large deletion errors by yeast DNA polymerase δ. *Nucleic Acids Research* **34**, 4335-4341
161. Pursell, Z. F., Isoz, I., Lundström, E.-B., Johansson, E., and Kunkel, T. A. (2007) Yeast DNA Polymerase ε Participates in Leading-Strand DNA Replication. *Science* **317**, 127-130
162. Nick McElhinny, S. A., Stith, C. M., Burgers, P. M. J., and Kunkel, T. A. (2007) Inefficient Proofreading and Biased Error Rates during Inaccurate DNA Synthesis by a Mutant Derivative of Saccharomyces cerevisiae DNA Polymerase δ. *J Biol Chem* **282**, 2324-2332
163. Georgescu, R. E., Langston, L., Yao, N. Y., Yurieva, O., Zhang, D., Finkelstein, J., Agarwal, T., and O'Donnell, M. E. (2014) Mechanism of asymmetric polymerase assembly at the eukaryotic replication fork. *Nat Struct Mol Biol* **21**, 664-670
164. Liu, C. L., Bernstein, B. E., and Schreiber, S. L. (2008) Whole Genome Amplification by T7-Based Linear Amplification of DNA (TLAD): Overview. *CSH Protoc* **2008**, pdb.top42

165. Storici, F., Bebenek, K., Kunkel, T. A., Gordenin, D. A., and Resnick, M. A. (2007) RNA-templated DNA repair. *Nature* **447**, 338-341
166. Qi, H., and Zakian, V. A. (2000) The Saccharomyces telomere-binding protein Cdc13p interacts with both the catalytic subunit of DNA polymerase alpha and the telomerase-associated est1 protein. *Genes Dev* **14**, 1777-1788
167. Dahlen, M., Sunnerhagen, P., and Wang, T. S. (2003) Replication proteins influence the maintenance of telomere length and telomerase protein stability. *Mol Cell Biol* **23**, 3031-3042
168. Grossi, S., Puglisi, A., Dmitriev, P. V., Lopes, M., and Shore, D. (2004) Pol12, the B subunit of DNA polymerase alpha, functions in both telomere capping and length regulation. *Genes Dev* **18**, 992-1006
169. Derboven, E., Ekker, H., Kusenda, B., Bulankova, P., and Riha, K. (2014) Role of STN1 and DNA polymerase alpha in telomere stability and genome-wide replication in Arabidopsis. *PLoS Genet* **10**, e1004682
170. Williamson, J. R., Raghuraman, M. K., and Cech, T. R. (1989) Monovalent cation-induced structure of telomeric DNA: The G-quartet model. *Cell* **59**, 871-880
171. Smogorzewska, A., and de Lange, T. (2004) Regulation of telomerase by telomeric proteins. *Annu Rev Biochem* **73**, 177-208
172. Gilson, E., and Geli, V. (2007) How telomeres are replicated. *Nat Rev Mol Cell Biol* **8**, 825-838
173. Verdun, R. E., and Karlseder, J. (2006) The DNA damage machinery and homologous recombination pathway act consecutively to protect human telomeres. *Cell* **127**, 709-720
174. Diede, S. J., and Gottschling, D. E. (1999) Telomerase-mediated telomere addition in vivo requires DNA primase and DNA polymerases alpha and delta. *Cell* **99**, 723-733
175. Early, A., Drury, L. S., and Diffley, J. F. (2004) Mechanisms involved in regulating DNA replication origins during the cell cycle and in response to DNA damage. *Philos Trans R Soc Lond B Biol Sci* **359**, 31-38
176. Siddiqui, K., On, K. F., and Diffley, J. F. (2013) Regulating DNA Replication in Eukarya. *Cold Spring Harb Perspect Biol*
177. Nakamura, M., Nabetani, A., Mizuno, T., Hanaoka, F., and Ishikawa, F. (2005) Alterations of DNA and chromatin structures at telomeres and genetic instability in mouse cells defective in DNA polymerase alpha. *Mol Cell Biol* **25**, 11073-11088
178. Casper, A. M., PA; Gawel, M; Petes, TD. (2008) Low Levels of DNA Polymerase Alpha Induce Mitotic and Meiotic Instability in the Ribosomal DNA Gene Cluster of Saccharomyces cerevisiae. *PLoS Genet*
179. Bartlett, E. J., Brissett, N. C., and Doherty, A. J. (2013) Ribonucleolytic resection is required for repair of strand displaced nonhomologous end-joining intermediates. *Proc Natl Acad Sci U S A* **110**, E1984-1991
180. Guilliam, T. A., Keen, B. A., Brissett, N. C., and Doherty, A. J. (2015) Primase-polymerases are a functionally diverse superfamily of replication and repair enzymes. *Nucleic Acids Research*

181. De Falco, M., Fusco, A., De Felice, M., Rossi, M., and Pisani, F. M. (2004) The DNA primase of Sulfolobus solfataricus is activated by substrates containing a thymine-rich bubble and has a 3'-terminal nucleotidyl-transferase activity. *Nucleic Acids Res* **32**, 5223-5230
182. Hu, J., Guo, L., Wu, K., Liu, B., Lang, S., and Huang, L. (2012) Template-dependent polymerization across discontinuous templates by the heterodimeric primase from the hyperthermophilic archaeon Sulfolobus solfataricus. *Nucleic Acids Res* **40**, 3470-3483
183. Babudri, N., Achilli, A., Martinelli, C., Moore, E., Lancioni, H., and Pavlov, Y. I. (2011) The role of DNA polymerase alpha in the control of mutagenesis in cells starved for nutrients. **9**, 53-61
184. Longhese, M. P., Jovine, L., Plevani, P., and Lucchini, G. (1993) Conditional mutations in the yeast DNA primase genes affect different aspects of DNA metabolism and interactions in the DNA polymerase alpha-primase complex. *Genetics* **133**, 183-191
185. Jin, Y. H., Clark, A. B., Slebos, R. J., Al-Refai, H., Taylor, J. A., Kunkel, T. A., Resnick, M. A., and Gordenin, D. A. (2003) Cadmium is a mutagen that acts by inhibiting mismatch repair. *Nat Genet* **34**, 326-329
186. Cleary, J. D., and Pearson, C. E. (2003) The contribution of cis-elements to disease-associated repeat instability: clinical and experimental evidence. *Cytogenet Genome Res* **100**, 25-55
187. Suzuki, M., Niimi, A., Limsirichaikul, S., Tomida, S., Miao Huang, Q., Izuta, S., Usukura, J., Itoh, Y., Hishida, T., Akashi, T., Nakagawa, Y., Kikuchi, A., Pavlov, Y., Murate, T., and Takahashi, T. (2009) PCNA mono-ubiquitination and activation of translesion DNA polymerases by DNA polymerase {alpha}. *J Biochem* **146**, 13-21
188. Niimi, A., Limsirichaikul, S., Yoshida, S., Iwai, S., Masutani, C., Hanaoka, F., Kool, E. T., Nishiyama, Y., and Suzuki, M. (2004) Palm Mutants in DNA Polymerases and Alter DNA Replication Fidelity and Translesion Activity. *Mol Cell Biol* **24**, 2734-2746
189. Balakrishnan, L., and Bambara, R. A. (2013) Okazaki fragment metabolism. *Cold Spring Harb Perspect Biol* **5**